ISAR GEOMETRY AND SIGNAL MODELLING

SPOTLIGHT SYNTHETIC APERTURE

- The antenna can be steered in order to increase the synthetic aperture

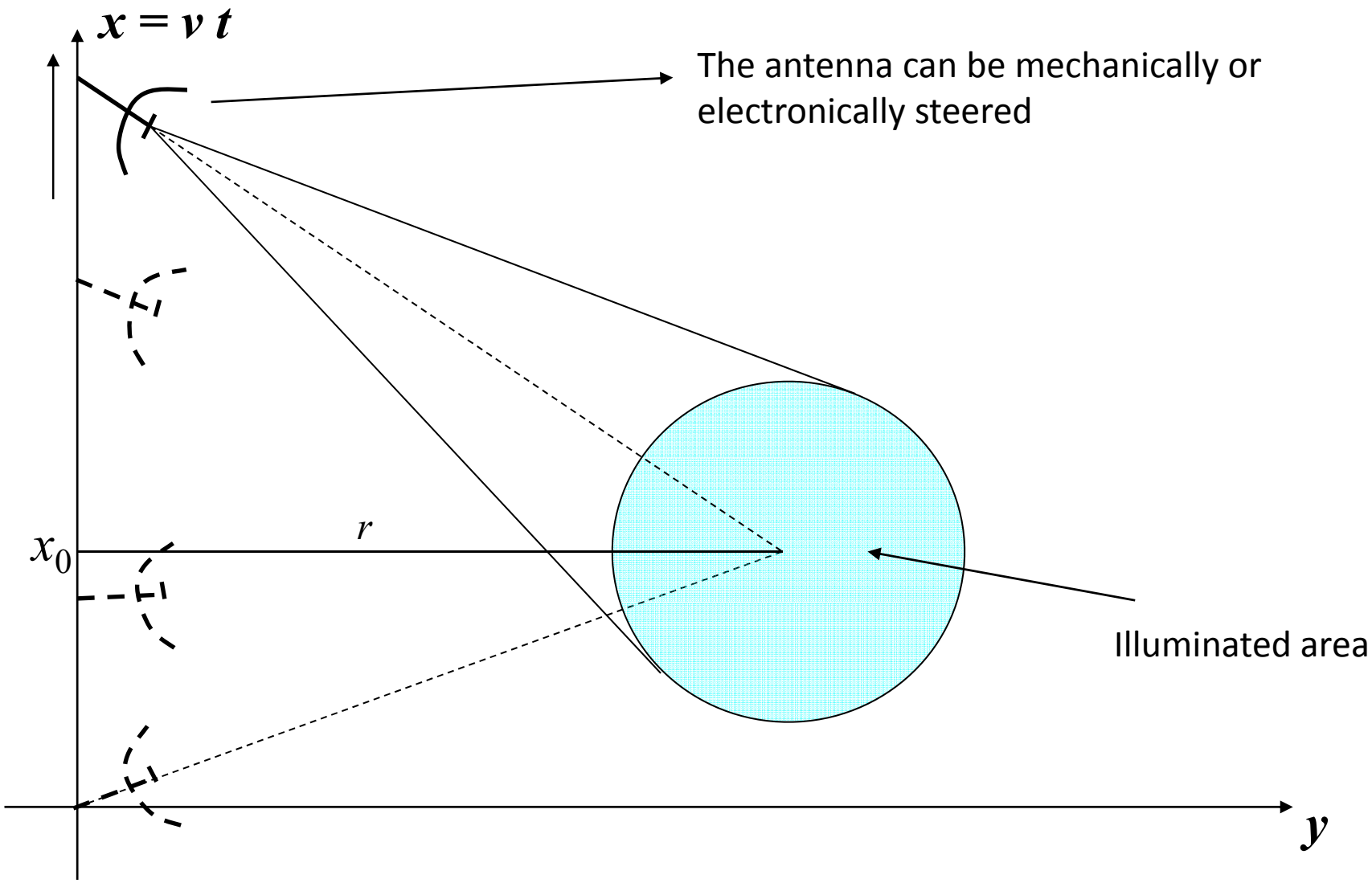

From SAR to ISAR

• The name Inverse SAR refers to the fact that the synthetic aperture is not formed by means of the movement of the platform that carries the radar but rather it is formed by exploiting the movement of the target.

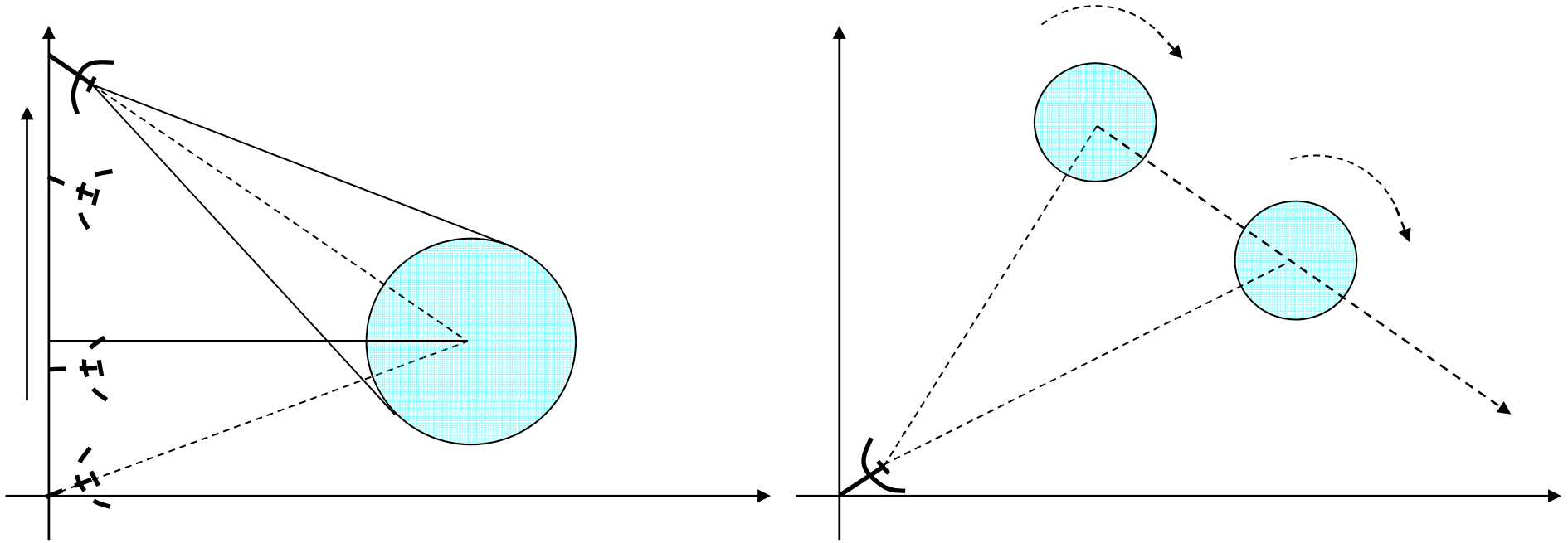

• The synthetic aperture can be seen as a coherent processing of echoes that comes from different view angles.

• The inverse synthetic aperture is achieved when there is a variation of the target-radar aspect angle.

THE TURNTABLE EXPERIMENT

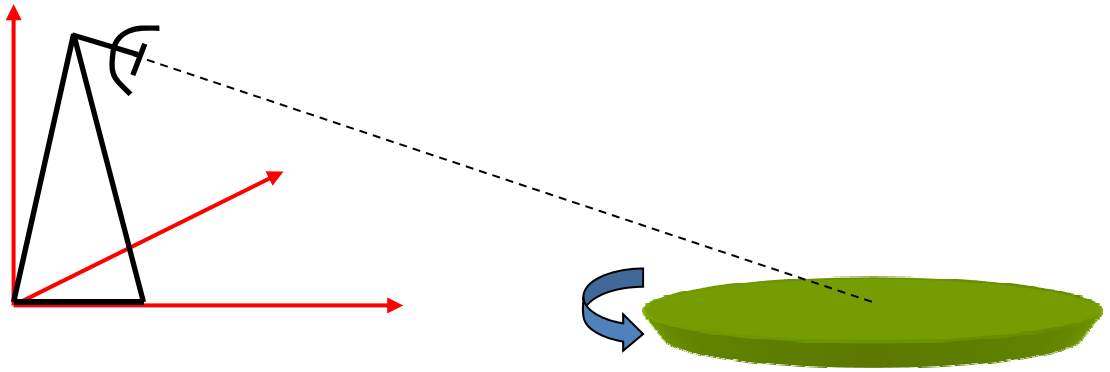

The turntable experiment can be interpreted as a SAR experiment where the antenna array is formed along a circular path.

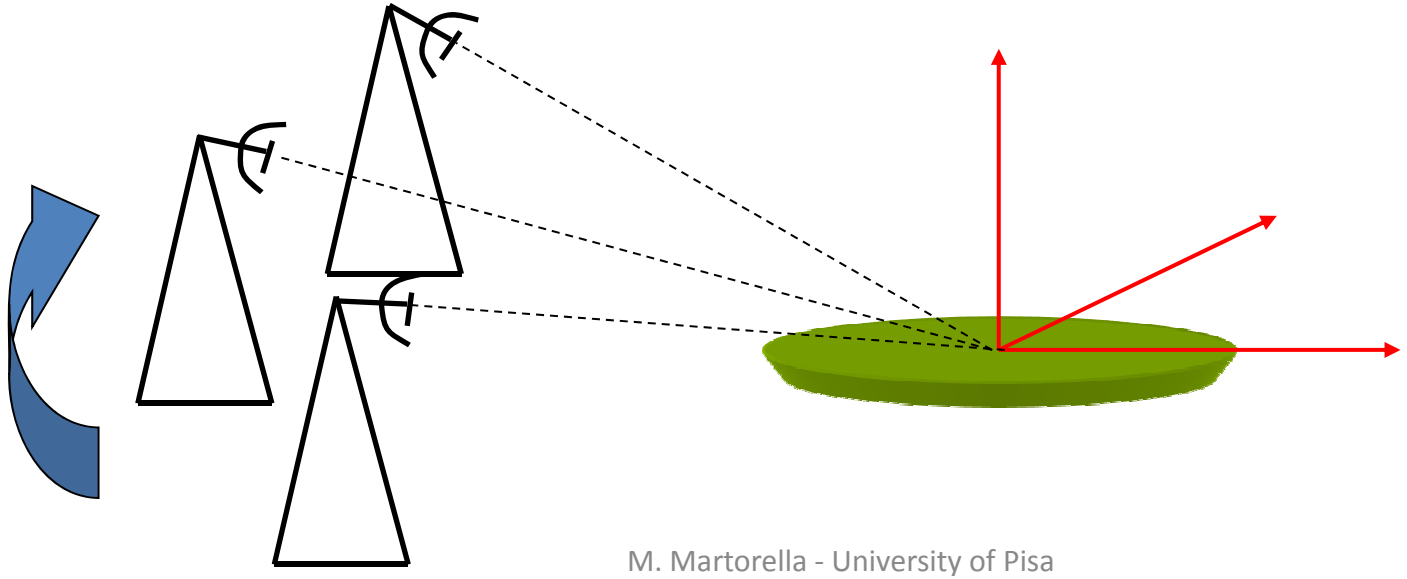

ISAR SYSTEM GEOMETRY

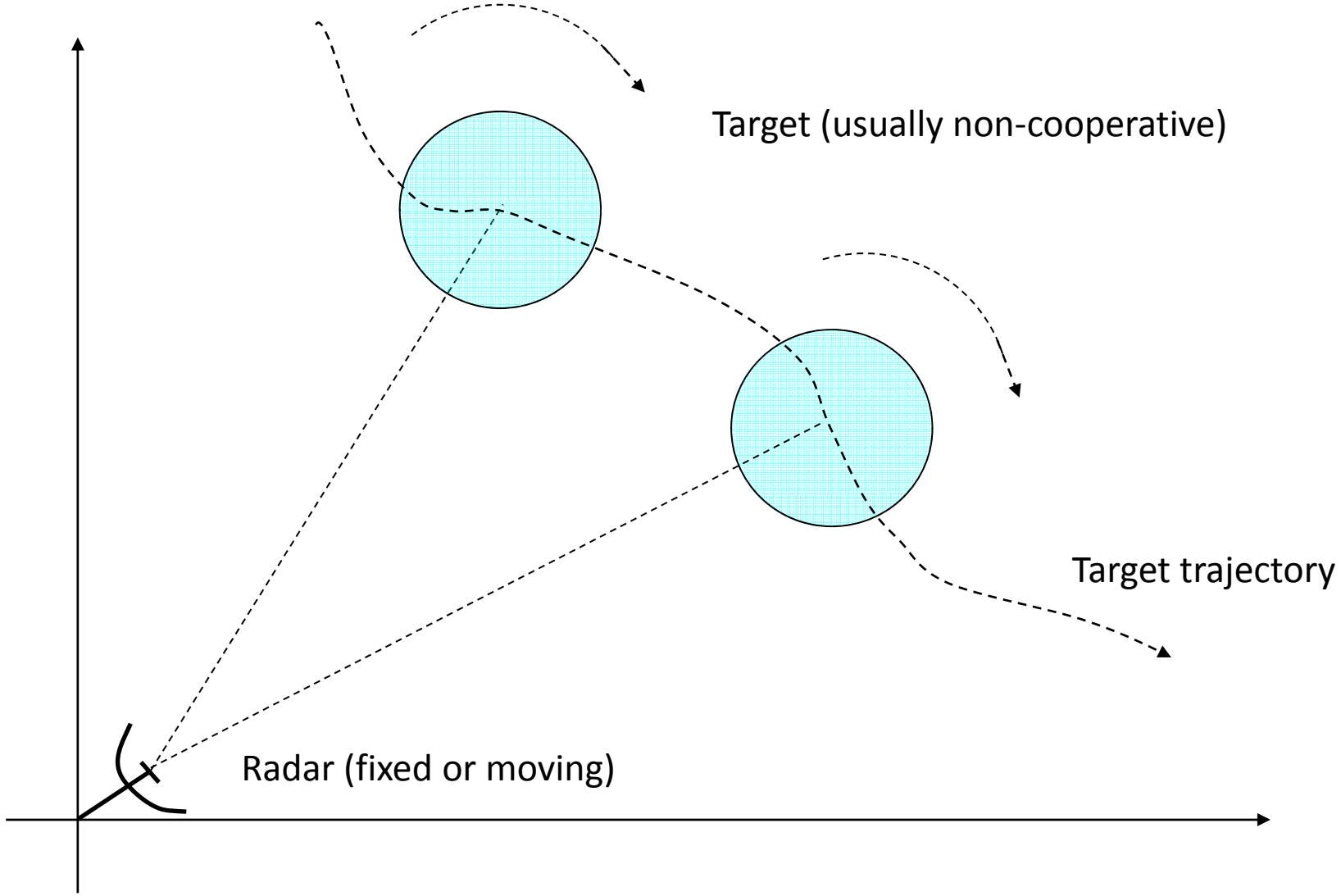

EXAMPLES OF ISAR SYSTEMS

FGAN - TIRA

- Initially used for detecting and tracking ballistic missiles,FGAN-TIRA is now used as a powerful ISAR system.

- It is able to form images of satellites

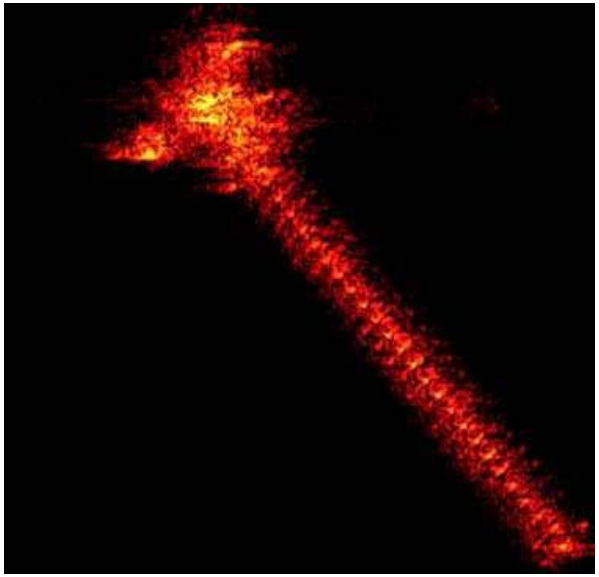

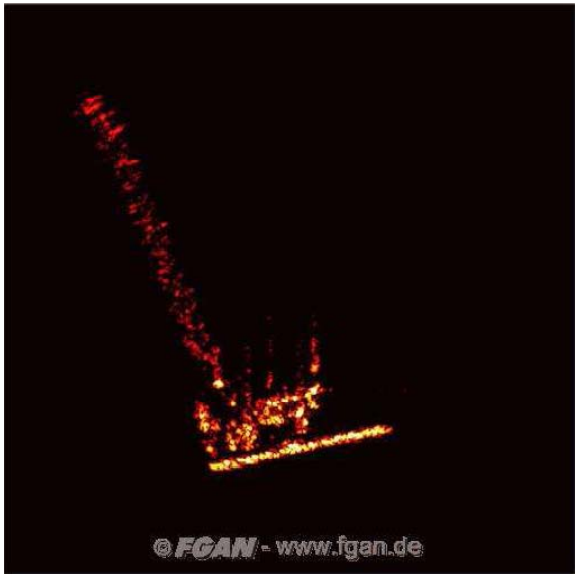

DSTO - INGARA

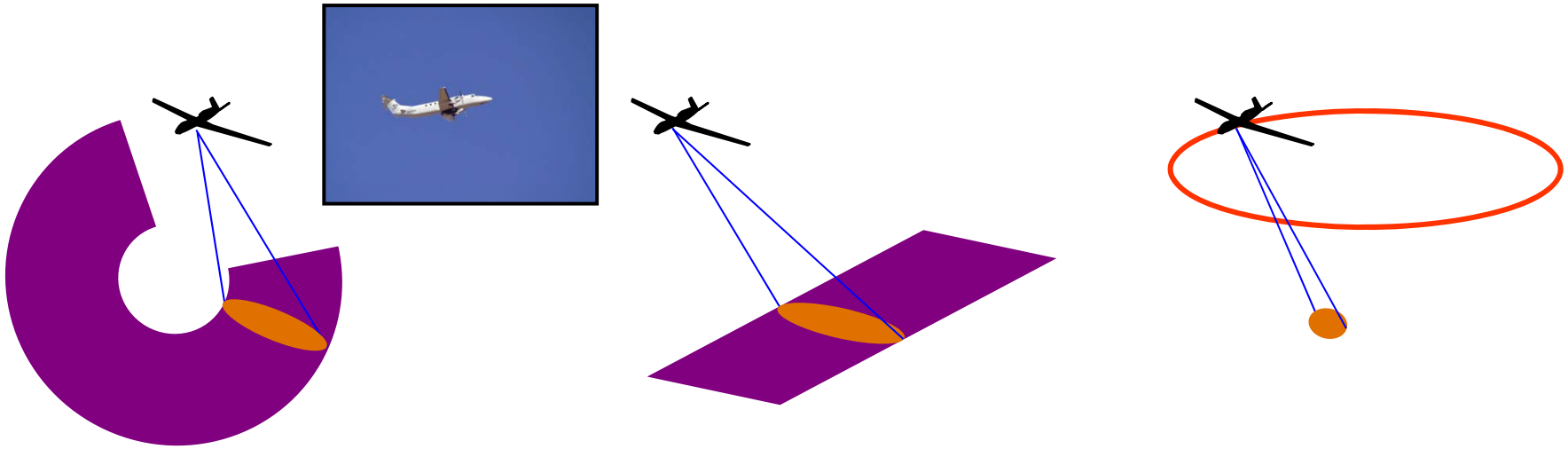

SCAN MODES	
GMTI	>5 km/hr MDV, 6 km swath
Maritime	2 m @ 12 km swath
	12 m @ 48 km swath

STRIP MODES	
SAR	2 m res, 12 km swath
	4 m res, 24 km swath
	8 m res, 48 km swath
Full-Pol SAR	
	4 m x 1.33 m res,
	< 8 km swath

SPOT MODES	
SAR	0.3 m res, 1 km spot
ISAR	0.3 m res, 1 km spot
Full-Pol SAR-ISAR	
	0.3 m res, 0.5 km spot
	1.0 m res, 1.5 km spot

Radar Parameters	
Frequency	9.8-10.4 GHz
Incidence Angles	$45^o \rightarrow 89^o$
Scan Angles	up to 240^o
2 Receive Channels	

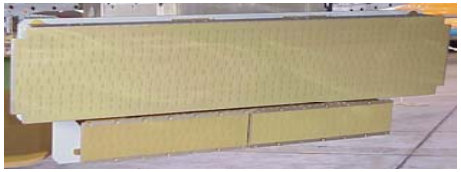

ATI Antenna

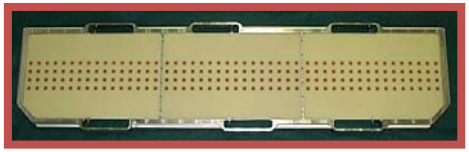

Dual Pol Antenna

ISAR SIGNAL MODELING

M. Martorella - University of Pisa

SIGNAL MODELLING

Transmitted signal (base band representation)

$$s_T(t) = \sum_{k=1}^{N} s(t - kT_R)$$

$A(t)$ = Amplitude Modulation

$$s(t) = A(t)\exp\left[j\vartheta(t)\right]$$

$\vartheta(t)$ = Phase Modulation

The *k*-th transmitted pulse

$$s_T(t,k) = s(t - kT_R) \Leftrightarrow S_T(f,k) = S(f)\exp(-j2\pi kfT_R)$$

Amplitude and/or phase modulations are needed in order to obtain wide-band signals and therefore high range resolution

Phase Modulations are preferred because they do not need linear power amplifiers.

SIGNAL MODELLING

Received signal (base band representation)

Assumption: the target is composed of ideal independent scatterers

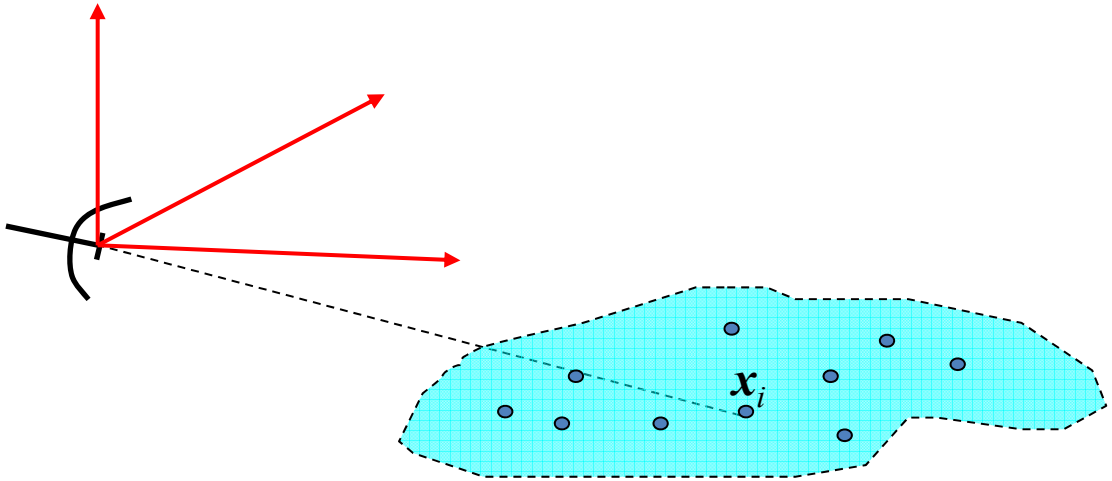

$$s_R(t,k) = \sum_{i=1}^{M} a_i s\left(t - kT_R - \tau_i\right)$$

M = Number of scattering centres

$$a_i = \alpha_i e^{j\psi_i}$$

$$\tau_i = \frac{2R(t,\boldsymbol{x}_i)}{c}$$

$$S_R(f,k) = S(f)\sum_{i=1}^{M} a_i \exp\left[-j2\pi\left(kfT_R + \frac{2R(t,\boldsymbol{x}_i)}{c}\right)\right]$$

SIGNAL MODELLING

Continuous target

In real scenarios the target must be represented by means of a continuous function in the spatial domain. Such a function is called *target reflectivity*.

$$\sum_{i=1}^{M} a_i \delta(\boldsymbol{x}_i) \longrightarrow \xi(\boldsymbol{x}) \quad where \quad \xi(\boldsymbol{x}) \neq 0 \quad when \quad \boldsymbol{x} \in \boldsymbol{V}$$

$\boldsymbol{V} =$ volume where the target is defined

For continuous targets, the received signal can be rewritten in this form:

$$S_R(f,k) = S(f) \int \xi(\boldsymbol{x}) \exp\left[-j2\pi f \left(kT_R + \frac{2R(t,\boldsymbol{x})}{c} \right) \right] d\boldsymbol{x}$$

And the phase associated with the radar-target distance:

$$\varphi(t,\boldsymbol{x}) = -2\pi f \frac{2R(t,\boldsymbol{x})}{c}$$

SIGNAL MODELLING

Straight iso-range approximation

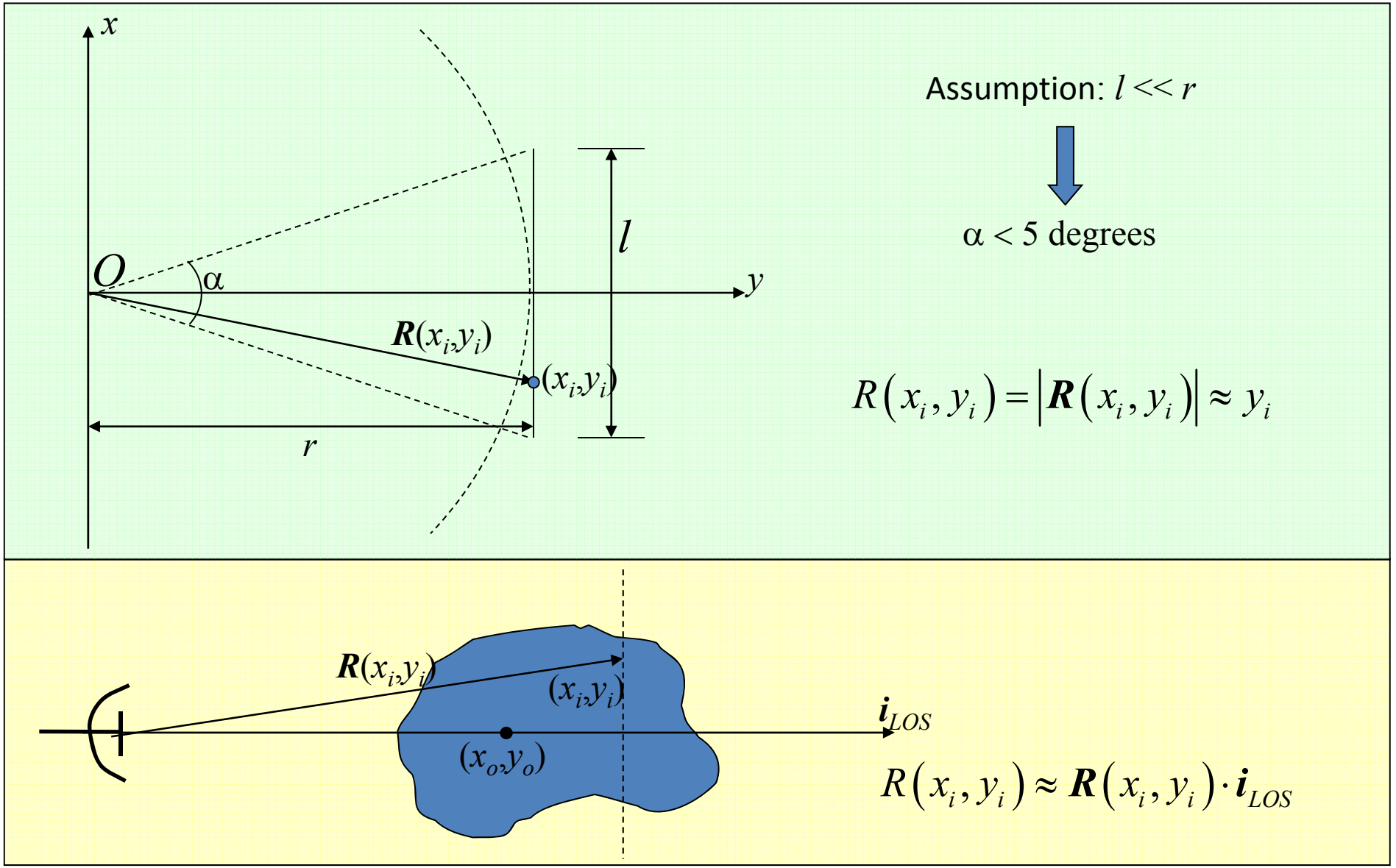

SIGNAL MODELLING

Static model

Reference system embedded on the target

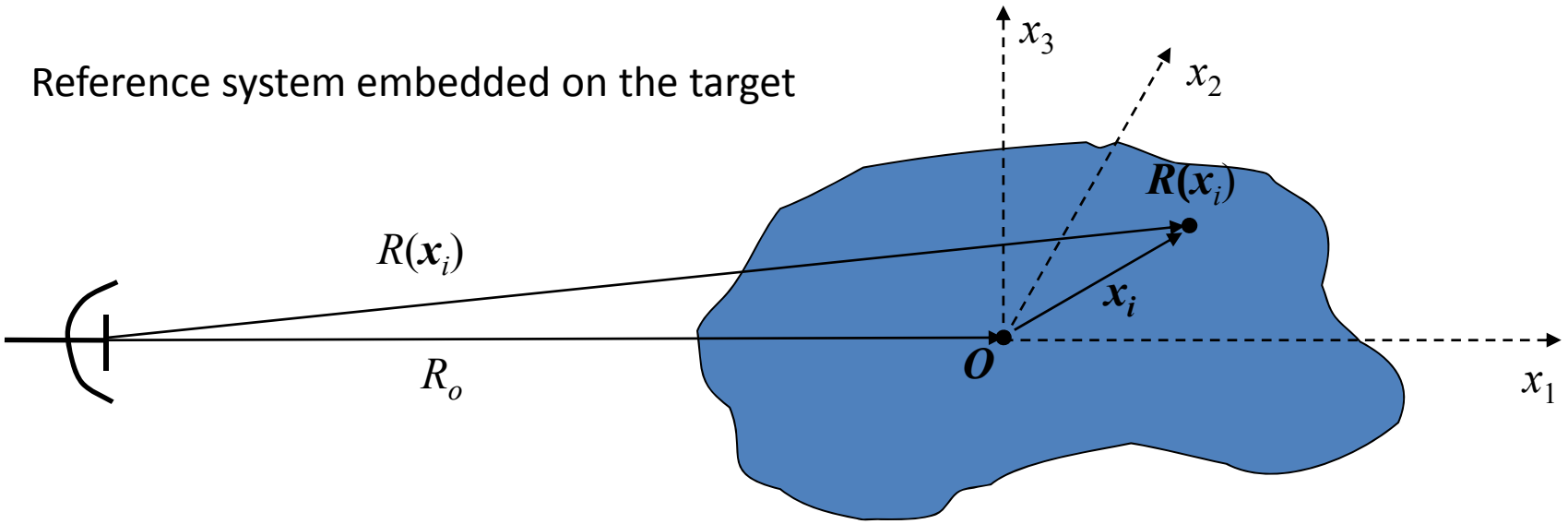

The distance between the radar and a generic target scatterer can be represented as follows:

$$R(x_i) \cong \boldsymbol{R}(x_i) \cdot \boldsymbol{i}_{LOS} \cong R_O + \boldsymbol{x}_i \cdot \boldsymbol{i}_{LOS}$$

Therefore, the received signal at the *k*-th sweep is:

$$S_R(f,k) = S(f) \exp\left[-j2\pi\left(kfT_R + \frac{2R_o}{c}\right)\right] \sum_{i=1}^{M} a_i \exp\left(-j\frac{4\pi}{c}\boldsymbol{x}_i \cdot \boldsymbol{i}_{LOS}\right)$$

SIGNAL MODELLING

Dynamic model (pulsed radar)

When the platform moves along a given trajectory the aspect angle changes. Therefore the $\boldsymbol{i}_{LOS}$ changes as well.

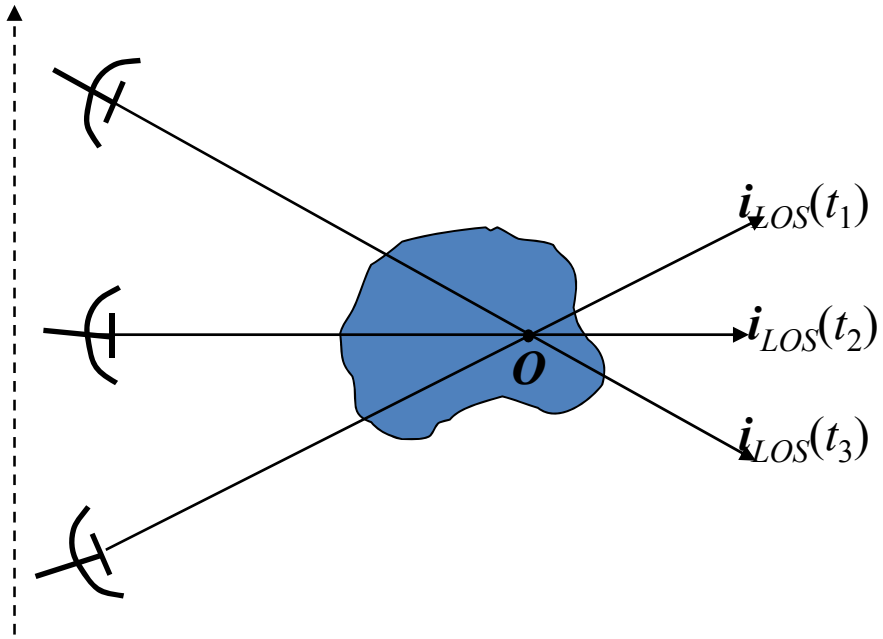

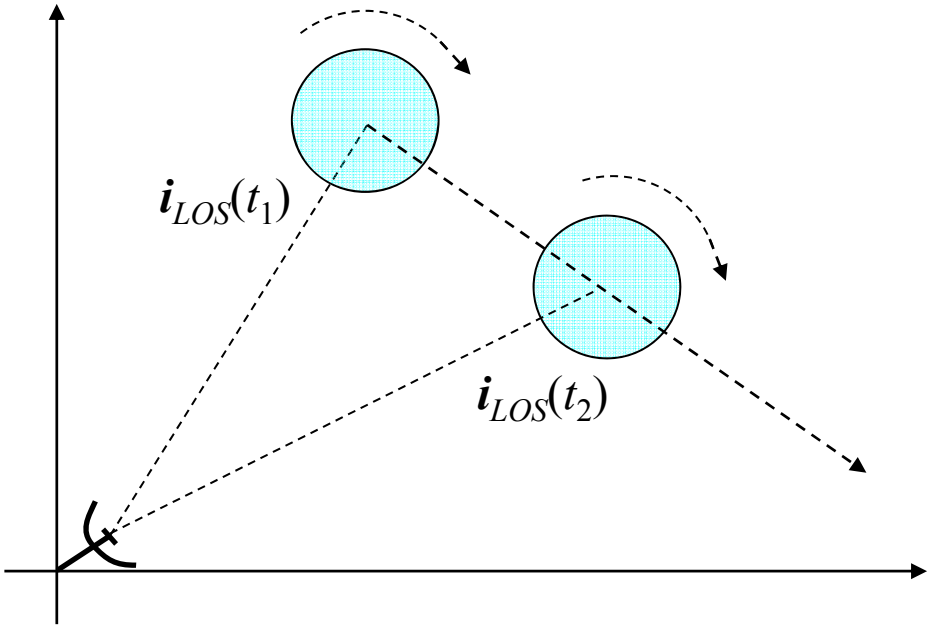

In the dynamic case the received signal at the k–th sweep is:

$$S_R(f,k) = S(f)\exp\left[-j2\pi f\left(kT_R + \frac{2R_O(kT_R)}{c}\right)\right]\sum_{i=1}^{M} a_i \exp\left(-j\frac{4\pi f}{c}\boldsymbol{x}\cdot\boldsymbol{i}_{LOS}(kT_R)\right)$$

REAL AND APPARENT TARGET ROTATION

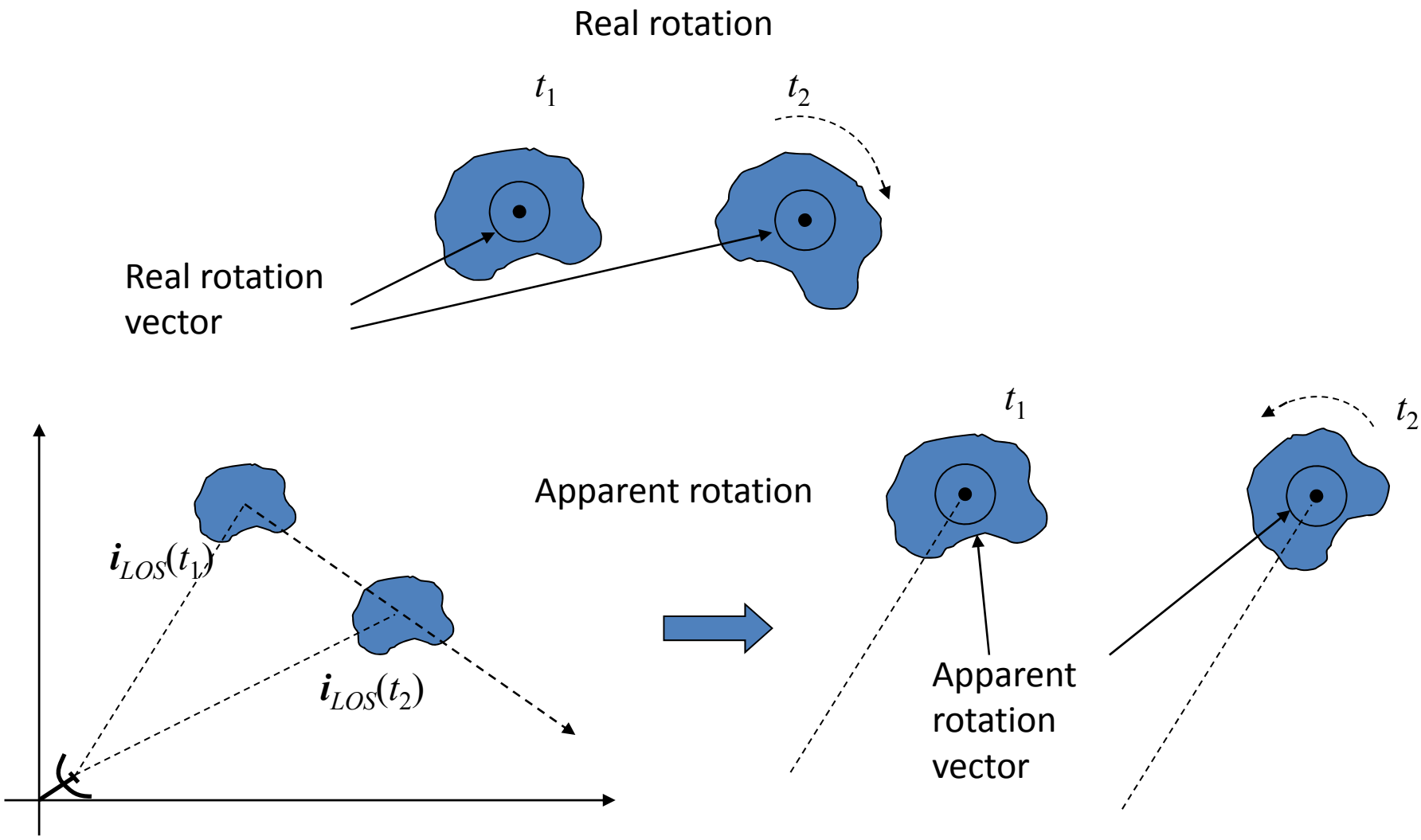

COORDINATE TRANSFORMATION

2D Problem

• The total rotation vector can be seen as a superposition (sum) of the apparent rotation vector and the target's own motion rotation vector

$$\Omega(kT_R) = \Omega_{ap}(kT_R) + \Omega_{tm}(kT_R)$$

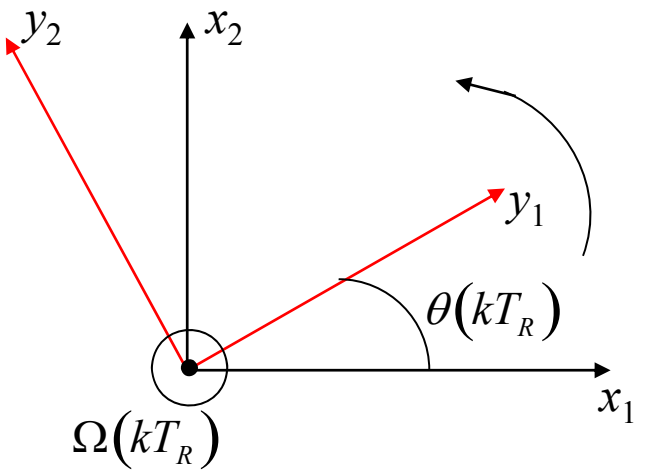

$T(x_1,x_2)$ Reference system embedded on the target

$T(y_1,y_2)$ Reference system centred on the Scene centre and rotating along with the LOS

COORDINATE TRANSFORMATION

2D Problem

Coordinate transformation:

$$\begin{bmatrix} y_1 \\ y_2 \end{bmatrix} = \begin{bmatrix} \cos\left[\theta\left(kT_R\right)\right] & -\sin\left[\theta\left(kT_R\right)\right] \\ \sin\left[\theta\left(kT_R\right)\right] & \cos\left[\theta\left(kT_R\right)\right] \end{bmatrix} \begin{bmatrix} x_1 \\ x_2 \end{bmatrix}$$

With respect to $\mathrm{T}(y_1,y_2)$ the radar-target LOS $\boldsymbol{i}_{LOS}(kT_R)$ is represented by coordinates (0,1). Therefore, by inverting the coordinate transformation, we obtain the coordinate of $\boldsymbol{i}_{LOS}(kTR)$ relative to the reference system $\mathrm{T}(x_1,x_2)$

$$\boldsymbol{i}_{LOS}^{(T(x_1,x_2))}\left(kT_R\right) = \begin{bmatrix} \sin\left[\theta\left(kT_R\right)\right] \\ \cos\left[\theta\left(kT_R\right)\right] \end{bmatrix}$$

SIGNAL MODELLING

Therefore, the received signal at the *k*–th sweep is:

$$S_R(f,k) = S(f)\exp\left[-j2\pi f\left(kT_R + \frac{2R_O(kT_R)}{c}\right)\right]$$
$$\cdot\sum_{i=1}^{M} a_i \exp\left\{-j\frac{4\pi f}{c}\left[x_1(i)\sin\left[\theta(kT_R)\right] + x_2(i)\right]\cos\left[\theta(kT_R)\right]\right\}$$

Where $\left(x_1(i), x_2(i)\right)$ are the coordinates of the *i*-th scatterer.

Let the transformation Ψ be defined as

$$\Psi:\begin{cases} X_1 = \dfrac{2f}{c}\sin\left[\theta(kT_R)\right] \\ X_2 = \dfrac{2f}{c}\cos\left[\theta(kT_R)\right] \end{cases}$$

Therefore, the received signal…

$$S_R(f,k) = S(f)\exp\left[-j2\pi f\left(kT_R + \frac{2R_O(kT_R)}{c}\right)\right]\sum_{i=1}^{M} a_i \exp\left\{-j2\pi\left[X_1x_1(i) + X_2x_2(i)\right]\right\}$$

Received Signal Interpretation

In order to give an interpretation of the received signal we will consider the continuous time and continuous target version of the signal model

$$S_R(f,t) = S(f,t)\exp\left[-j2\pi f\left(t+\frac{2R_O(t)}{c}\right)\right]\iint \xi(x_1,x_2)\exp\left\{-j2\pi\left[X_1x_1+X_2x_2\right]\right\}dx_1\,dx_2$$

Known

Phase term associated with the focusing pont

2D-FT of the target distributed reflectivity

If the last term could be extracted from the received signal, it would be possible to obtain the reflectivity function of the target, i.e. we would be able to obtain a radar image that is equivalent to the reflectivity of the target.

Such a result is ideal!!!

Received Signal Interpretation

Comments

- The knowledge of the reflectivity function FT is only limited to a region of the FT domain

$$\zeta(X_1, X_2) = \int\int \xi(x_1, x_2) \exp\left\{-j2\pi\left[X_1 x_1 + X_2 x_2\right]\right\} dx_1\, dx_2 \qquad (X_1, X_2) \in D$$

Such a constraint limits the resolution of the radar imaging system

- The target reflectivity function is defined in a 3D space whereas the image is defined in a 2D space.

$$\xi(x_1, x_2) = G\left[\xi'(x_1, x_2, x_3)\right]$$

G represents a function that maps the 3D reflectivity function onto the image plane

ISAR IMAGE FORMATION

IMAGE RECONSTRUCTION

$$S_R(f,t) = S(f,t)\exp\left[-j2\pi f\left(t+\frac{2R_O(t)}{c}\right)\right]\iint \xi(x_1,x_2)\exp\left\{-j2\pi\left[X_1x_1+X_2x_2\right]\right\}dx_1\,dx_2$$

1 2 3

Steps

1. Deconvolution

$$S'_R(f,t) = S^{-1}(f,t)\exp(-j2\pi ft)S_R(f,t)$$

$$= \exp\left[-j\frac{4\pi fR_O(t)}{c}\right]\iint \xi(x_1,x_2)\exp\left\{-j2\pi\left[X_1x_1+X_2x_2\right]\right\}dx_1\,dx_2$$

2. Motion Compensation

$$S''_R(f,t) = \exp\left[j\frac{4\pi fR_O(t)}{c}\right]S'_R(f,t)$$

$$= \iint \xi(x_1,x_2)\exp\left\{-j2\pi\left[X_1x_1+X_2x_2\right]\right\}dx_1\,dx_2$$

3. 2D Inverse Fourier Transform

$$I_C(\tau,\nu) = 2D-IFT\left\{S''_R(f,t)\right\}$$

IMAGE RECONSTRUCTION

Functional Block Scheme Interpretation

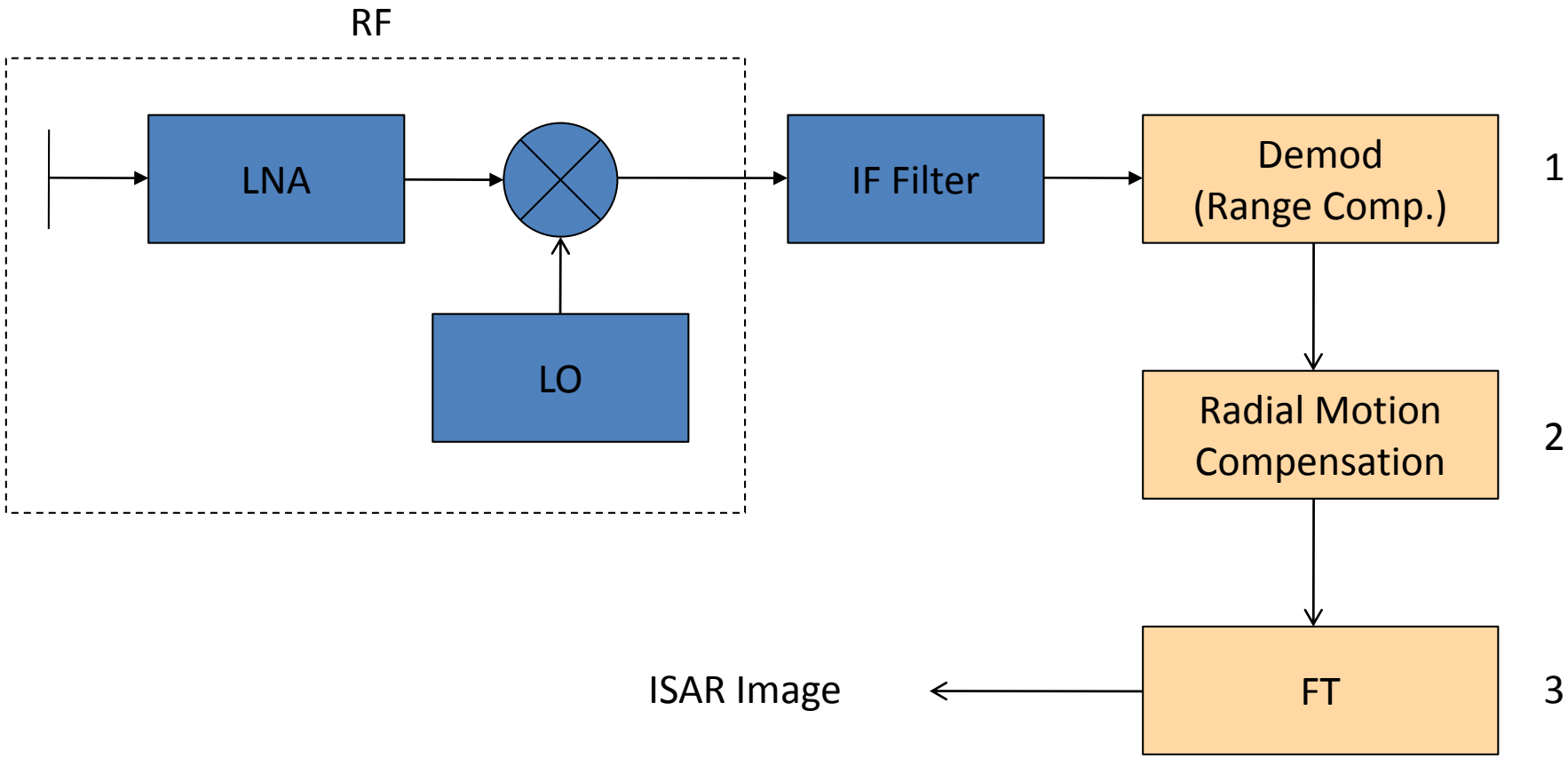

MOTION COMPENSATION

• The operation of Motion Compensation requires the knowledge or the estimation of the quantity $R_o(t)$.

• In SAR systems the geometry is generally known and therefore the operation of motion compensation is not too critical.
Example: for a linear trajectory, the distance between the radar and the scene centre can be written as:

$$R_o(t) = \sqrt{r^2 + \left(u(t) - x_o\right)^2}$$

Where x_o is the azimuth coordinate

Nevertheless GPS measurement errors and platform fluctuations must be compensated.

• In ISAR system the geoetry is generally not known. Therefore, a blind motion compensation must be performed.

Autofocusing techniques

IMAGE FORMATION

Signal after deconvolution and motion compensation

$$S_R''(f,t) = \int\int \xi(x_1, x_2) \exp\left\{-j2\pi\left[X_1 x_1 + X_2 x_2\right]\right\} dx_1 dx_2$$

Fourier domain:

$$\Psi_{(t,f)\to(X_1,X_2)} : \begin{cases} X_1 = \dfrac{2f}{c}\sin\left[\theta(t)\right] \\ X_2 = \dfrac{2f}{c}\cos\left[\theta(t)\right] \end{cases}$$

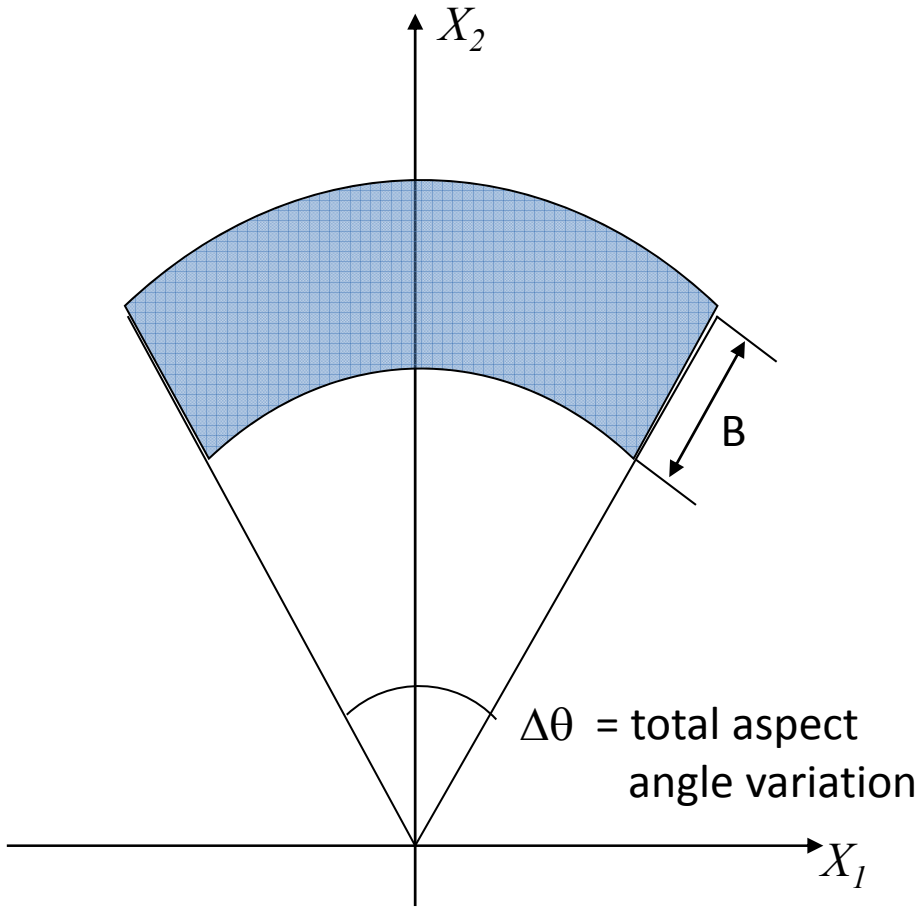

The knowledge of the target reflectiviy in the Fourier domain is limited by the:

- total aspect angle variation $\Delta\theta$
- transmitted signal bandwidth B

IMAGE FORMATION

The deconvoluted and compensated signal can be rewritten as follows:

$$S_R''(f,t) = \iint_D \xi(x_1,x_2)\exp\left\{-j2\pi\left[X_1x_1 + X_2x_2\right]\right\} dx_1dx_2 =$$

$$= W(X_1,X_2)\int_{-\infty}^{\infty}\int_{-\infty}^{\infty} \xi(x_1,x_2)\exp\left\{-j2\pi\left[X_1x_1 + X_2x_2\right]\right\} dx_1dx_2$$

Therefore, the complex image that we obtain by means of a 2D-IFT is a filtered version of the reflectivity:

$$I_C(x_1,x_2) = \xi(x_1,x_2) \otimes\otimes w(x_1,x_2)$$

where

$$w(x_1,x_2) = 2D - IFT\left[W(X_1,X_2)\right]$$

is called Point Spread Function (PSF).

IMAGE FORMATION

Point Spread Function

The point Spread Function is an indicator of the system performance, because it determines the system resolution.

$$W(X_1, X_2) = \begin{cases} 1 & when \quad (X_1, X_2) \in D \\ 0 & otherwise \end{cases}$$

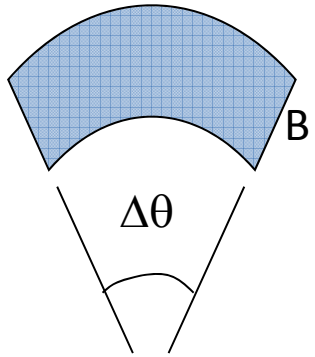

Because of a simple property of the Fourier Transform, the larger the domain *D* , the narrower the PSF, and therefore, the better the resolution.

Being the domain *D* related to the parameters B and $\Delta\theta$ by means of Ψ, it is clear that the larger the signal bandiwith and the total aspect angle variation, the better the resolution.

This is the reason why high resolution systems need large bandwidths and large synthetic aperture, in order to generate a large variation of the aspect angle.

IMAGE FORMATION

From continuous to discrete

•Almost all the signals employed in modern systems for radar imaging are discrete signals.

• By referring to our signal model, frequency and time are discrete and hence the received signal samples are mapped onto the Fourier domain on a grid.

• For each aspect angle (radar sweep) one sample is collected for each transmitted frequency. Therefore, the signal samples are mapped on a polar grid. The samples are generally not evenly spaced because the rotation vector is not constant.

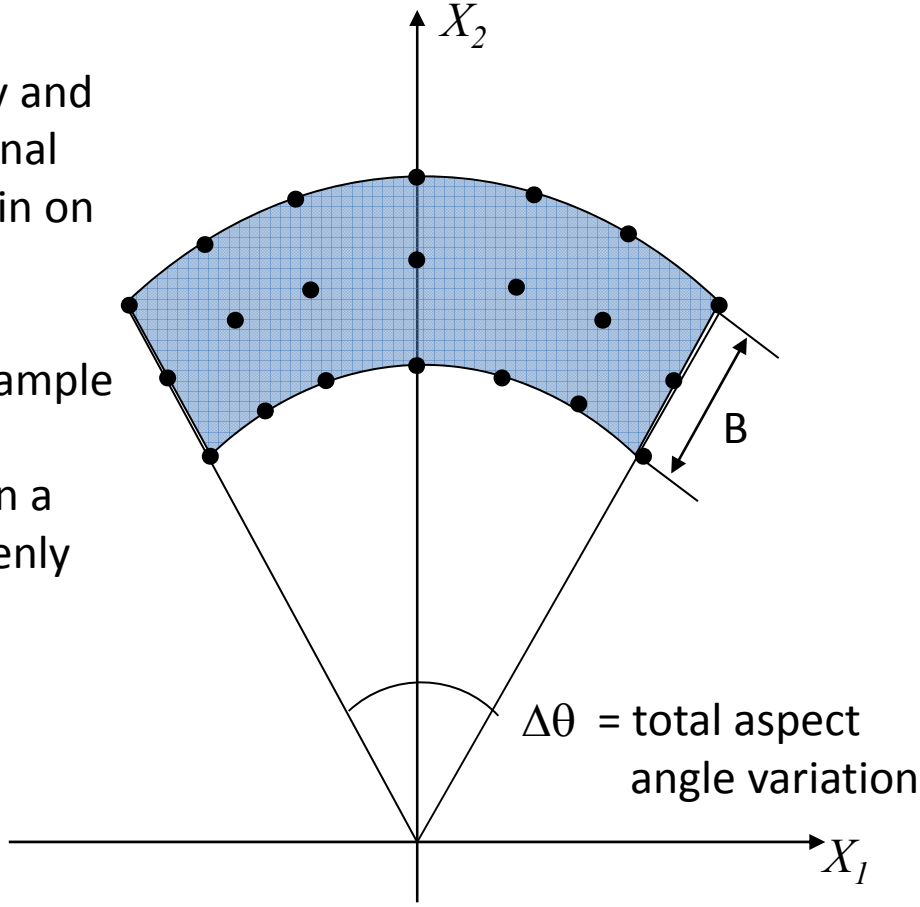

IMAGE FORMATION

Numerical problem

• The calculation of the 2D-IFT on a generic domain is too expensive in terms of **computational load**. In fact, any calculation of the Fourier Transform is expensive, unless a Fast Fourier Transform (**FFT**) technique can be applied.

• The conditions that guarantee a succesful calculation of the FT by means of a FFT are:

- **evenly spaced samples**
- **rectangular grid**

• The grid of the signal samples in the Fourier Domain is **not rectangular** and moreover is generally **not evenly spaced**.

• Several solutions to this problem have been proposed. The main solutions are:

- **Range-Doppler** (directly iplementable)
- **Polar Reformatting** (requires the knowledge of the effective rotation vector, directly applicable in turn-table experiments)
- **Backprojection** (requires the knowledge of the effective rotation vector, directly applicable in turn-table experiments)

RANGE-DOPPLER

RANGE DOPPLER

The Range-Doppler (RD) technique can be applied when:

• the total aspect angle variation is small enough (< 5 degrees). In such a condition the domain W can be approximated by means of a rectangle.

• the grid is evenly spaced. This is achieved when the rotation vector is constant (for short observation time this is true).

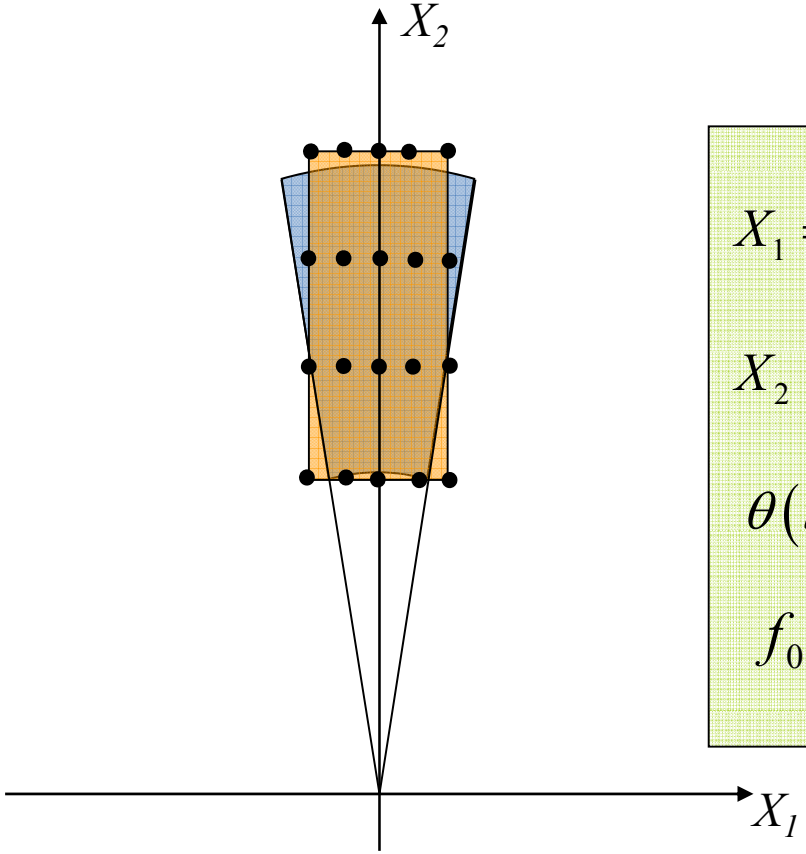

$$X_1 = \frac{2f}{c}\sin\left[\theta(t)\right] \approx \frac{2f}{c}\theta(t) = \frac{2f\Omega t}{c} \approx \frac{2f_0\Omega t}{c}$$

$$X_2 = \frac{2f}{c}\cos\left[\theta(t)\right] \approx \frac{2f}{c}$$

$$\theta(t) = \Omega t \quad |t| \le \frac{T_{obs}}{2}$$

f_0 Central frequency

ISAR Signal Processing

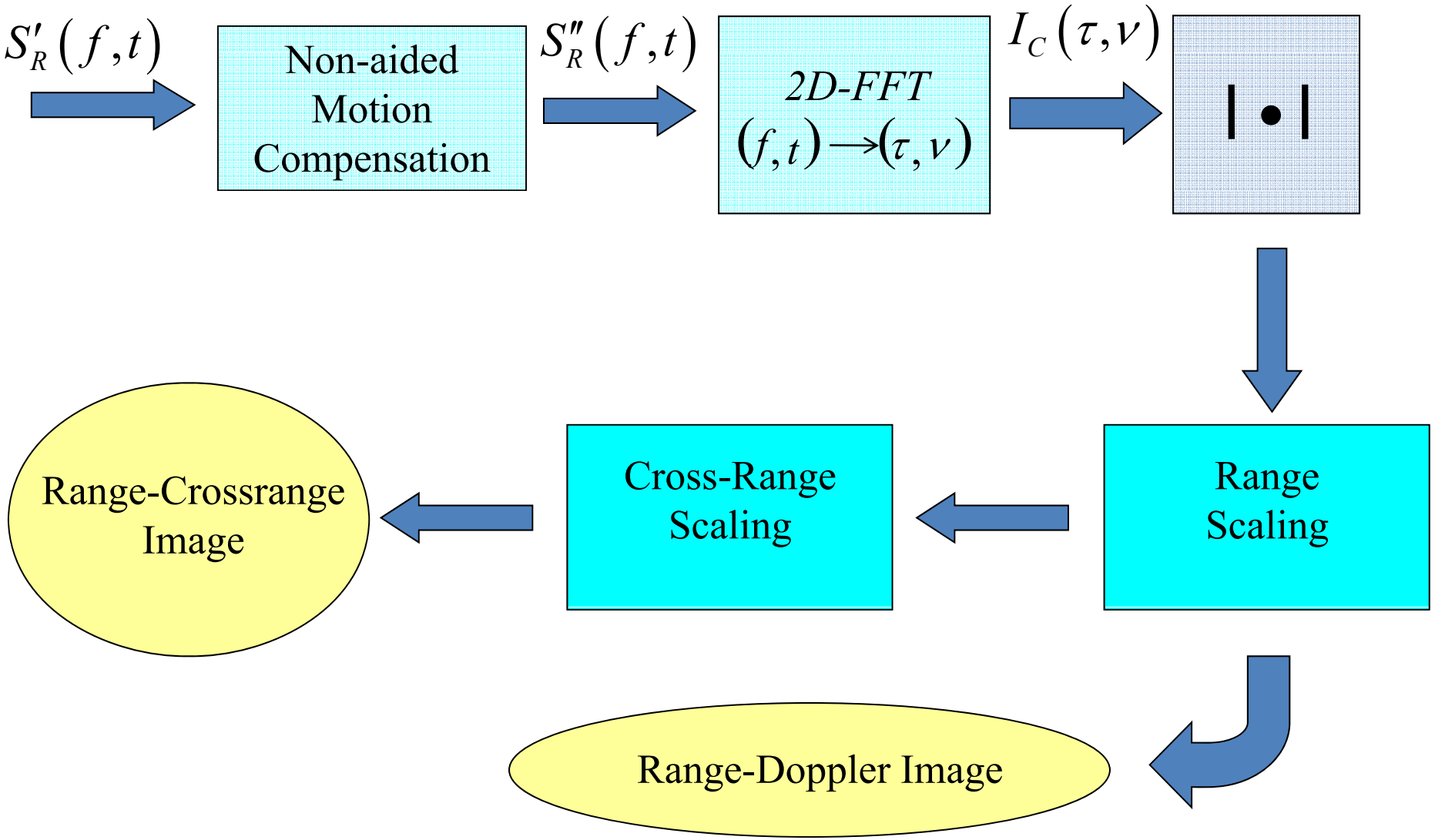

POLAR REFORMATTING

POLAR REFORMATTING

• The aim of the use of Spotlight SAR is to achieve high resolution, therefore the total aspect angle variation is usually larger than 5 degrees.

• The Range Doppler technique is not applicable because the assumptions on which it is based are not satisfied.

•The numerical computation is still the main problem whenever a 2D DFT has to be calculated on given domain.

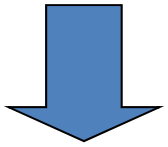

Polar Reformatting

• The polar domain is first transformed into a rectangular domain

• The DFT can be performed by means of a FFT

POLAR REFORMATTING

Transformation from polar grid to regularly spaced rectangular grid

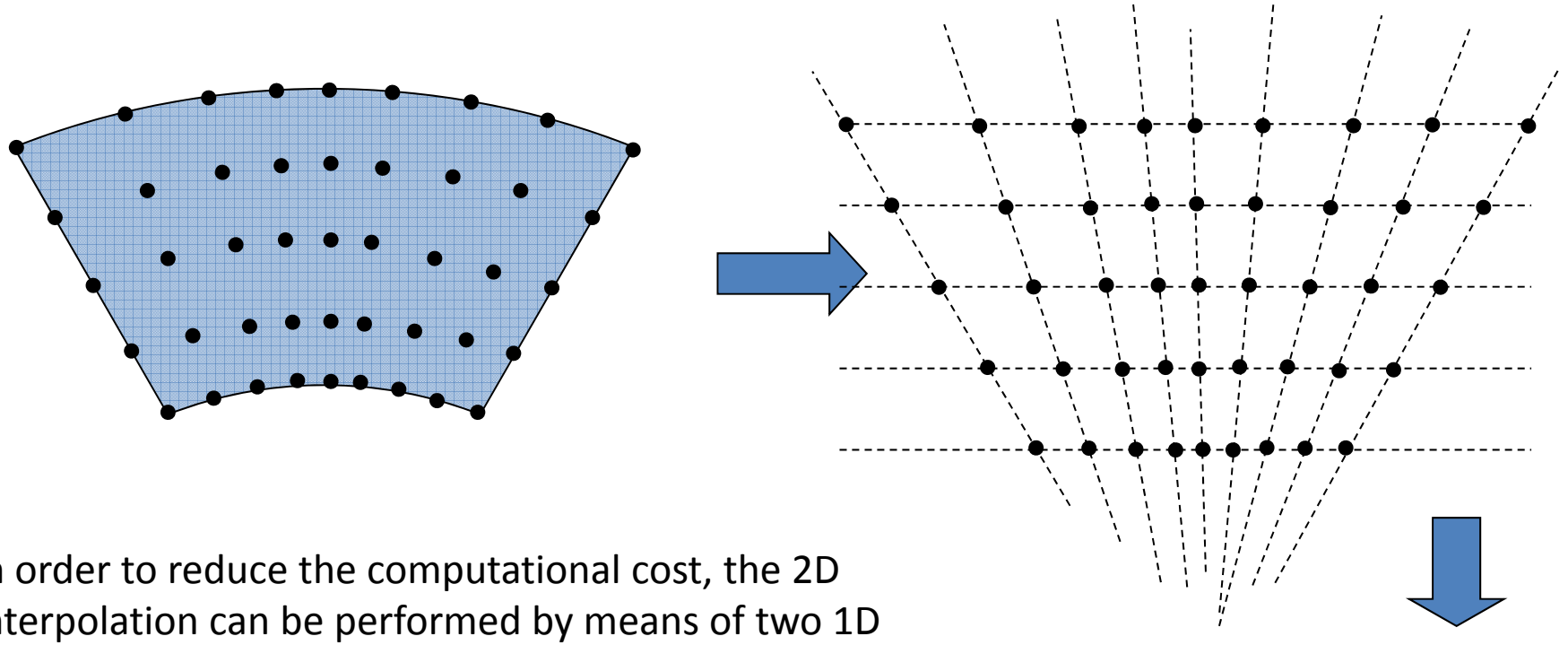

In order to reduce the computational cost, the 2D interpolation can be performed by means of two 1D interpolations (keystone):

- the first interpolation is performed along the coordinate f
- the second interpolation is performed along the coordinate X

BACK-PROJECTION

TOMOGRAPHIC APPROACH

• The derivation of the theory for SAR image formation can also be obtained by means of a tomographic approach.

• Computer Tomography (CT) was first formally suggested by
G. N. Hounsfield in 1972 and found direct application in medical imaging.

• The need to reveal small amounts of abnormal tissues in the middle of healthy tissue drove the scientist towards the development of CT.

• The analytical formulation of the medical problem and the reconstruction of the SAR image are formally identical. Therefore, the application of the CT to the problem of reconstructing SAR images is straightforward.

• In the case of rectilinear trajectory of the platform, the 3D scenario can be simply derived from the 2D scenario.

TARGET PROJECTION

2D CASE:

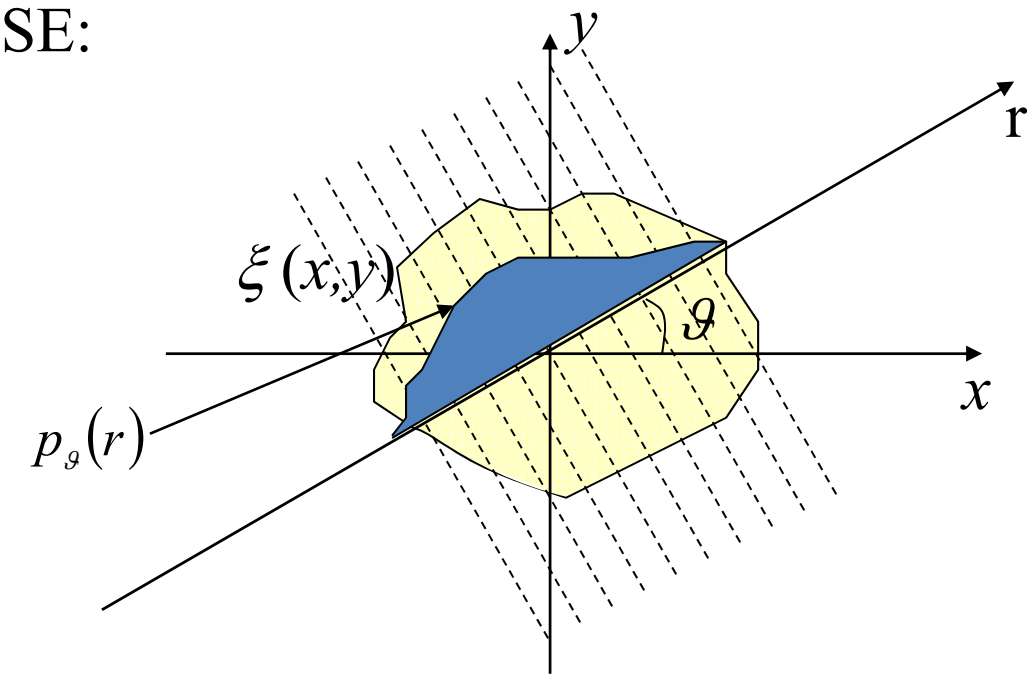

Given a function $\xi(x,y)$ and a value of the orientation angle ϑ

the function projection along the angle ϑ can be defined as:

$$p_\vartheta(r) = \iint f(x,y)\,\delta(x\cos\vartheta + y\,\mathrm{sen}\,\vartheta - r)\,dx\,dy$$

TARGET PROJECTION

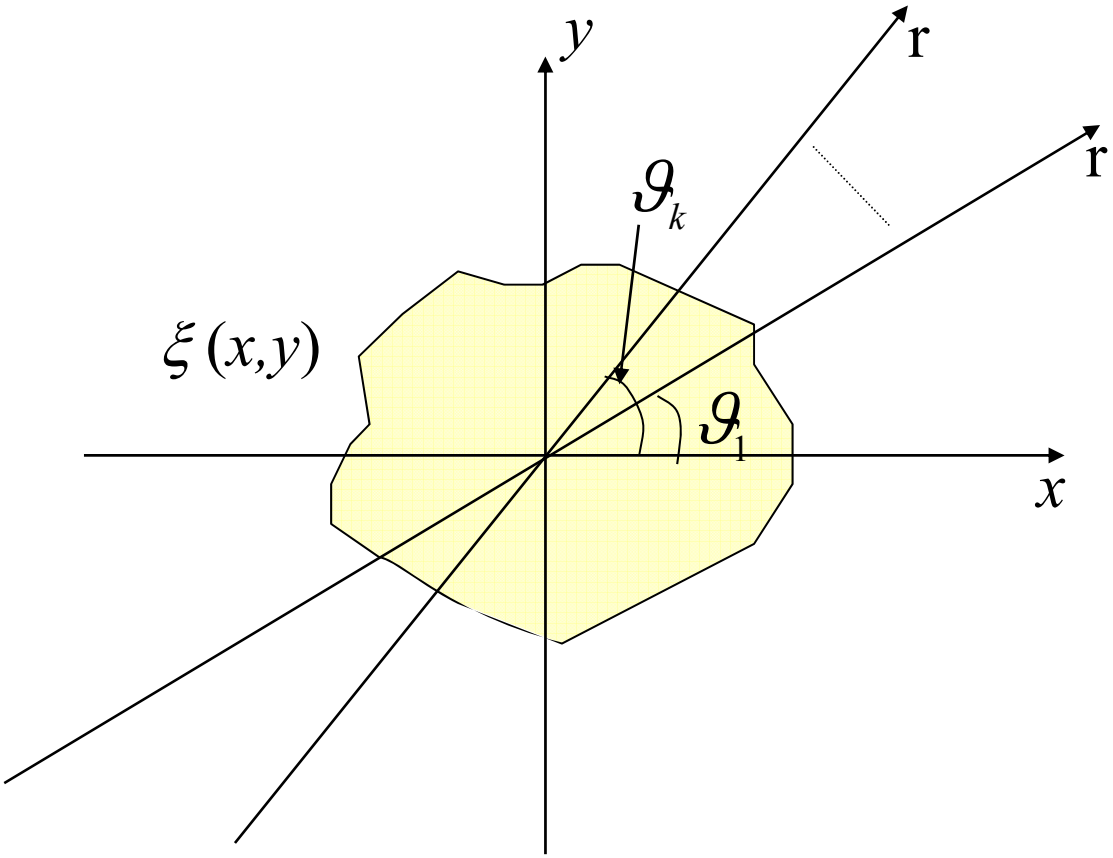

$$p_{\vartheta_1}(r) = \iint f(x,y)\,\delta(x\cos\vartheta_1 + y\,\mathrm{sen}\,\vartheta_1 - r)\,dx\,dy$$

$$p_{\vartheta_k}(r) = \iint f(x,y)\,\delta(x\cos\vartheta_k + y\,\mathrm{sen}\,\vartheta_k - r)\,dx\,dy$$

k target projections, relative to k different aspect angles, are collected.

PROJECTION-SLICE THEOREM

Fourier Transform of a projection

$$P_\vartheta(R) = \int_{-\infty}^{+\infty} p_\vartheta(r)\, e^{-j2\pi rR}\, dr = \int_r \int_x \int_y \xi(x,y)\, \delta(x\cos\vartheta + y\,\mathrm{sen}\,\vartheta - r)\, dx\, dy\, e^{-j2\pi rR}\, dr =$$

$$= \int_x \int_y \xi(x,y)\quad e^{-j2\pi(x\cos\vartheta + y\,\mathrm{sen})R}\quad dx\, dy = \Theta(X,Y)\Big|_{\substack{X=R\cos\vartheta \\ Y=R\,\mathrm{sen}\,\vartheta}}$$

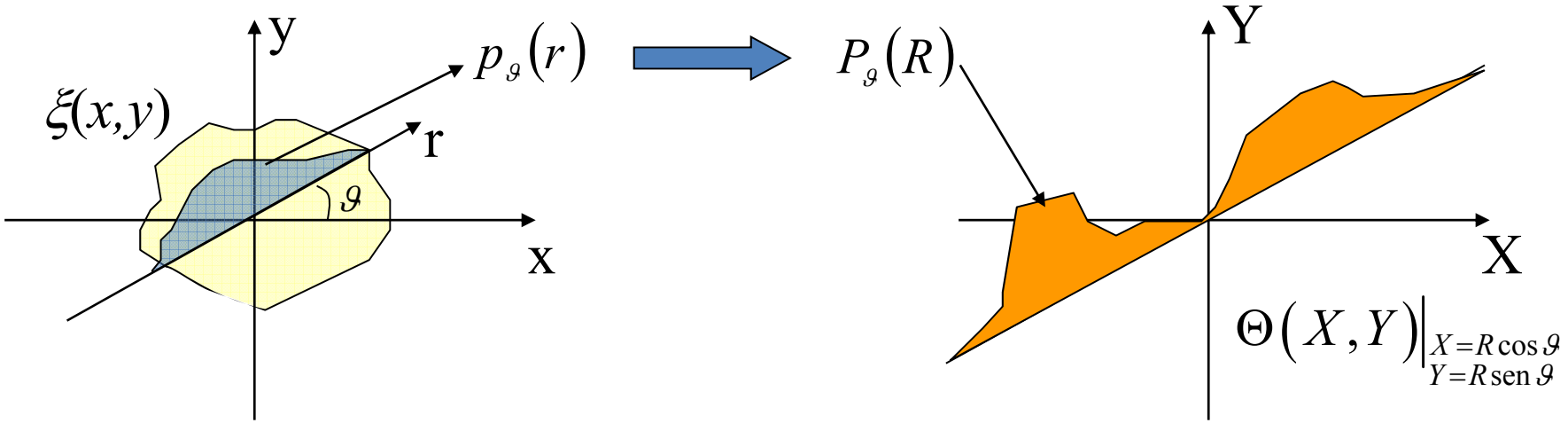

FOURIER DOMAIN

By Fourier transforming the N projections we obtain slices of the Fourier Transform of the target reflectevity function.

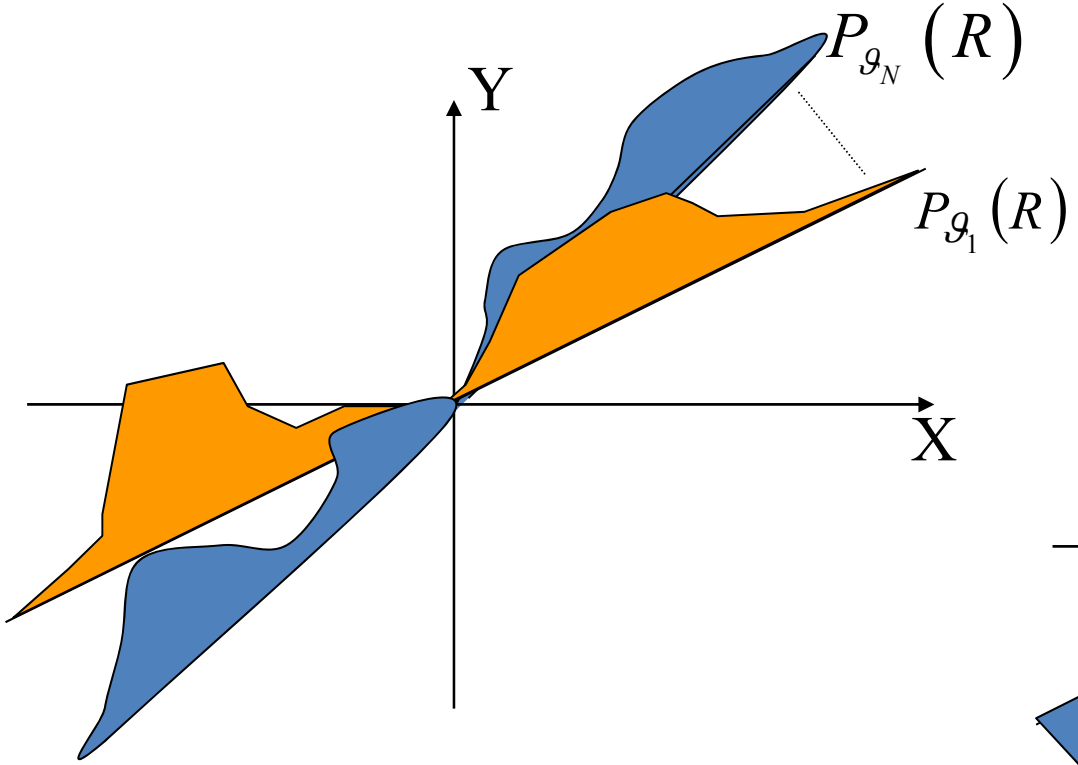

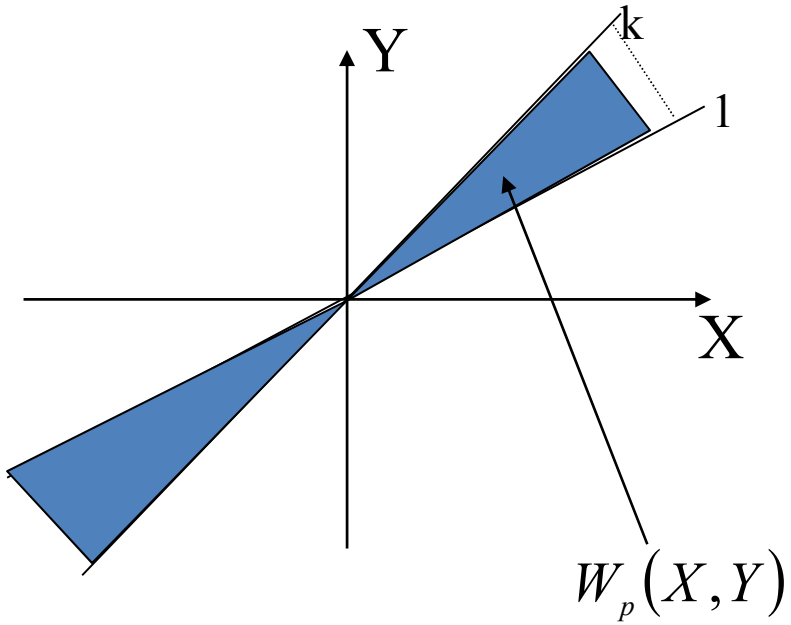

Fourier domain where the target reflectivity function is known

FOURIER PROPERTY

Relationships between the Fourier Transform and the cartesian to polar coordinate transformation.

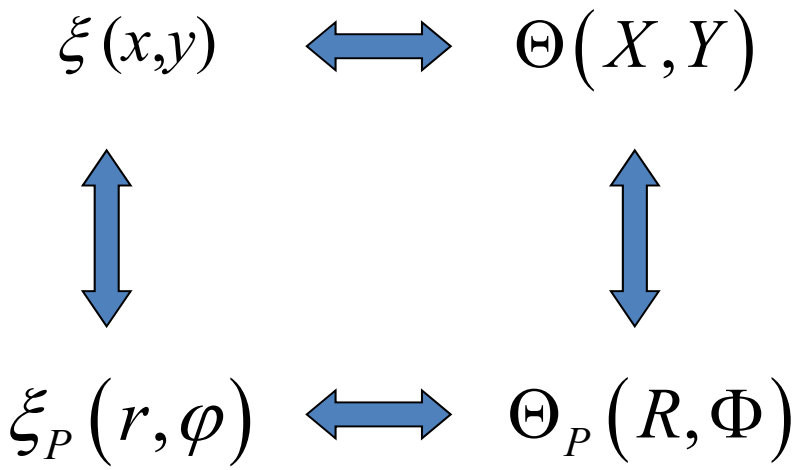

$$\xi(x,y) = \iint \Theta(X,Y) \quad e^{j2\pi(xX+yY)}\, dX\, dY$$

$$\Theta_P(R,\Phi)\big|_{\Phi=\vartheta} = P_\vartheta(R)$$

$$\xi_P(r,\varphi) = \iint \Theta_P(R,\Phi) \quad e^{j2\pi Rr\cos(\Phi-\varphi)}\, R\, dR\, d\Phi$$

$$\Theta_P(R,\Phi+\pi)\big|_{\Phi=\vartheta} = P_\vartheta(-R)$$

BACK-PROJECTION ALGORITHM

$$\xi(x,y) = \left.\xi_P(r,\varphi)\right|_{\substack{r=\sqrt{x^2+y^2} \\ \varphi=\text{arctg}\left(y/x\right)}} = \int_0^{+\infty}\int_0^{2\pi} R\,\Theta_P(R,\Phi)\; e^{j2\pi R(x\cos\Phi+y\,\text{sen}\,\Phi)}\,dR\,d\Phi$$

$$\xi(x,y) = \int_0^{\pi}\left[\int_{-\infty}^{+\infty} |R|\left\{P_\vartheta(R)\right\}_{\vartheta=\Phi} e^{j2\pi R(x\cos\Phi+y\,\text{sen}\,\Phi)}\,dR\right]d\Phi$$

Inverse Fourier Transform of a product of two functions wrt the variable R, calculated in the coordinate $x\cos\Phi + y\,\text{sen}\,\Phi$

$$\xi(x,y) = \int_0^{\pi}\left[FT^{-1}\left\{|R|\left\{P_\vartheta(R)\right\}_{\vartheta=\Phi}\right\}_{x\cos\Phi+y\,\text{sen}\,\Phi}\right]d\Phi$$

BACK-PROJECTION ALGORITHM

The product in the Fourier domain corresponds to the convolution in the spatial domain

$$g(x) = f(x) \otimes h(x) \quad \Longleftrightarrow \quad G(X) = F(X)H(X)$$

$$f(x) \otimes h(x) = g(x)$$

$$F(X) \cdot H(X) = G(X)$$

- $$FT^{-1}\left[\left\{P_{\vartheta}(R)\right\}_{\vartheta=\Phi}\right]_{x\cos\Phi + y\,\mathrm{sen}\,\Phi} = p_{\Phi}\left(x\cos\Phi + y\,\mathrm{sen}\,\Phi\right)$$
- $$FT^{-1}\left[|R|\right] = ? \quad \Longrightarrow \quad |R| = \frac{1}{j2\pi} j2\pi R\,\mathrm{sgn}(R)$$

BACK-PROJECTION ALGORITHM

- $FT^{-1}\left[\, j\,2\pi R \,\right] = \dfrac{d}{dr}$ ⟸ Derivative

- $FT^{-1}\left[\, \mathrm{sgn}\,(R) \,\right] = \mathrm{Hilbert}\,(r)$ ⟸ Hilbert's Transform

Let $q_{\vartheta=\Phi}\left(x\cos\Phi + y\,\mathrm{sen}\,\Phi\right)$ be the filtered projection

$$q_{\vartheta=\Phi}\left(x\cos\Phi + y\,\mathrm{sen}\,\Phi\right) = FT^{-1}\left\{\left|R\right|\left\{P_{\vartheta}\left(R\right)\right\}_{\vartheta=\Phi}\right\}_{x\cos\Phi+y\,\mathrm{sen}\,\Phi} =$$

$$= \frac{1}{j2\pi}\left\{\frac{d}{dr}\left[p_{\vartheta=\Phi}\left(r\right)\right]\otimes h\left(r\right)\right\}\Bigg|_{r=x\cos\Phi+y\,\mathrm{sen}\,\Phi} = \frac{1}{j2\pi}\left\{\frac{d}{dr}\left[p_{\vartheta=\Phi}\left(r\right)\otimes h\left(r\right)\right]\right\}\Bigg|_{r=x\cos\Phi+y\,\mathrm{sen}\,\Phi}$$

BACK-PROJECTION ALGORITHM

The reconstruction of the reflectivity function follows:

$$\xi(x,y) = \int_0^{\pi} q_{\vartheta=\Phi}\left(x\cos\Phi + y\,\mathrm{sen}\,\Phi\right) d\Phi$$

In practical scenarios, the number of projections is limited and therefore the integral must be substituted with a sum.

$$\hat{\xi}(x,y) = \sum_{i=1}^{N} q_{\vartheta_i}\left(x\cos\vartheta_i + y\,\mathrm{sen}\,\vartheta_i\right)$$

Where $\hat{\xi}(x,y)$ is the reconstructed reflectivity function, which represents an estimation of the actual function. N is the number of available projections.

BACK-PROJECTION ALGORITHM

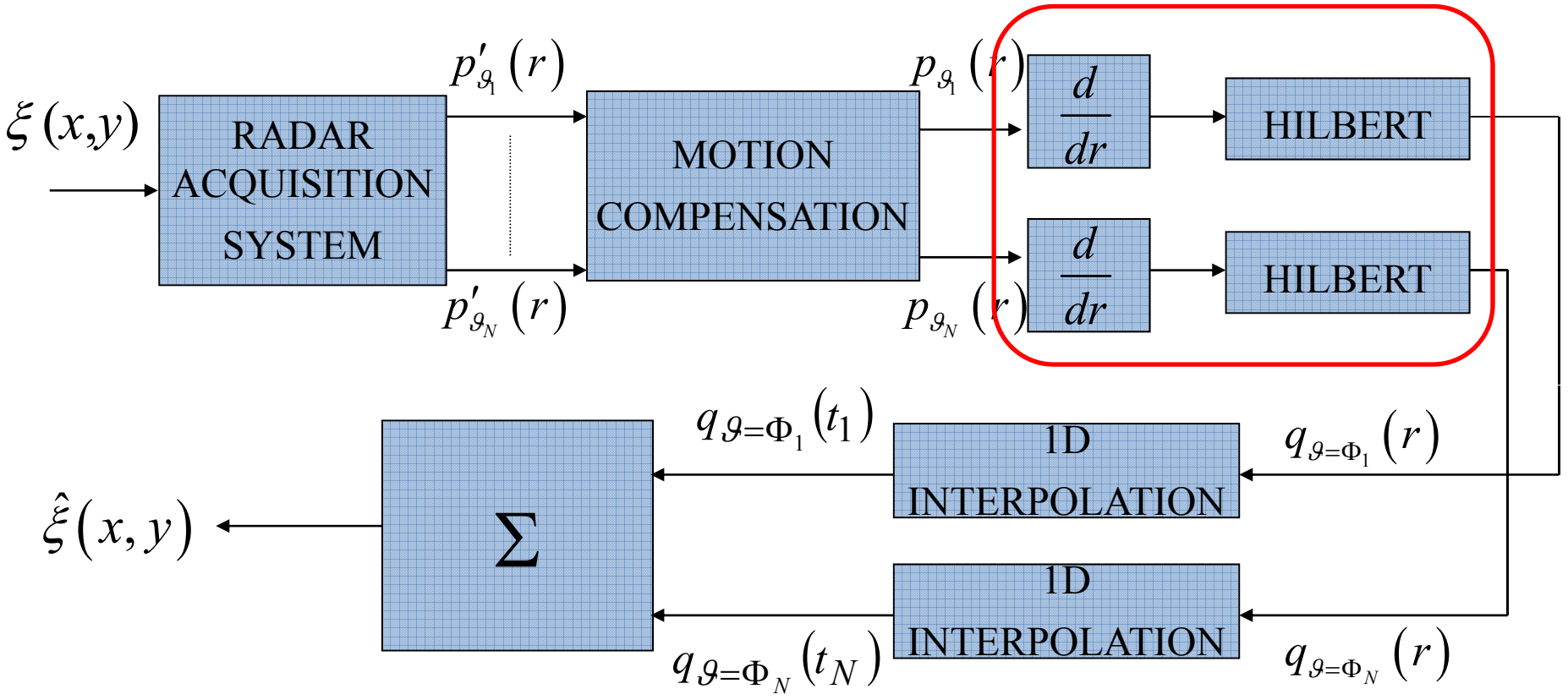

Interpolation: the value of r must be mapped onto values of t according to the cartesian grid given by the coordinates (x,y)

$$r \quad \Rightarrow \quad t_i = x\cos\Phi_i + y\sin\Phi_i$$

BACK-PROJECTION ALGORITHM

Frequency Approach

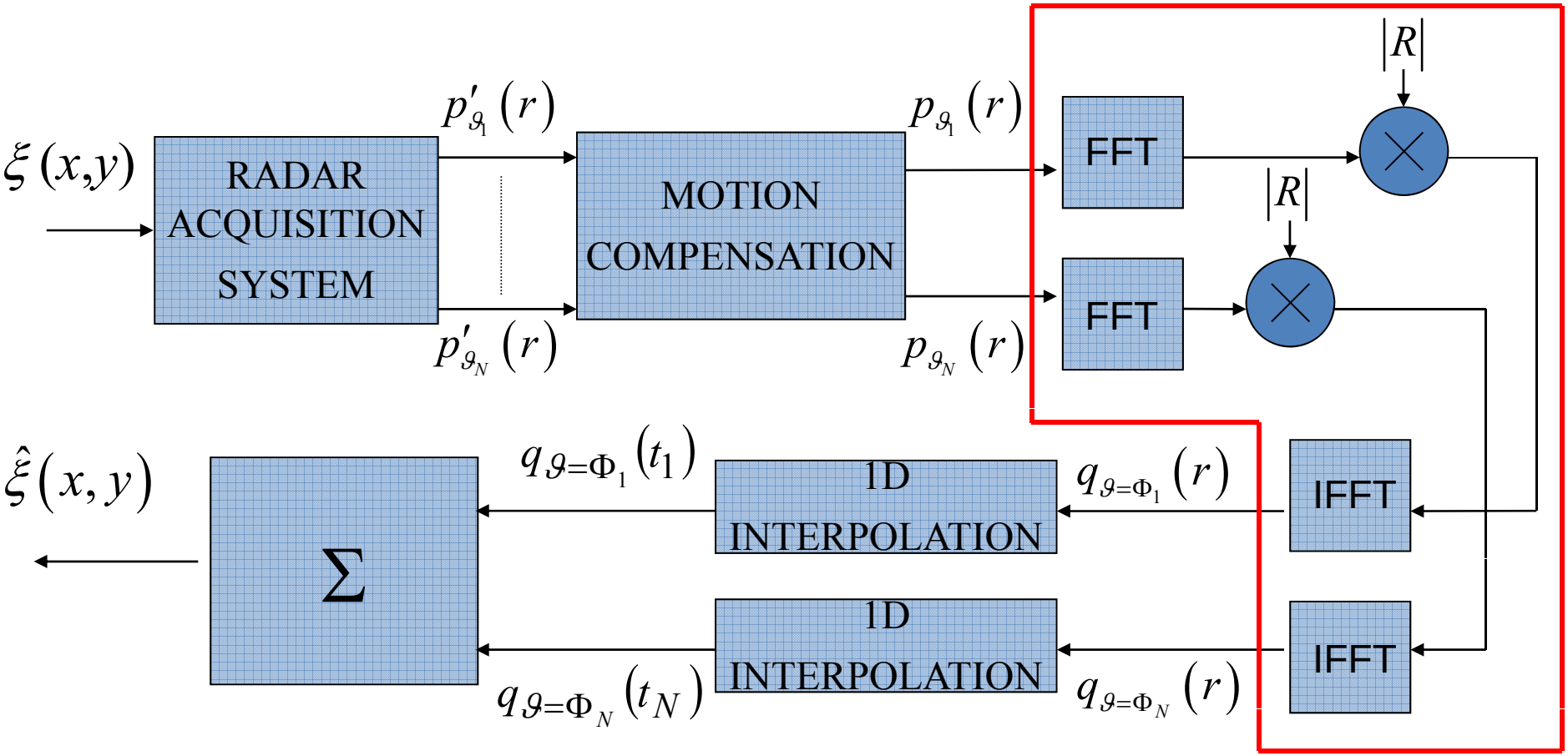

EXAMPLE

Set-up

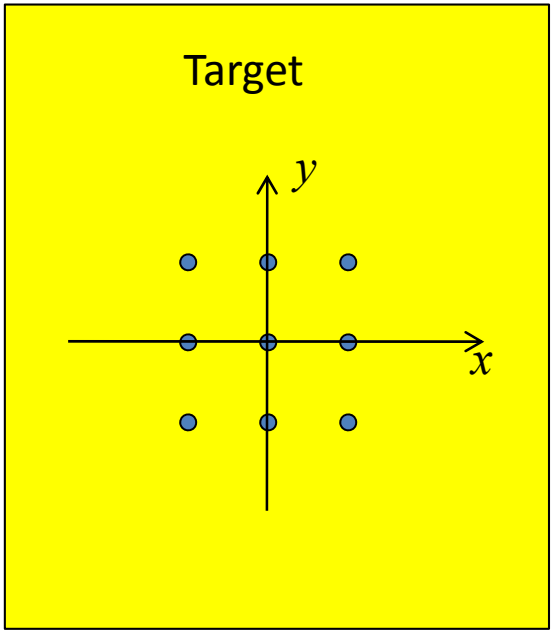

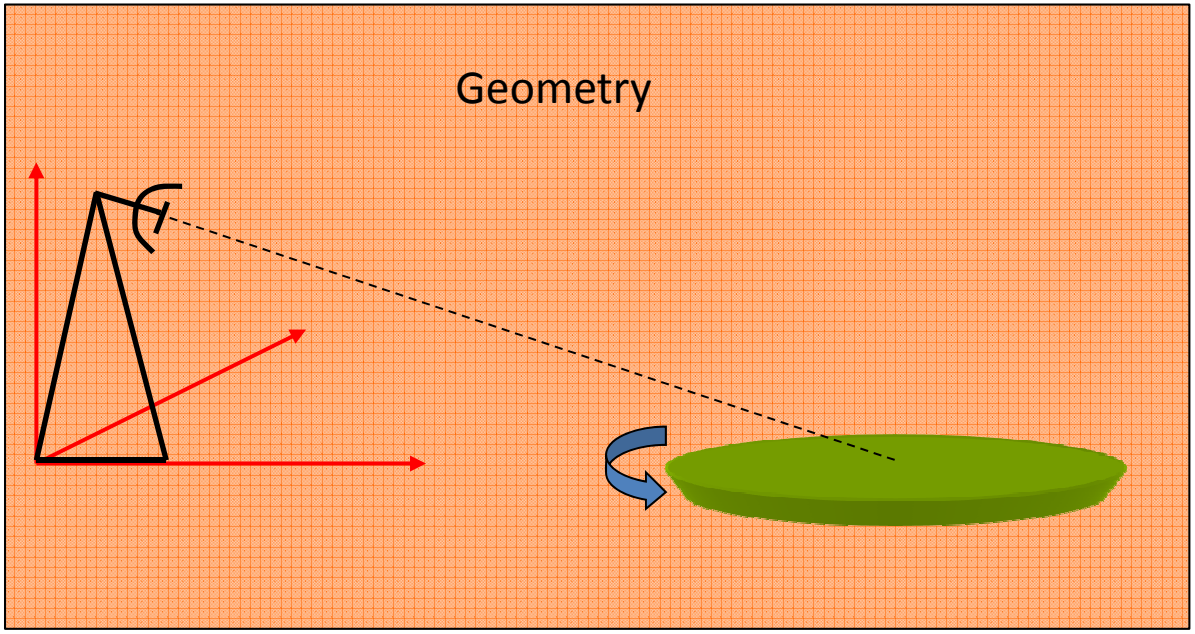

- Stepped frequency radar
- 48 view angles
- 32 tx frequencies

EXAMPLE

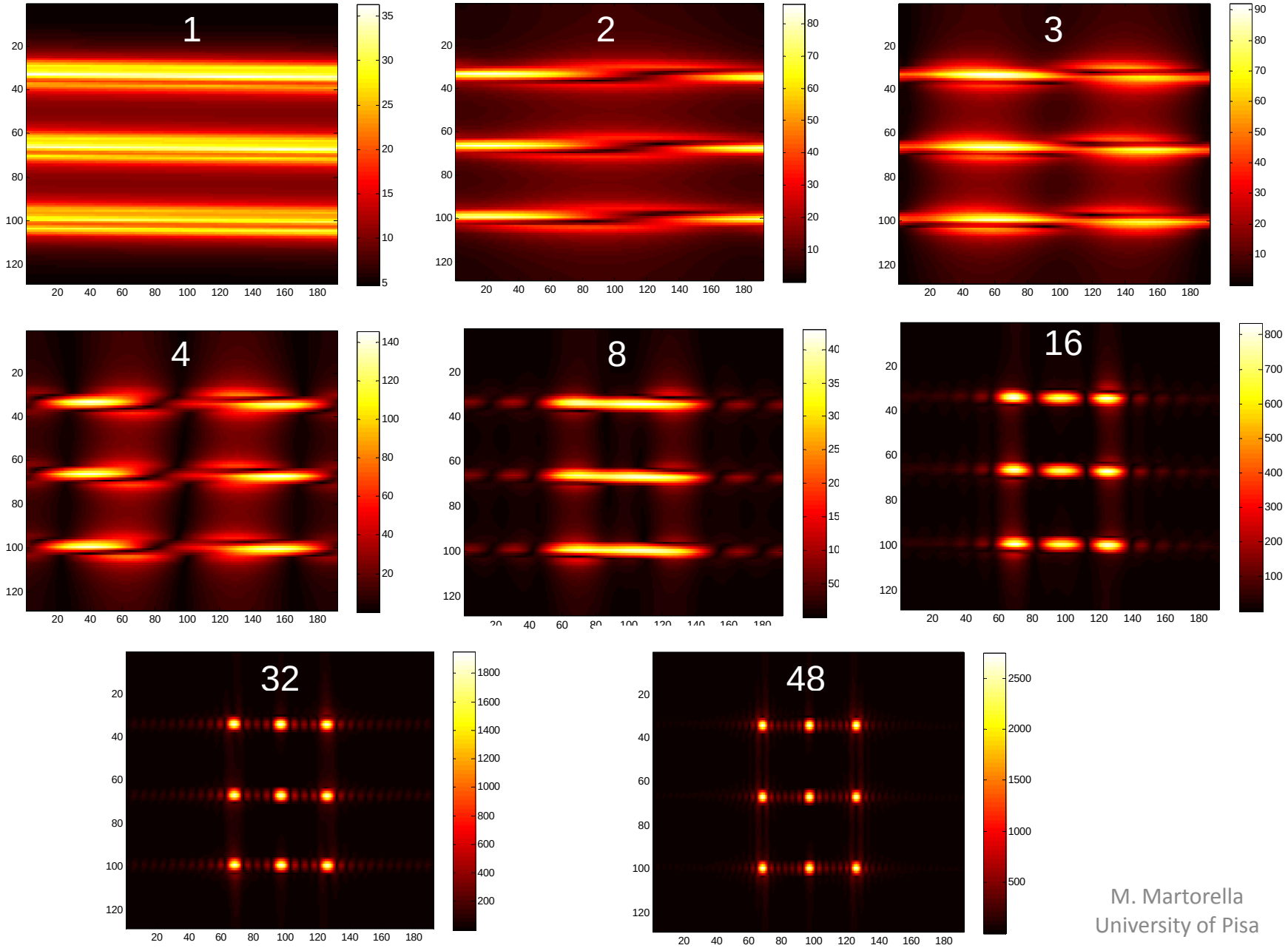

M. Martorella
University of Pisa

EXAMPLE

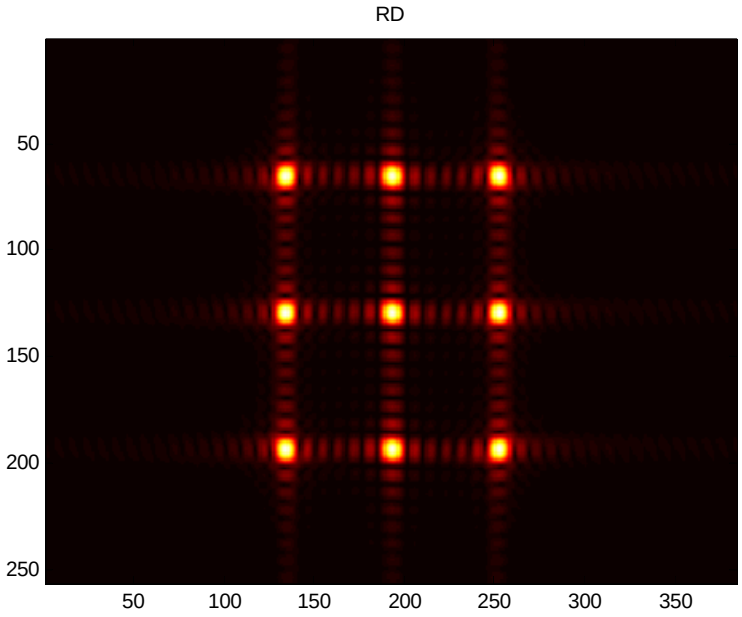
RD
50
100
150
200
250
50
100
150
200
250
300
350

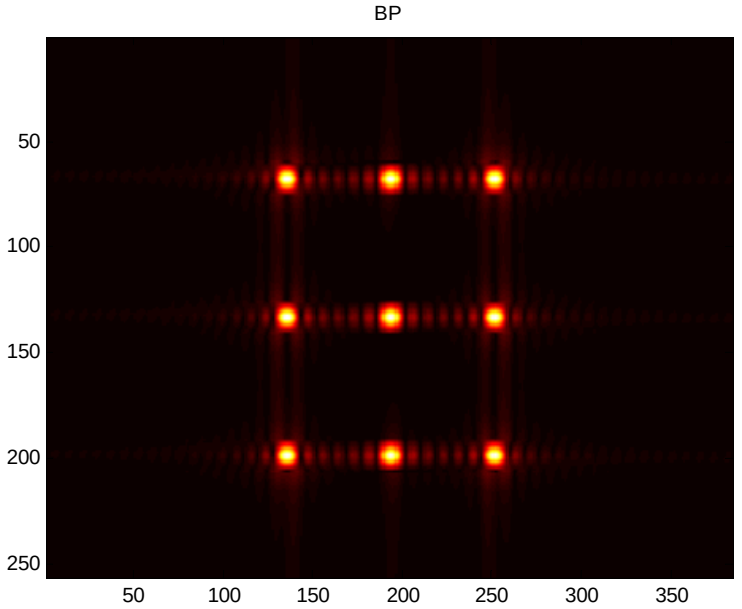
BP
50
100
150
200
250
50
100
150
200
250
300
350

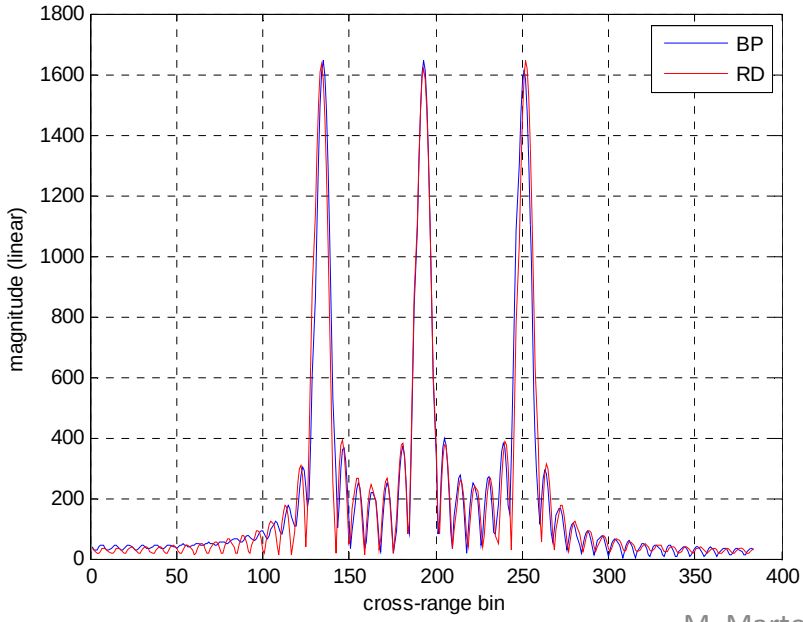
BP
RD
magnitude (linear)
cross-range bin
0
200
400
600
800
1000
1200
1400
1600
1800
0
50
100
150
200
250
300
350
400

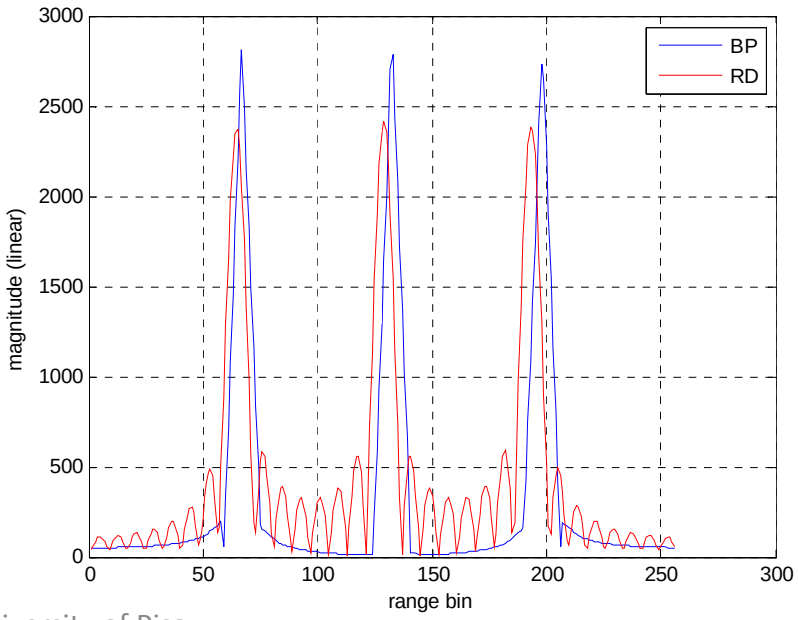
BP
RD
magnitude (linear)
range bin
0
500
1000
1500
2000
2500
3000
0
50
100
150
200
250
300

Turntable experiment

Set-up

Fully polarimetric radar

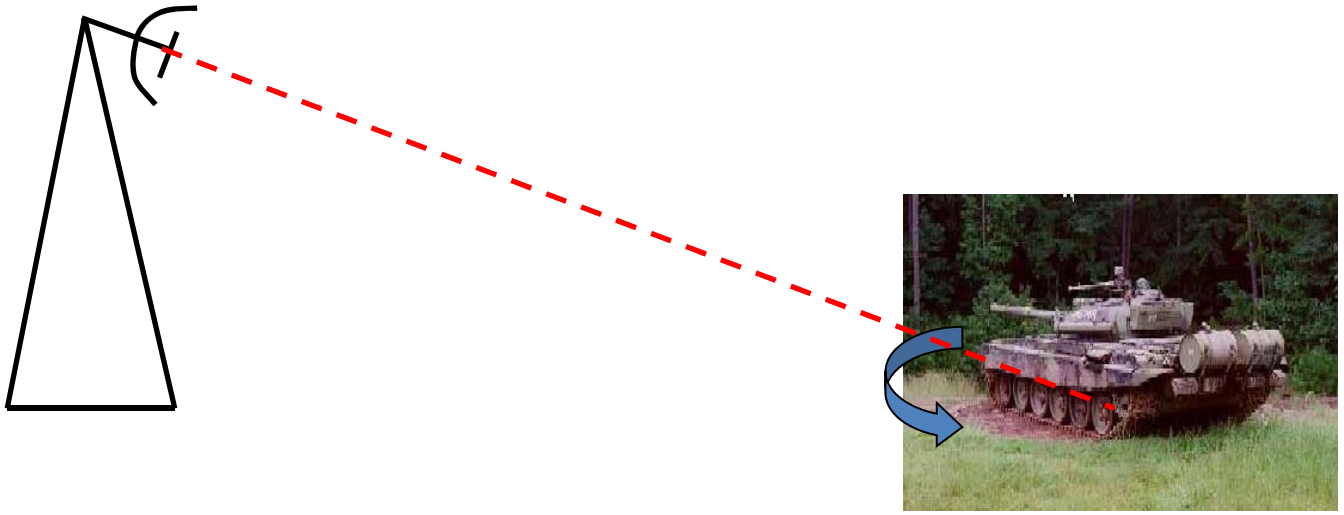

Turntable

Parameters	Value
f_0	9.6 GHz
frequency step	3 MHz
N° transmitted frequencies	221
azimuthal sampling rate	0.05°
N° sweeps	79
total aspect angle for each file	3.9°
range and cross range resolution	1 foot

No radial motion compensation is needed

Turntable experiment

Results

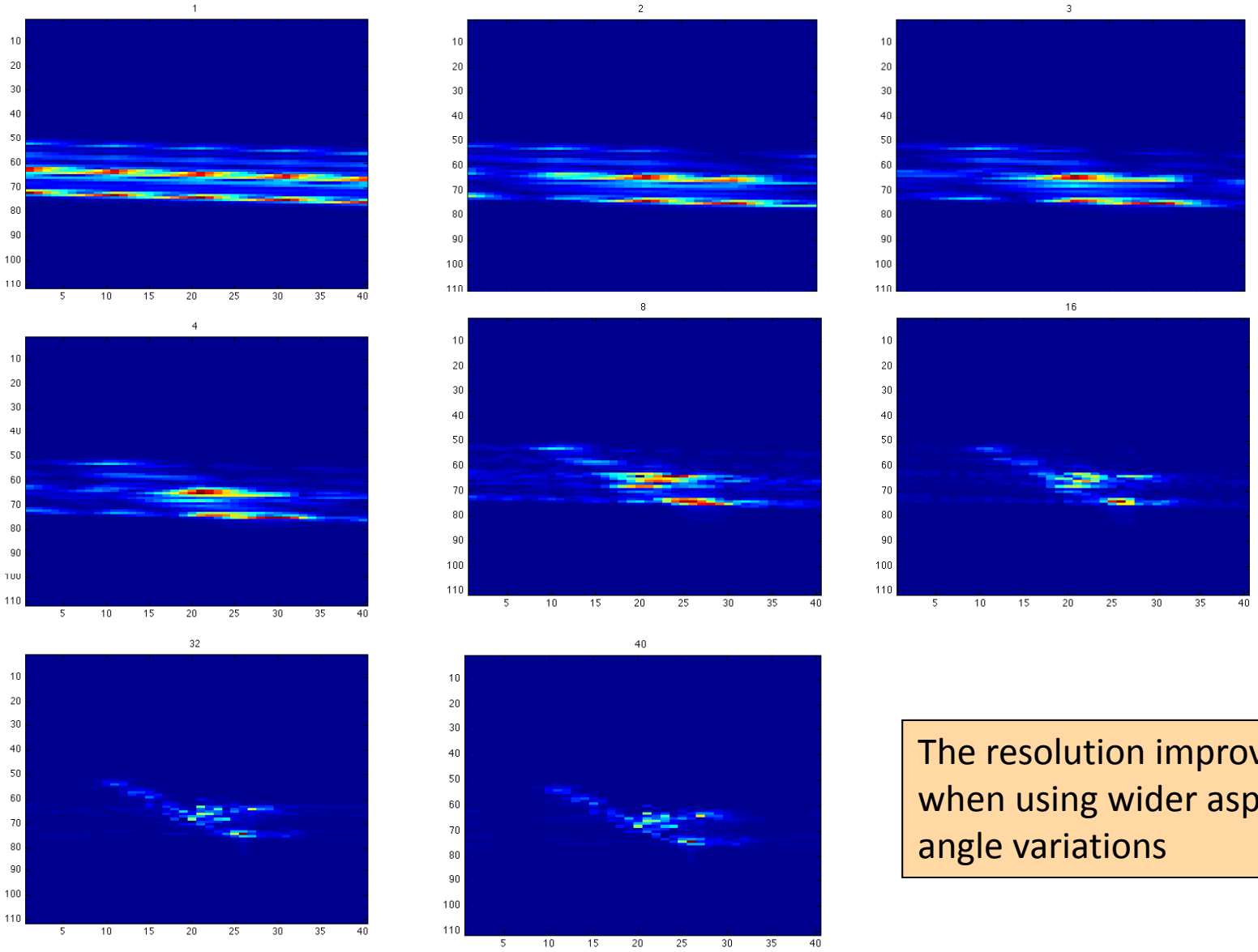

The resolution improves when using wider aspect angle variations

JOINT TIME-FREQUENCY ANALYSIS (JTFA)

Range-Doppler Limitation

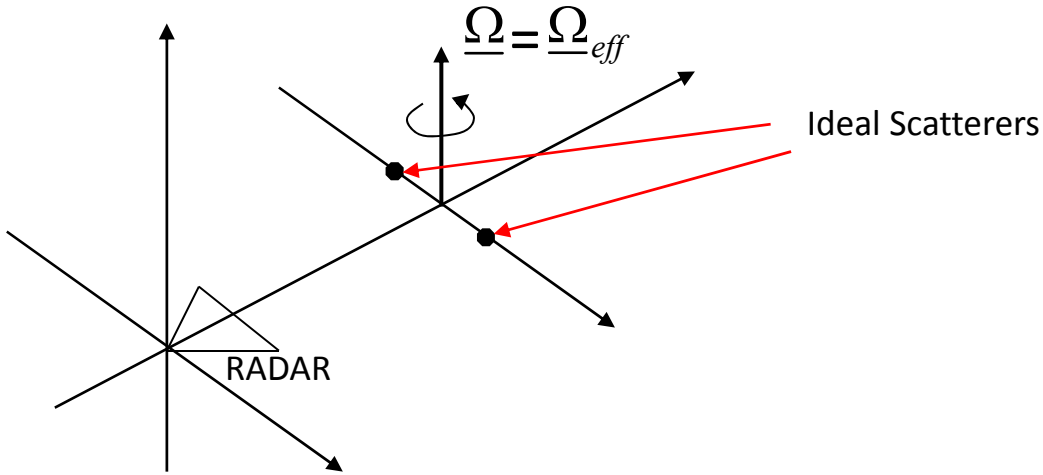

At low resolution:
- Short observation time
- Constant Doppler
- components

At high resolution:
- Long observation time
- LM Doppler components

DOPPLER PROFILES

Tob=1.5 s

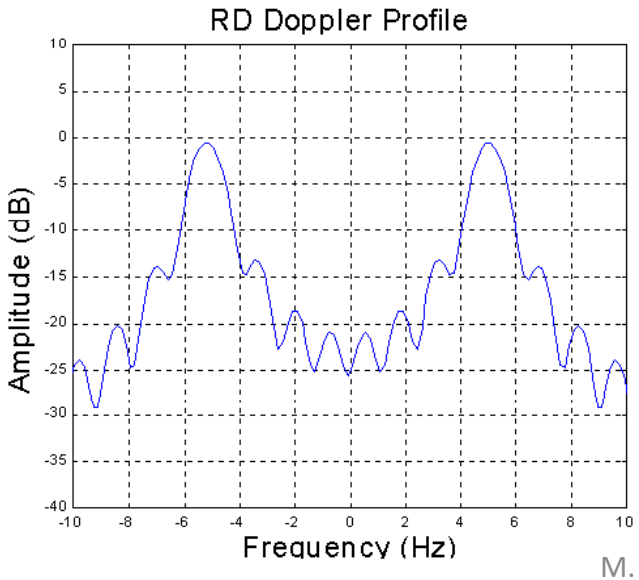

Tob=2.5 s

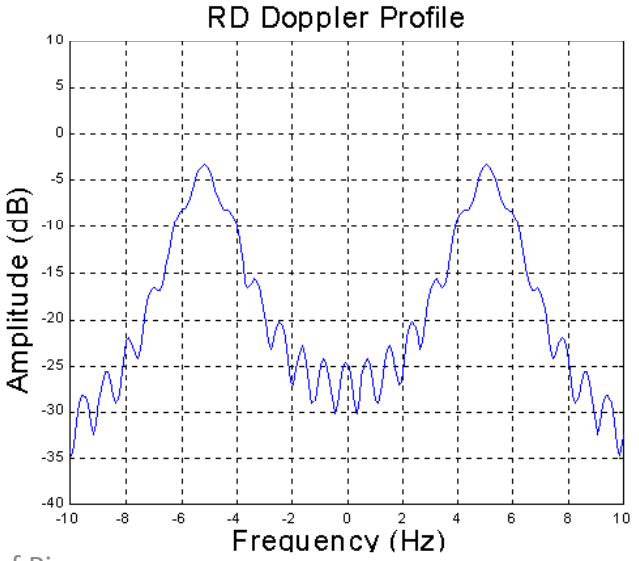

Fourier Transform and Time-Frequency Transform

• The Fourier Transform is a powerful tool for analysis of stationary signals, i.e. those signals that have a stationary frequency signature.

• When the frequency content of a signal varies with respect to time, the Fourier analysis is not capable to retrieve the time varying frequency content.

• A modification of the Fourier Transform, which is able to track the frequency signature is the Short Time Fourier Transform (STFT).

$$S_w(f,t) = \int s(\tau)\, w(\tau - t) \exp(-j2\pi f \tau)\, d\tau$$

Where $w(t)$ is a time window.

• The definition of the time window affects the time and frequency resolutions.

• Unfortunately the two resolution cannot arbitrarily chosen: if we enhance the time resolution, the frequency resolution is automatically degraded.

Time-Frequency Trasnform

• In order to enhance the frequency resolution, a long integration time is needed. Therefore, long time windows are needed.

• In order to enhance the time resolution, short time windows are needed.

Trade off

• The limits of the STFT can be relaxed by using different Time-Frequency Transforms (TFTs).

• A general TFT is not necessarily linear.

• A particular class of non-linear TFT is the Wigner-Ville (WV) transform, which is a bilinear transform.

• Following the WV transform, other bilinear transforms have been introduced: Margenau-Hill, Choi, Pseudo Wigner-Ville, …

• All these bilinear TFTs have been grouped into a general bilinear class of TFTs by Cohen.

Time-Frequency Trasnform

Bilinear Time-Frequency Transforms:
the Cohen class Time Frequency Distributions (CTFD)

$$CTFD(t,\omega)=\iiint e^{-j\theta t}e^{-j\xi\omega}e^{j\theta u}\ K(\theta,\xi)\,s^*\left(u-\frac{\xi}{2}\right)s\left(u+\frac{\xi}{2}\right)du\ d\xi\ d\theta$$

$K(\theta,\xi)$ Is the kernel of the CTFD. The kernel defines the particular CTFD.

Basic Time-Frequency Transform: Wigner-Ville

$$WV(t,\omega)=\int s^*\left(t-\frac{\xi}{2}\right)s\left(t+\frac{\xi}{2}\right)\cdot e^{-j\omega\xi}d\xi$$

Cross-terms:

- Non-linear transforms introduce cross-terms (CTs).
- CTs must be eliminated by defining suitable kernels $K(\theta,\xi)$

Smoothed Pseudo Wigner Ville (SPWV)

$$K(\theta,\xi)=F(\theta)G(\xi)$$

$F(\theta)$ and $G(\xi)$ are generic smoothing windows, such as Hamming, Kaiser, Gaussian, etc

Range-Instantaneous Doppler

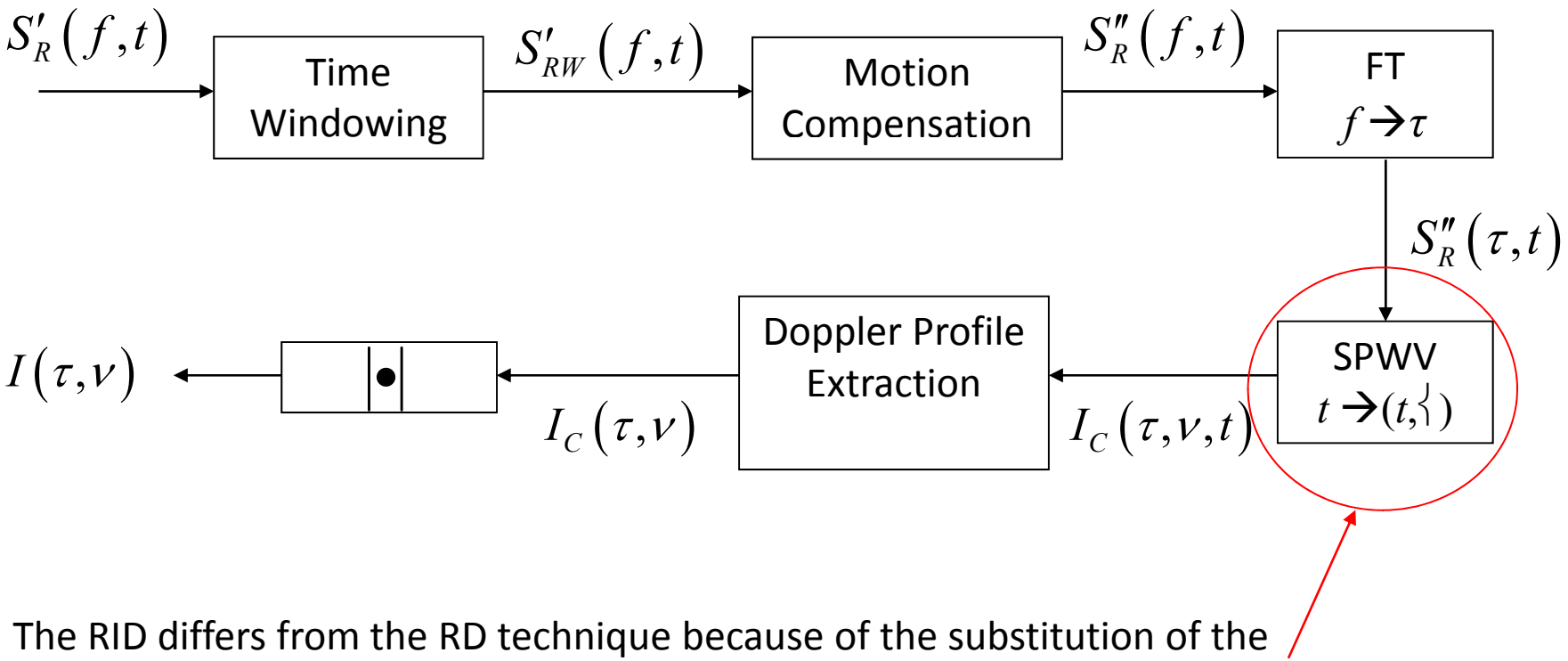

• The RID differs from the RD technique because of the substitution of the Fourier analysis with the Time-Frequency Analysis.

• Among all the possible choices of TFTs, the SPWV better solves the trade off between cancelling the cross-terms and loosing cross-range resolution.

• The narrower the kernel windows, the lower the level of the cross-terms and the worse the resolution loss.

Range-Instantaneous Doppler

(Tob=2.5 s)

SMEARED PEAKS

LFM TERMS

SINC-LIKE SHAPES

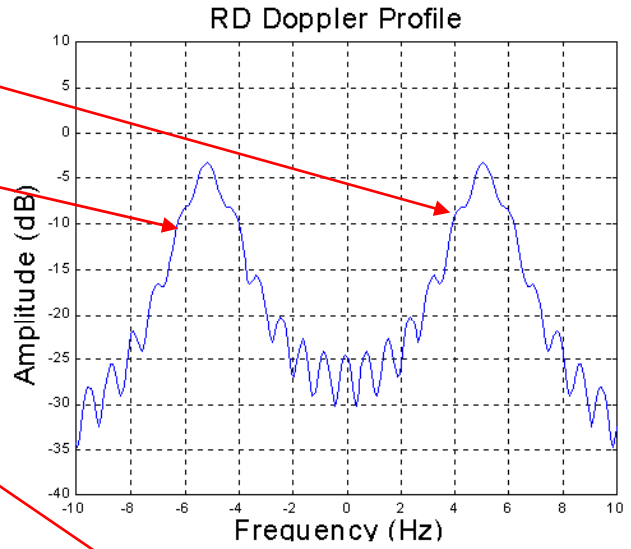

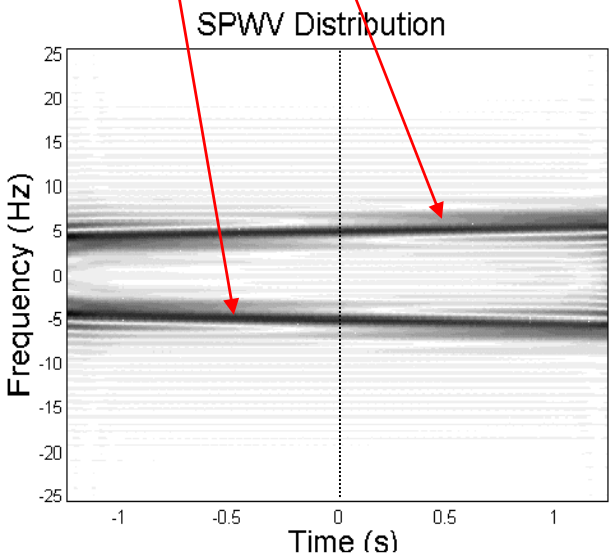

Doppler Profile Extraction (central time instant)

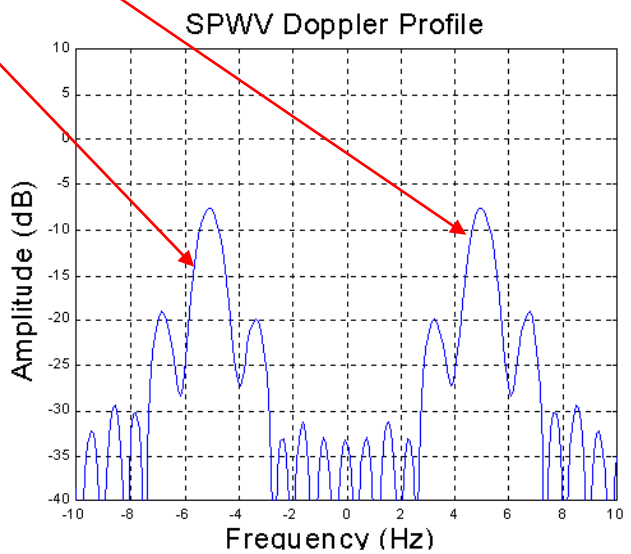

Simulation Results

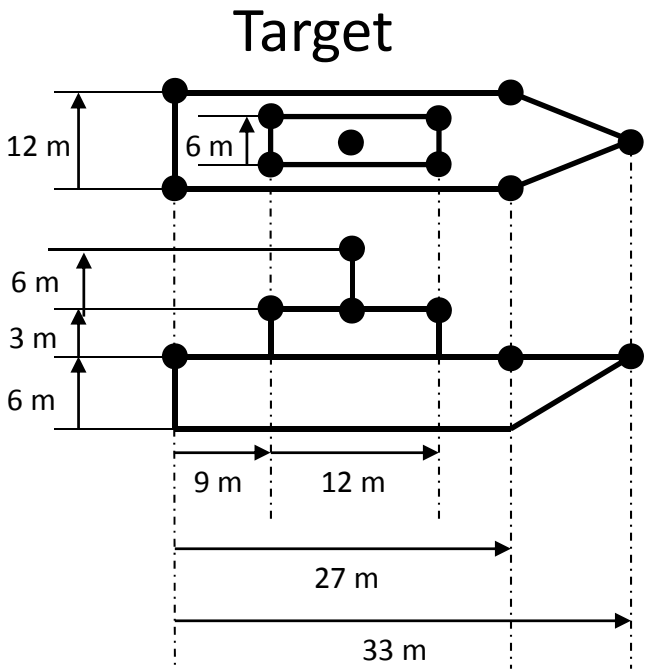

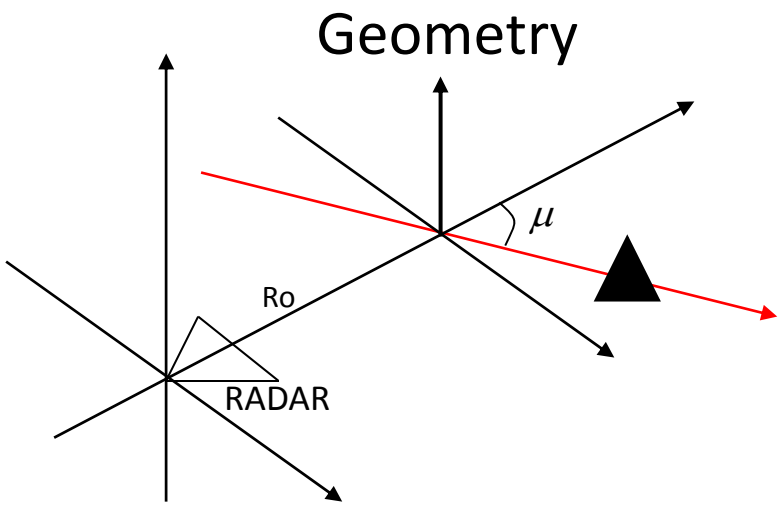

Geometrical parameters

Radar-Target Distance (Km)	15
Target Velocity Direction (degree)	60
Target Oscillation Amplitudes (degree)	[1 4.5 1.125]
Target Oscillation Periods (s)	[10 9.5 8]
Target Velocity (Knots)	15

RADAR Parameters

Carrier Frequency (GHz)	10
Bandwidth (MHz)	300
Observation Time (s)	0.9
Number of Echoes	256
Number of Range Cells	128

Resolutions

RANGE RESOLUTION (m)	0.5
CROSS-RANGE RESOLUTION (m)	0.3

Simulation Results

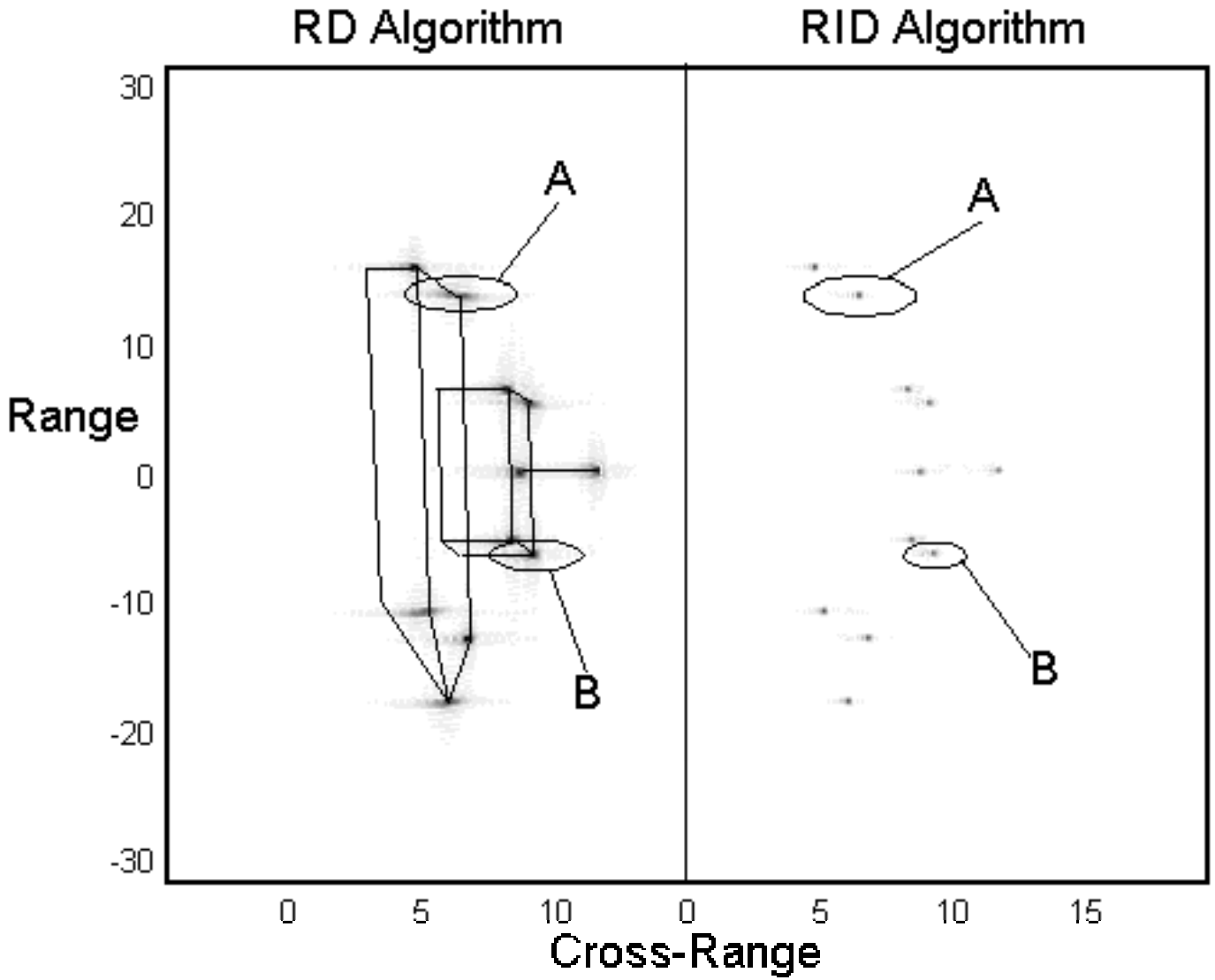

Simulation Results

Results:

- The scatterer A is
  - smeared when the RD algorithm is used
  - well focused when the RID algorithm is used

- The RD technique produces a spatially variant response whereas the RID produces a spatially invariant response

RD PROFILES

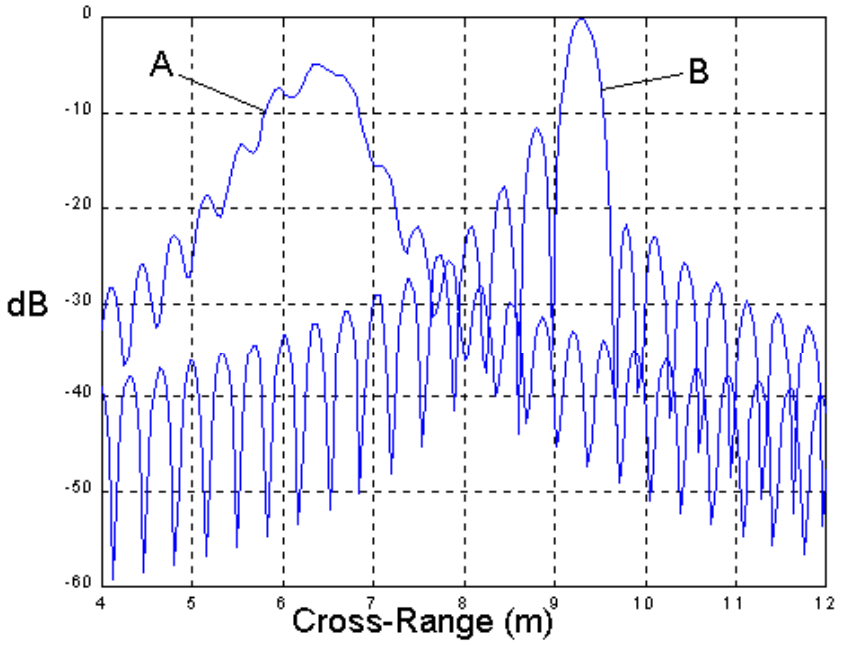

RID PROFILES

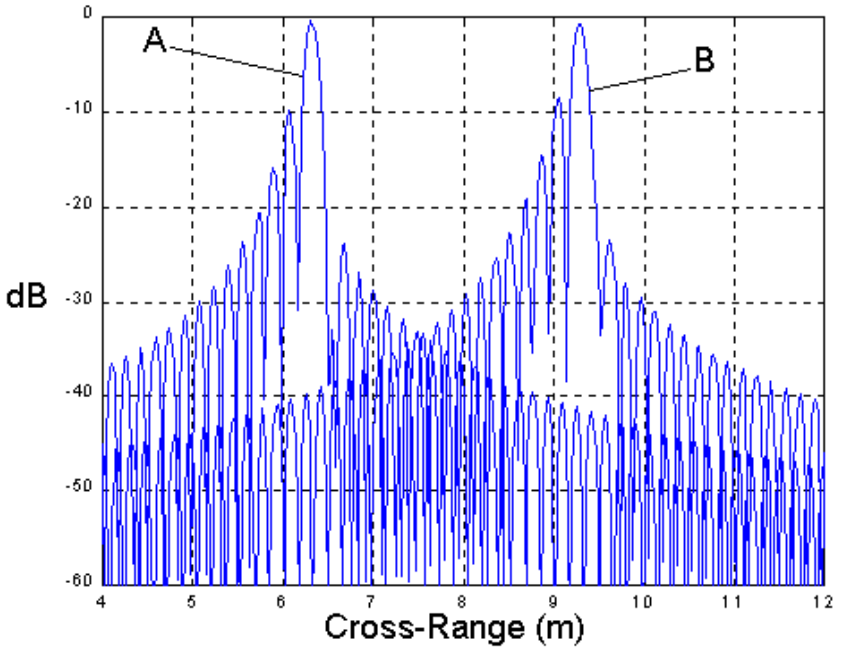

Statistical Analysis

Statistics generation criterion:

- Radar parameters are kept constant
- Target oscillation amplitudes, periods and initial phases are changed
- The observation time is chosen to have the best resolution

Longer observation time allowed

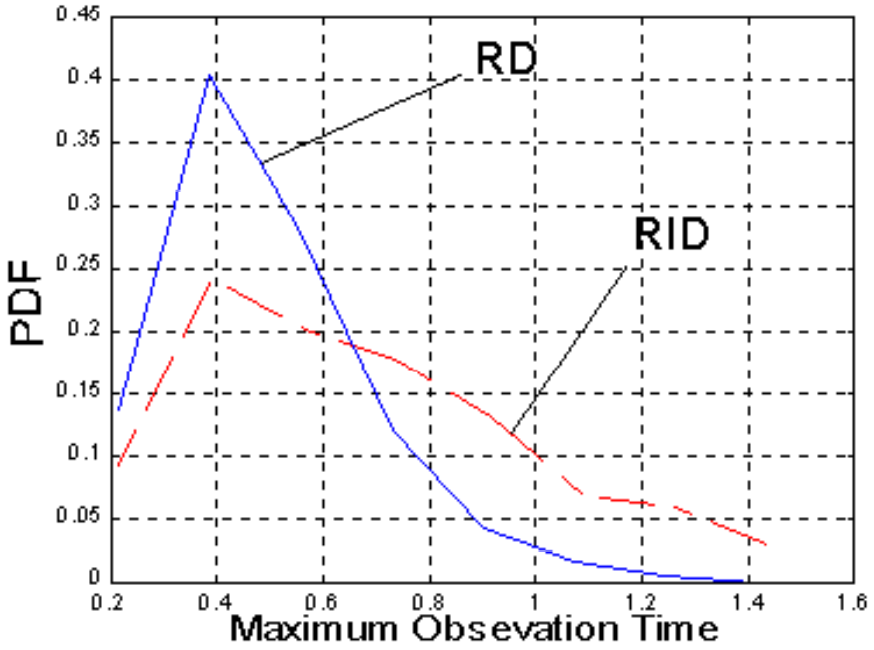

Spatial Resolution Improvement

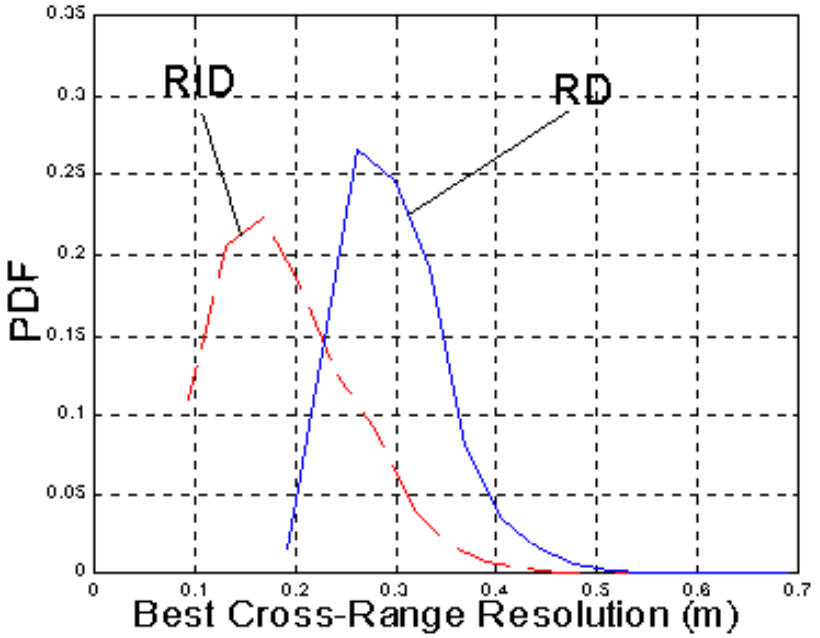

Real Data Results: Bulk Loader

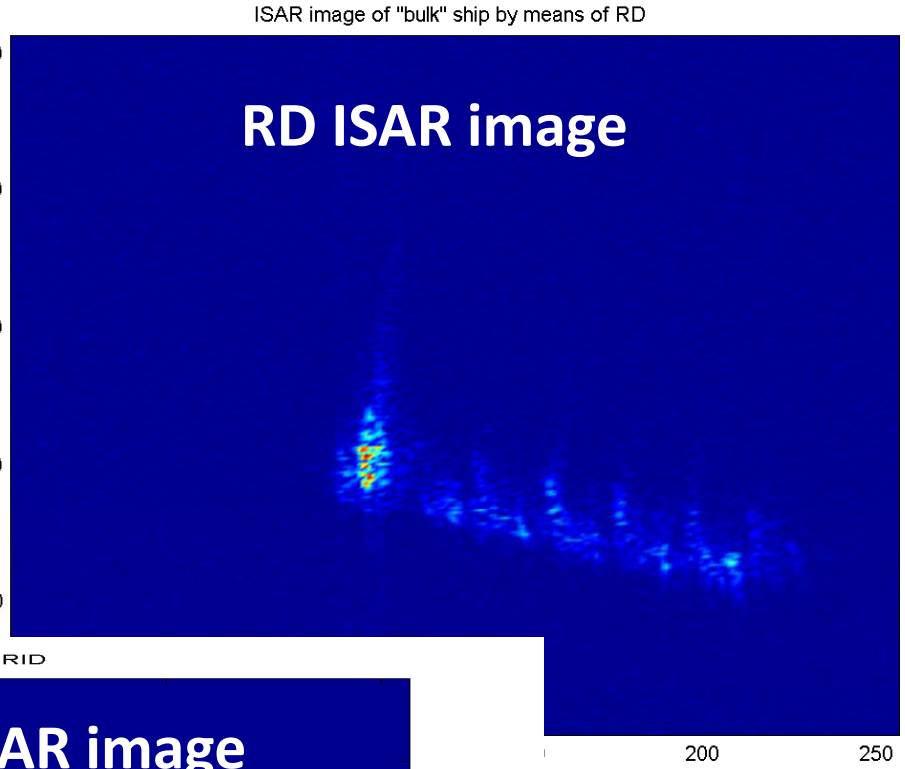

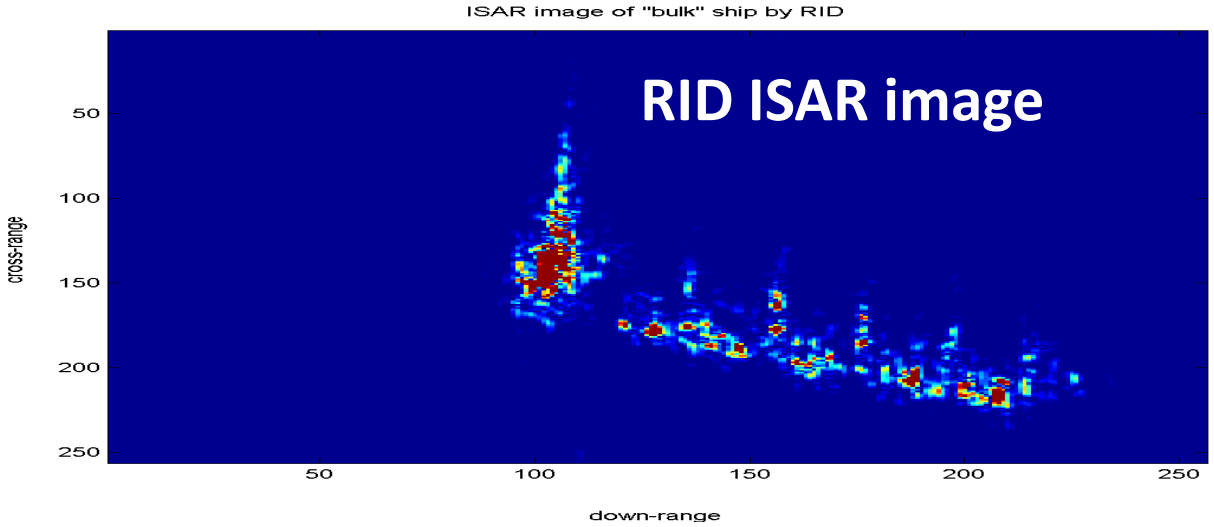

INTERPRETATION OF ISAR IMAGES

Received Signal Interpretation

From 3D to 2D

- The reference system embedded on the target is totally arbitrary
- The received signal does not depend on the choice of the particular reference system

$$S_R(f,k) = S(f)\sum_{i=1}^{M} a_i \exp\left\{-j2\pi f\left[kT_R + \frac{2R(t,\boldsymbol{x}_i)}{c}\right]\right\}$$

Point-like scatterers

$$S_R(f,k) = S(f)\iiint \xi(\boldsymbol{x})\left\{-j2\pi f\left[kT_R + \frac{2R(t,\boldsymbol{x})}{c}\right]\right\}d\boldsymbol{x}$$

Distributed target

$\boldsymbol{x}_i$ and $\boldsymbol{x}$ have three components, since they represent 3D coordinates

EFFECTIVE ROTATION VECTOR

• The radar is only able to measure **time delays** and **phases**

• A target's rotation around the LOS axis does not produce any time delay or phase changes in the received signal

The radar is blind to any target's rotation with respect to the LOS

• An Effective Rotation Vector can be defined as the component of the total rotation vector that is orthogonal to the LOS

$$\boldsymbol{\Omega}_{eff}(t) = \boldsymbol{i}_y(t) \times \left[\boldsymbol{\Omega}(t) \times \boldsymbol{i}_y(t)\right]$$

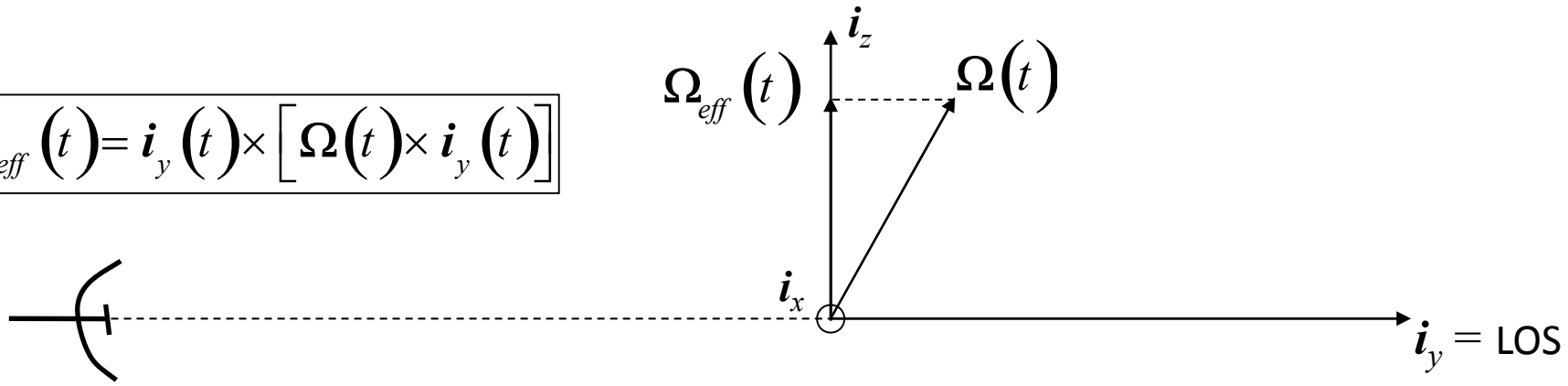

IMAGE PLANE INTERPRETATION

- The aspect angle variation
  - is responsible for the synthetic aperture formation
  - is produced by the effective rotation vector
  - occurs on the plane orthogonal to the effective rotation vector

Image Plane: the image plane can be defined when the effective rotation vector direction is constant.

$$\left(\boldsymbol{i}_{cr}, \boldsymbol{i}_{r}\right) = \left(\boldsymbol{i}_{y} \times \Omega_{eff}, \boldsymbol{i}_{y}\right)$$

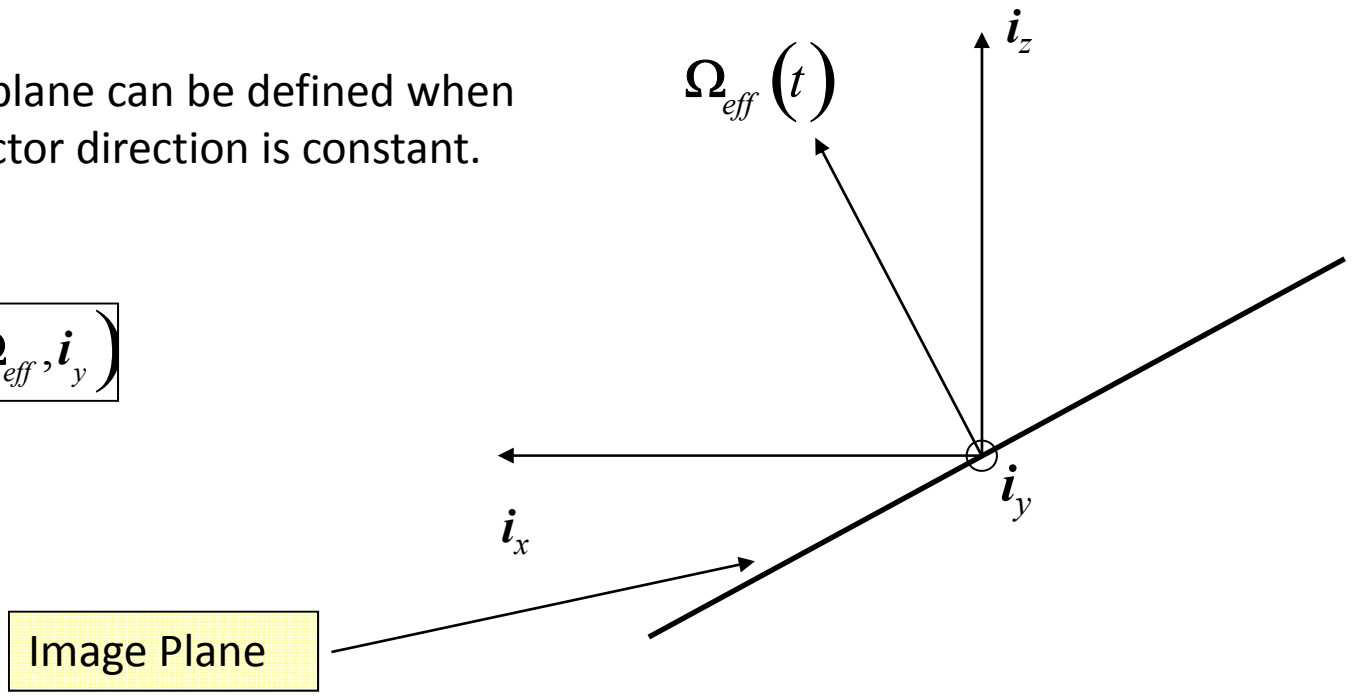

IMAGE PLANE INTERPRETATION

From 3D to 2D

- The reference system embedded on the target can be chosen as shown in figure

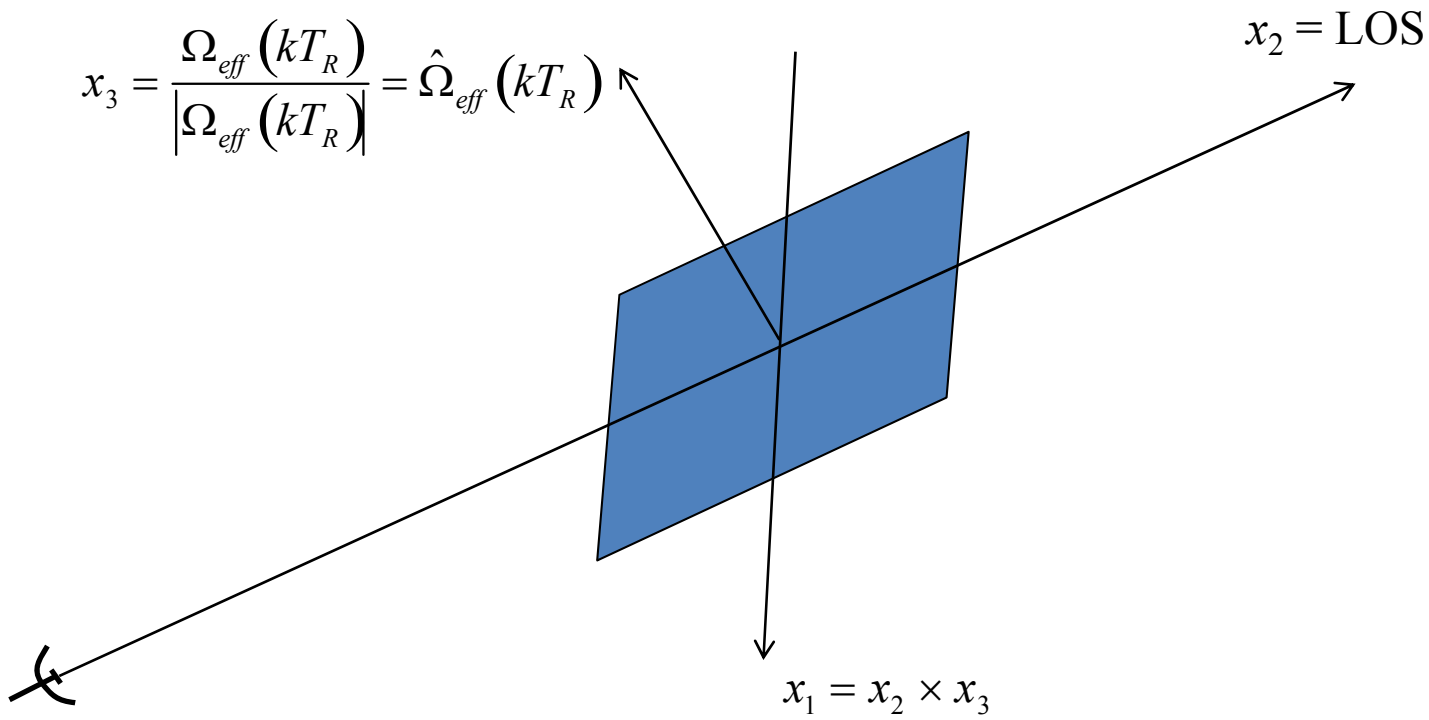

FROM 3D TO 2D

• By considering a distributed 3D reflectivity function and by choosing the reference system as previously described, the received signal can be rewritten as follows

$$S_R(f,k) = S(f)\exp\left[-j2\pi f\left(kT_R + \frac{2R_O(kT_R)}{c}\right)\right]$$
$$\cdot \iiint \xi(x_1,x_2,x_3)\exp\left\{-j\frac{4\pi f}{c}\left[x_1\sin\left[\theta(kT_R)\right] + x_2\cos\left[\theta(kT_R)\right]\right]\right\}dx_1\,dx_2\,dx_3$$

• It should be noted that the third coordinate (x_3) does not produce any phase change in the received signal. This is due to fact that the effective rotation vector produces position changes only on the plane orthogonal to itself.

FROM 3D TO 2D

The integral part can be manipulated as follows:

$$\iiint \xi'(x_1,x_2,x_3)\exp\left\{-j\frac{4\pi f}{c}\left[x_1\sin\left[\theta(kT_R)\right]+x_2\cos\left[\theta(kT_R)\right]\right]\right\}dx_1\,dx_2\,dx_3$$

$$=\iint\left[\int \xi'(x_1,x_2,x_3)dx_3\right]\exp\left\{-j\frac{4\pi f}{c}\left[x_1\sin\left[\theta(kT_R)\right]+x_2\cos\left[\theta(kT_R)\right]\right]\right\}dx_1dx_2$$

$$=\iint \xi(x_1,x_2)\exp\left\{-j\frac{4\pi f}{c}\left[x_1\sin\left[\theta(kT_R)\right]+x_2\cos\left[\theta(kT_R)\right]\right]\right\}dx_1\,dx_2$$

The function G that maps the 3D reflectivity function onto a 2D domain is, in facts, a projection

$$\xi(x_1,x_2)=G\left[\xi'(x_1,x_2,x_3)\right]=\int \xi'(x_1,x_2,x_3)dx_3$$

ISAR IMAGE AND REFLECTIVITY FUNCTION

• It is therefore correct to consider an equivalent 2D reflectivity function in the received signal

• The 2D reflectivity function is the projection of the 3D (real) reflectivity function onto the image plane

$$S_R(f,k) = S(f)\exp\left[-j2\pi f\left(kT_R + \frac{2R_O(kT_R)}{c}\right)\right]$$
$$\cdot \iint \xi(x_1,x_2)\exp\left\{-j\frac{4\pi f}{c}\left[x_1\sin\left[\theta(kT_R)\right] + x_2\cos\left[\theta(kT_R)\right]\right]\right\}dx_1\,dx_2$$

• The ISAR image is a linear convolution of the projection of the reflectivity function with the system PSF

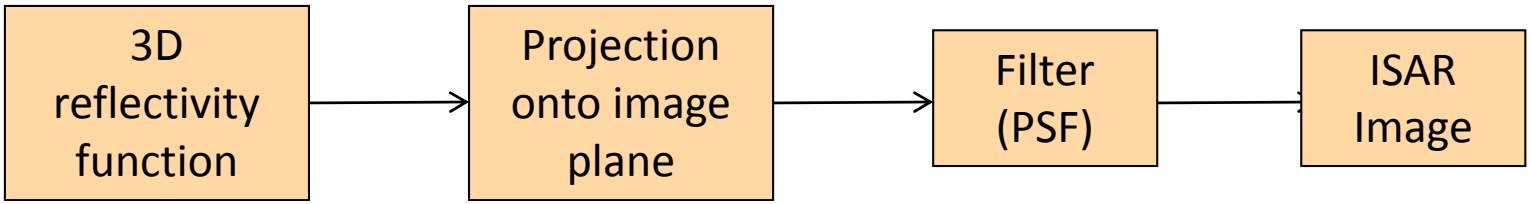

RANGE DOPPLER

Point Spread Function

Given a transmitted signal bandwidth B and an observation time T_{obs}., we can define a window $W(f,t)$, which can be related to $W(X_1,X_2)$

$$W(f,t) = rect\left[\frac{f-f_0}{B}\right] rect\left[\frac{t}{T_{obs}}\right]$$

By exploiting the relationship between (f,t) and (X_1,X_2), we obtain

$$W(X_1,X_2) = rect\left[\frac{X_2 - \frac{2f_0}{c}}{\frac{2B}{c}}\right] rect\left[\frac{X_1}{\frac{2f_0\Omega T_{obs}}{c}}\right]$$

System PSF

$$w(x_1,x_2) = sinc\left[\frac{x_2}{\frac{c}{2B}}\right] \exp\left(j2\pi\frac{2f_0}{c}x_2\right) sinc\left[\frac{x_1}{\frac{c}{2f_0\Omega T_{obs}}}\right]$$

RANGE DOPPLER

Point Spread Function

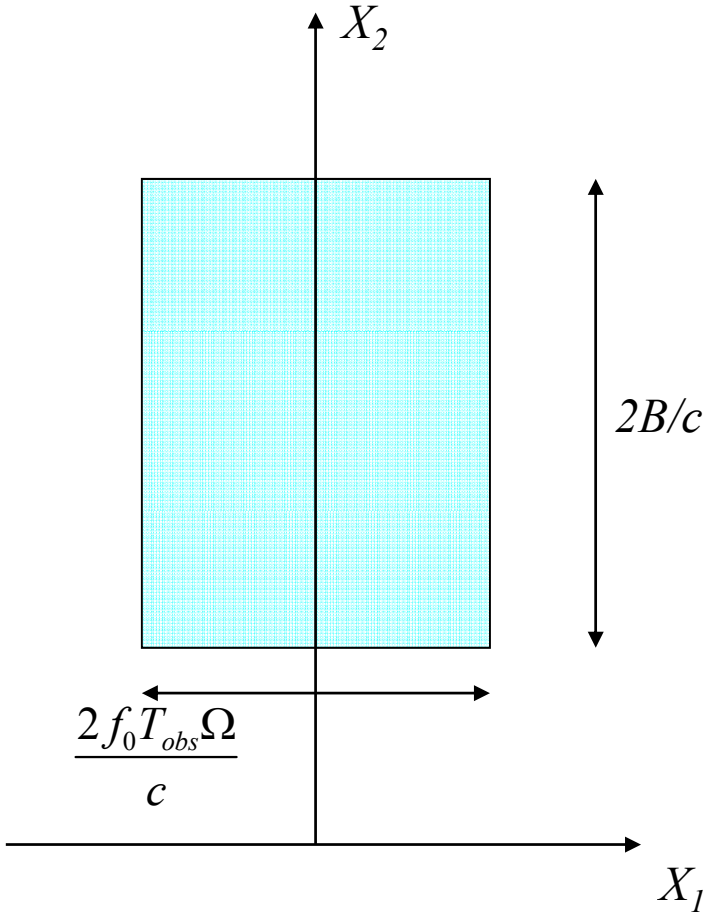

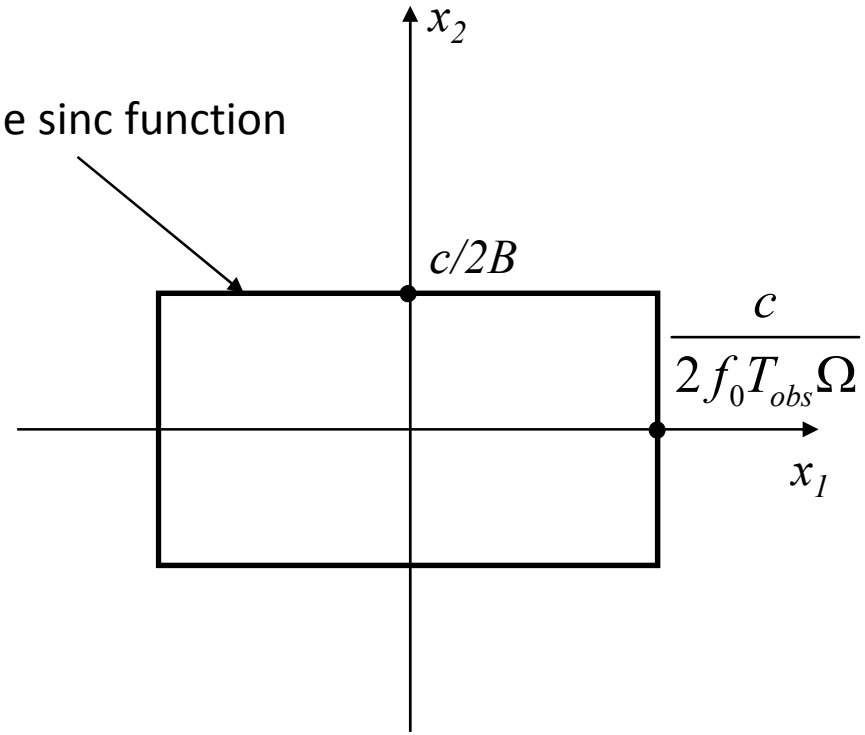

Resolution

Range Resolution: $\frac{c}{2B}$

Cross-range Resolution: $\frac{c}{2 f_0 T_{obs} \Omega}$

RANGE DOPPLER

Ambiguity

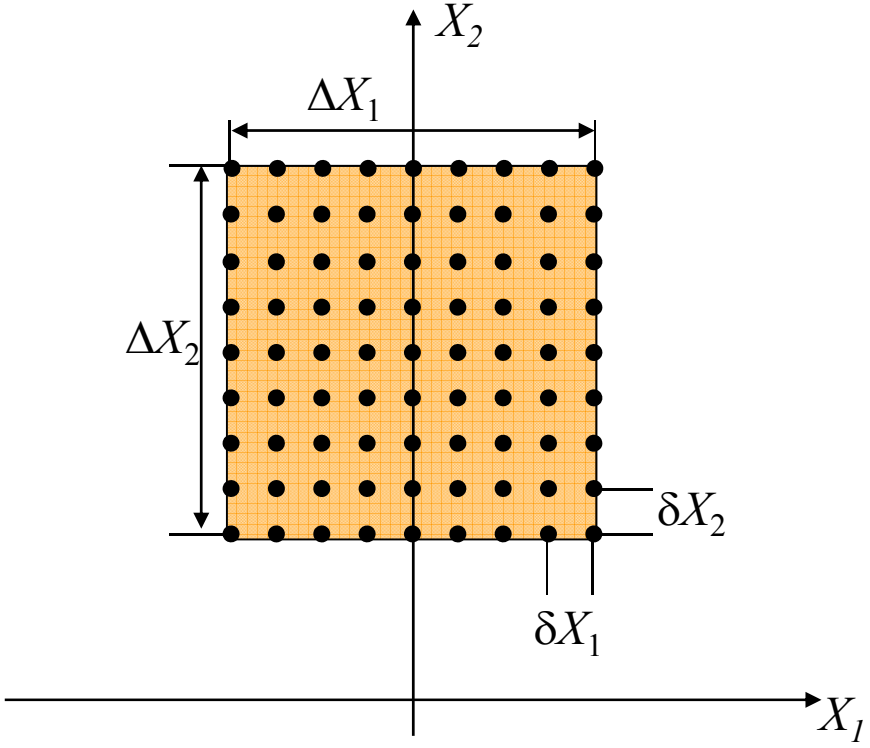

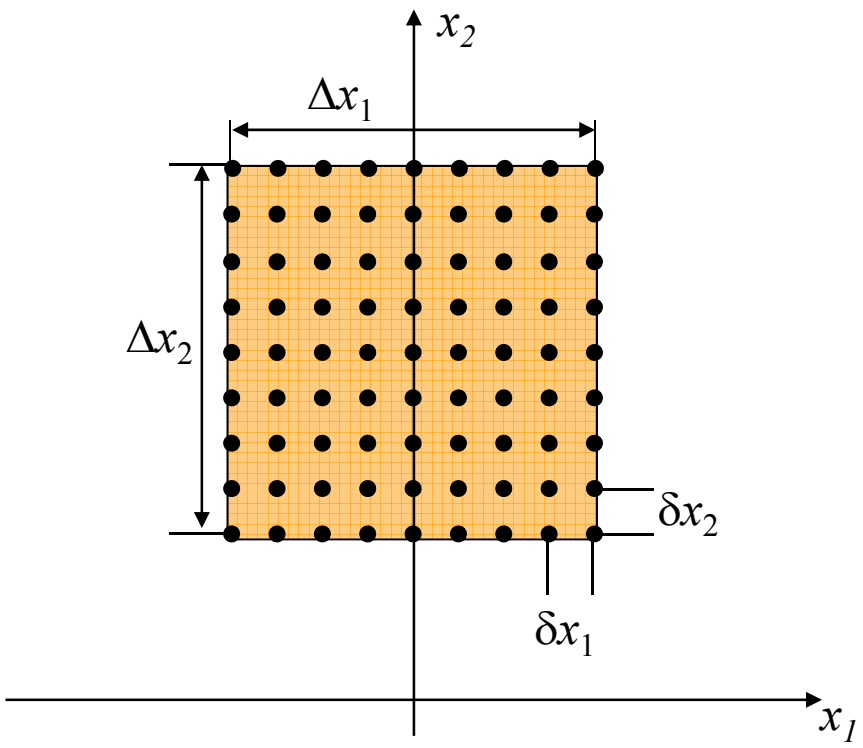

- $\delta X_1 = 1/\Delta x_1$
- $\delta X_2 = 1/\Delta x_2$

- $\delta x_1 = 1/\Delta X_1$
- $\delta x_2 = 1/\Delta X_2$

RANGE DOPPLER

Circular ambiguity - Examples

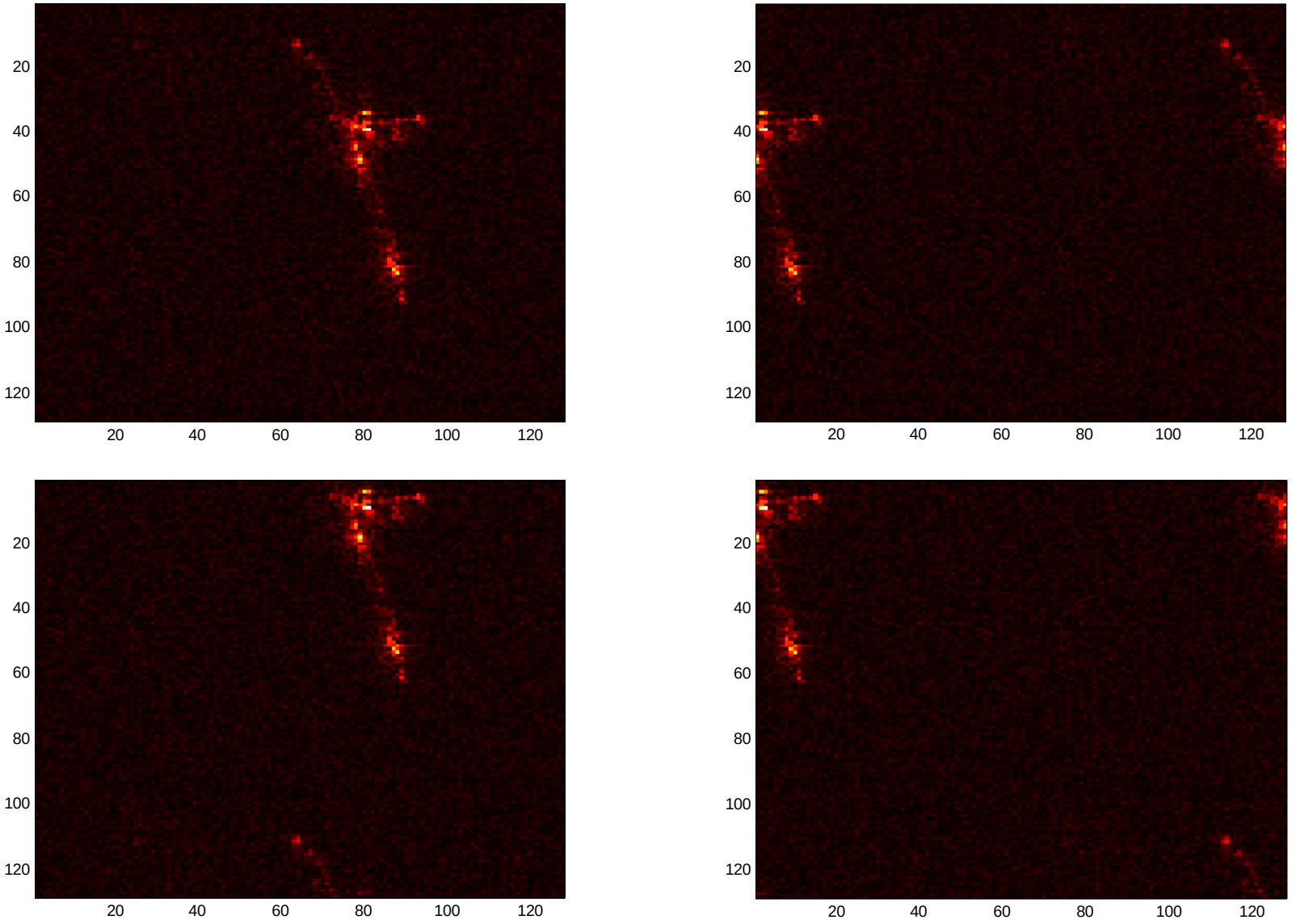

Differences and analogies between SAR and ISAR

SAR and ISAR: is it only a matter of reference systems?

• It seems that by simply changing the reference system we can look at synthetic aperture from a SAR or ISAR point of view.

• The only subtle difference that separates the two worlds is the target cooperativity.

• In ISAR scenarios the target motion is usually not known whereas in SAR scenarios the area illuminated by the antenna is usually static during the synthetic aperture formation.

• Target cooperation can be seen as system geometry knowledge. The knowledge of the geometry enables straightforward image formation processing.

• Most of the ISAR image formation techniques deal with the problem of target non-cooperativity and for this reason they differ from SAR image formation techniques

SAR and ISAR example

SAR Image with unfocussed ship targets (EMISAR data)

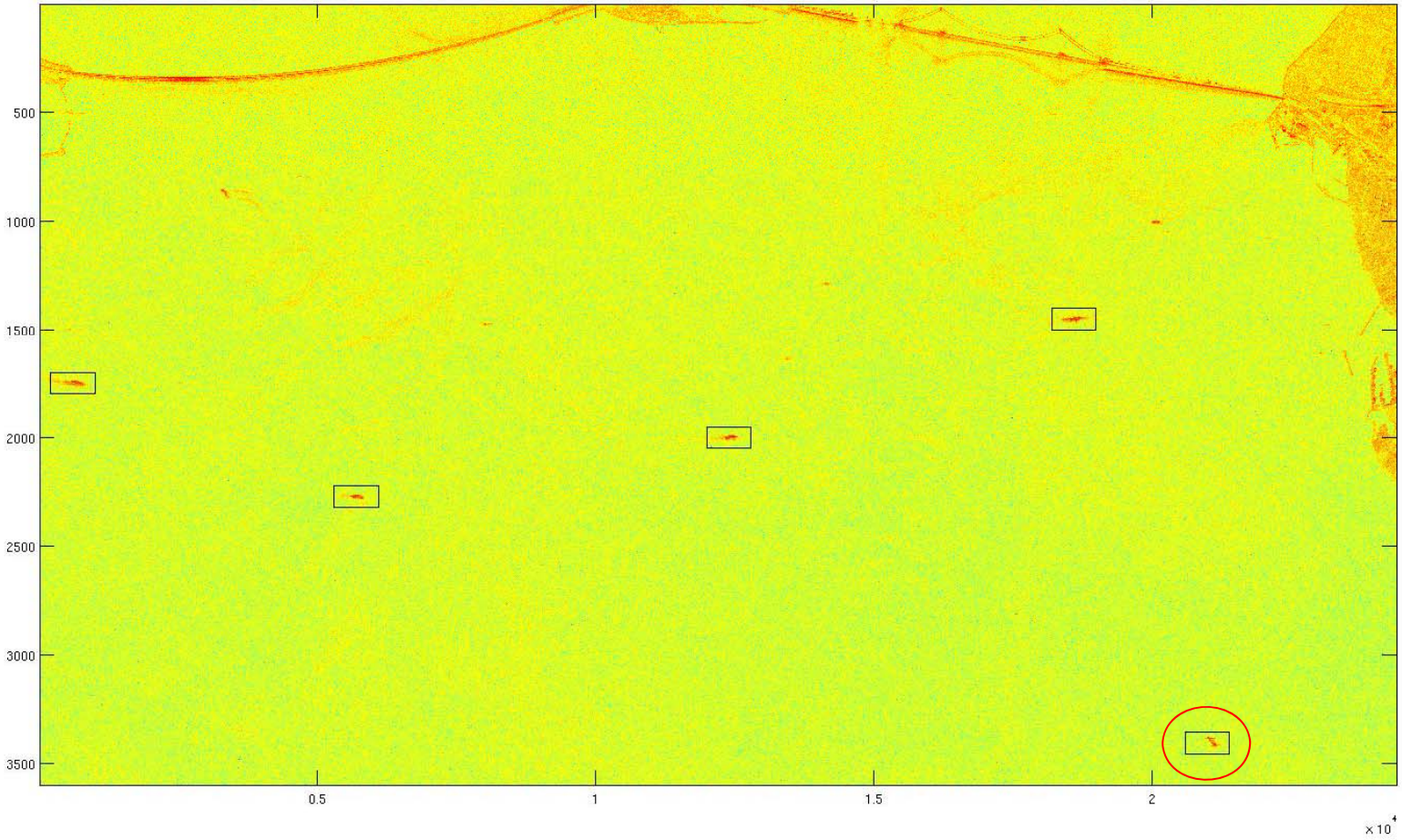

SAR and ISAR example

- The target's own motions are not considered when using a SAR processor
- ISAR imaging must be used to obtain a focussed target
- Focussed ISAR images of the ships can be obtained even starting from the SAR complex image

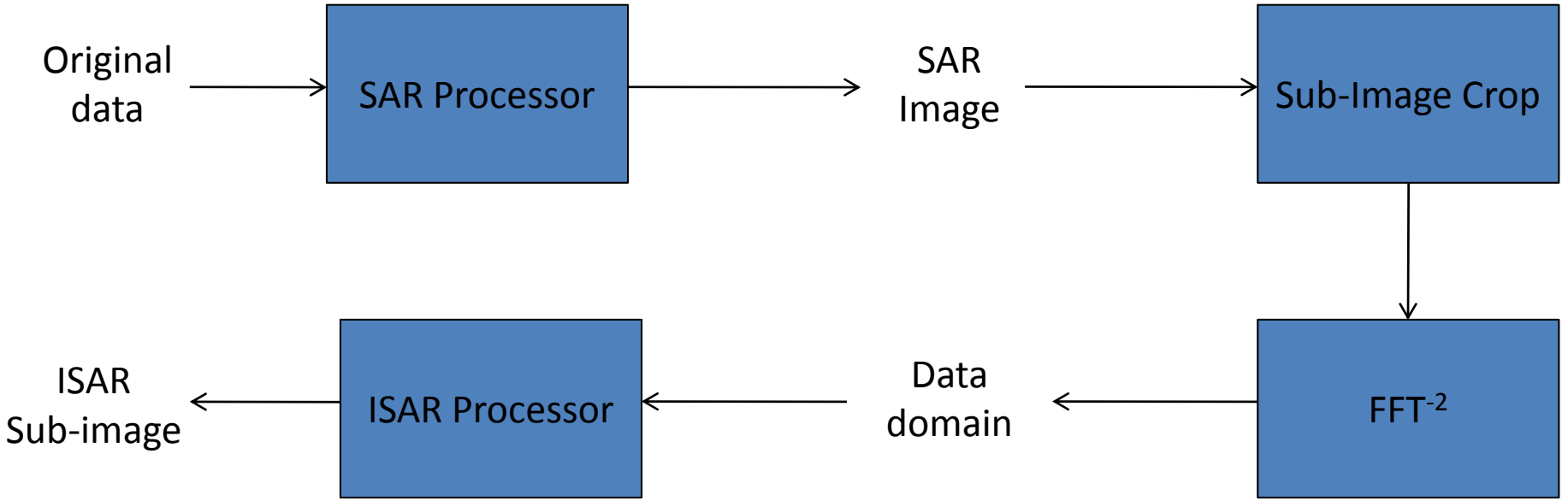

SAR and ISAR example

Unfocussed ship target (SAR processed data)

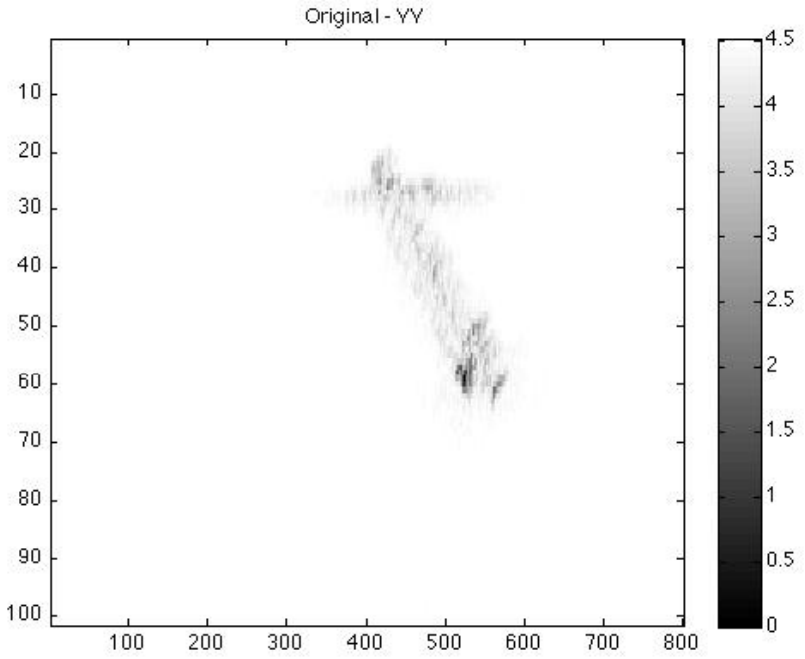

Focussed ship target (ISAR processed data)

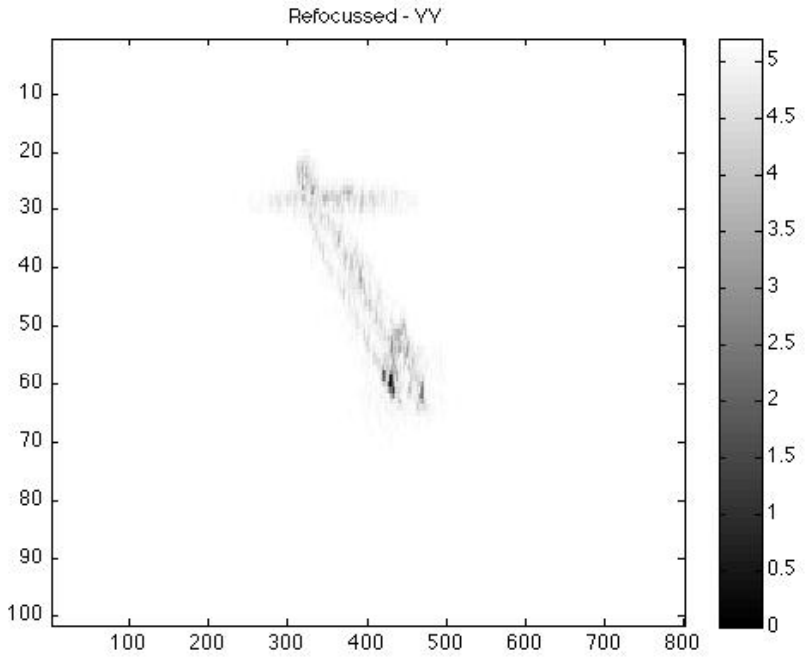

- The Focussed sub-image has the same number of pixels of the unfocussed sub-image (crop)

- The focussed ISAR sub-image can be reinserted in the original image by replacing the sub-image crop

Analogies and differences between SAR and ISAR

• The name Inverse SAR refers to the fact that the synthetic aperture is not formed by means of the movement of the platform that carries the radar but it is formed by exploiting the movement of the target.

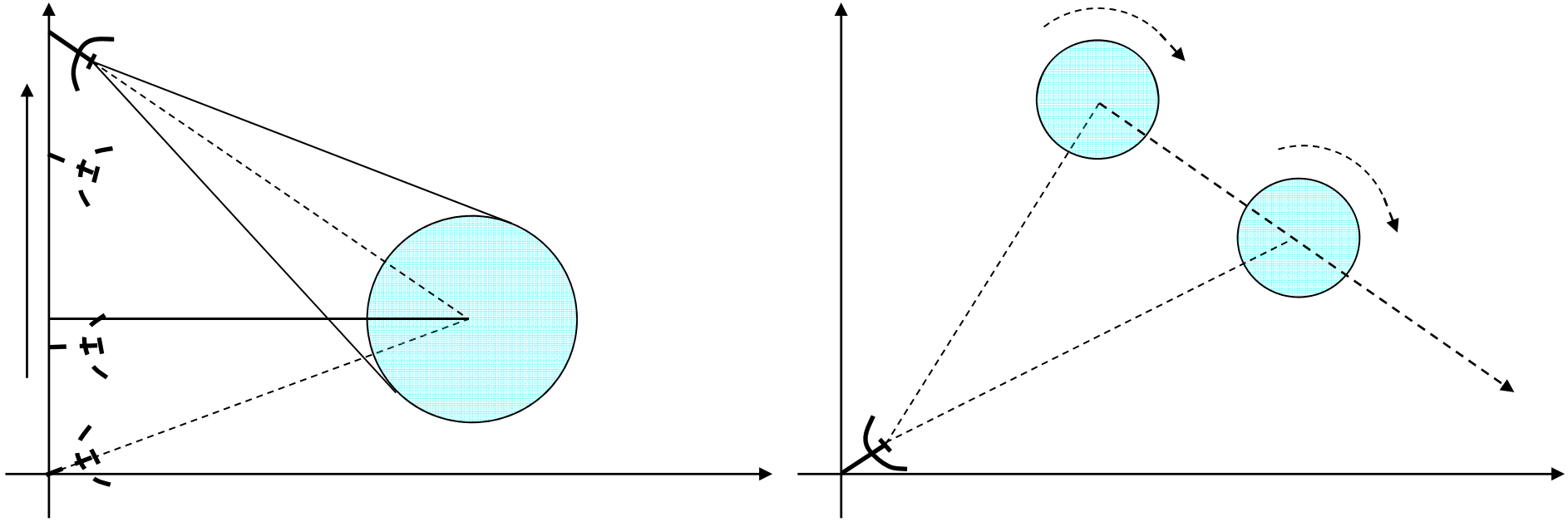

• The synthetic aperture can be seen as a coherent processing of echoes that comes from different view angles.

• The inverse synthetic aperture is achieved when there is a variation of the target-radar aspect angle.

Analogies and differences between SAR and ISAR

• Such an insight opens the horizons of SAR to another set of scenarios where the radar is fixed on the ground and the target moves with respect to it.

• Nevertheless, this view is limited and does not highlight the underlying difference between SAR and ISAR. In fact, by changing the reference system it is possible to consider either the radar or the target as fixed and the other moving. Therefore, one scenario would be completely equivalent to the other.

• The real substantial difference is given by the cooperation of the target.

  • Generally, for a SAR system, the target is cooperative because it is a static or quasi-static scene and the geometry and cinematic of the radar-target system is known a-priori.

  • For an ISAR system, the target is non-cooperative and hence the geometry and cinematic of the system cannot be known a-priori.

Analogies and differences between SAR and ISAR

• Because SAR and ISAR systems are equivalent apart from the non-cooperation of the target, most steps of the signal processing remain unchanged.

• Nevertheless, the non-cooperativity of the target causes a few problems:

- the motion compensation cannot be performed by exploiting the knowledge of the geometry

- the grid of samples in the Fourier domain is not evenly spaced because the rotation of the target with respect to the radar is not constant

- the scaling operation along the cross-range coordinate cannot be performed unless the total aspect angle variation is somehow estimated, therefore the image is generally scaled in range-Doppler coordinates

ISAR IMAGE AUTOFOCUS

Automatic Motion Compensation

• Because the target is non-cooperative, the motion compensation must be performed without any external aid.

• Such an operation is also known as: image autofocusing. In fact, the better such an operation is performed the higher the image focus is.

• Several techniques have been proposed. They can be grouped into two classes: parametric and non-parametric techniques.

• Parametric techniques make use of a signal model. The parameters of the signal model have to be estimated in order to achieve the target motion compensation.

• Non-parametric techniques do not make use of any signal model.

The use of either parametric or non-parametric techniques depends on the accuracy and computational cost required by the specific application.

Parametric and non-parametric techniques

Parametric techniques

Image Contrast Based Autofocus

Image Entropy Based Autofocus

Non-parametric techniques

Prominent Point Processing (Hot Spot)

Phase Gradient Autofocus

Image Contrast Based Autofocusing (ICBA)

• The implementation of the ICBA requires the definition of a signal model and a criterion for the estimation of the signal model parameters.

• The ICBA is based on:

  • the definition of a polynomial signal phase

  • the definition of the Image Contrast (IC)

• By defining a signal model it is possible to estimate the signal phase component associated with the radial motion of the phase centre.

• The estimation of such a signal phase component is equivalent to the estimation of the phase centre radial motion, therefore it has the physical meaning of estimating the radial motion of a single point that belongs to the target.

• The maximisation of the IC will be used as a criterion for optimal estimation of the radial motion parameters.

Motion Compensation (or Image Autofocusing)

Polynomial phase term

Deconvoluted received signal (continuous time, continuous target):

$$S'_R(f,t) = W(f,t)\exp\left[-j\frac{4\pi f R_o(t)}{c}\right]\int\int \xi(x_1,x_2)\exp\left\{-j2\pi\left[X_1x_1 + X_2x_2\right]\right\}dx_1dx_2$$

$$R_0(t) = \alpha_0 + \sum_{k=1}^{N}\alpha_k t^k$$

Shift term

Focusing parameters

(radial motion parameters)

Assumption:

The image plane must remain unchanged during the integration time.

- Physical meaning:
  - α_1 = radial velocity of the phase centre
  - α_2 = radial acceleration of the phase centre

Shift term

Parameter α_0 :

- provokes a shift along the range coordinate in the image
- does not affect the image focus

Demonstration:

Let $S'_R(f,t)$ be compensated by means of $R'_0(t)$, where $R'_0(t) = \sum_{k=1}^{N} \alpha_k t^k$

Hence,

$$S''_R(f,t) = W[f,t] \int\int \xi(x_1,x_2) \exp\{-j2\pi[X_1 x_1 + X_2 x_2]\} dx_1\, dx_2 \exp\left[-j\frac{4\pi f\, \alpha_o}{c}\right]$$

$$I_C(\tau,\nu) = \underset{\substack{f\to\tau \\ t\to\nu}}{FT^{-2}} \{S''_R(f,t)\} =$$

$$= T_{obs} B \sum_{k=1}^{K} sinc[T_{obs}\nu]\, sinc[B\tau]\, e^{-j2\pi f_0 \tau} \otimes\otimes \xi\left(\frac{c}{2}\tau, \frac{c}{2f_0\Omega}\nu\right) \otimes\otimes \delta(\nu)\delta\left(\tau - \frac{2\alpha_0}{c}\right)$$

Focusing Parameters

The focusing parameters α_k provoke a defocusing of the image

When the demodulated signal is compensated by means of an incorrect phase term $\ddot{R}_0(t) = \sum_{k=1}^{N} \alpha_k t^k$ it retains some residuals of the radial motion. Therefore, the reconstructed image is blurred by the effect of the residual phase term.

$$S_R''(f,t) = W[f,t] \int\int \xi(x_1,x_2) \exp\left\{-j2\pi[X_1 x_1 + X_2 x_2]\right\} dx_1\, dx_2 \sum_{k=1}^{N} \exp\left[-j\frac{4\pi f}{c}\alpha_k t^k\right]$$

Where $\tilde{\alpha}_k = \alpha_k - \hat{\alpha}_k$ are the focusing parameter residuals.

Hence, the reconstructed complex image is

Defocusing term

$$I_C(\tau,\nu) = T_{obs} B \sum_{k=1}^{K} sinc[T_{obs}\nu]\, sinc[B\tau]\, e^{-j2\pi f_0 \tau} \otimes\otimes \xi\left(\frac{c}{2}\tau, \frac{c}{2 f_0 \Omega}\nu\right) \otimes\otimes FT^{-2}\left[\sum_{k=1}^{N} \exp\left[-j\frac{4\pi f}{c}\alpha_k t^k\right]\right]$$

Image Focus and Image Contrast

• In order to maximise the image focus, the focusing parameter residuals (estimation errors) must be minimised.

• Optimal estimation techniques can provide an accurate estimate of the focusing parameters and therefore a minimisation of the focusing parameter residuals.

• Because the image focus is related to focusing parameter residuals, it can be convenient to define a new parameter that is able to provide a measure of the image focus.

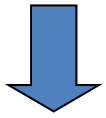

Image Contrast

$$IC(\alpha)=\frac{\sqrt{A\left\{I^2(\tau,\nu;\alpha)-A\left\{I^2(\tau,\nu;\alpha)\right\}\right]^2}\right\}}{A\left\{I^2(\tau,\nu;\alpha)\right\}}$$

$$\alpha=(\alpha_1,\alpha_2,\ldots,\alpha_N)$$

$$A\{\bullet\}=\text{spatial mean operator}$$

$$I(\tau,\nu;\alpha)=\text{ISAR image intensity}$$

Image Focus and Image Contrast

Example

The higher the Image Contrast
the better the image focus

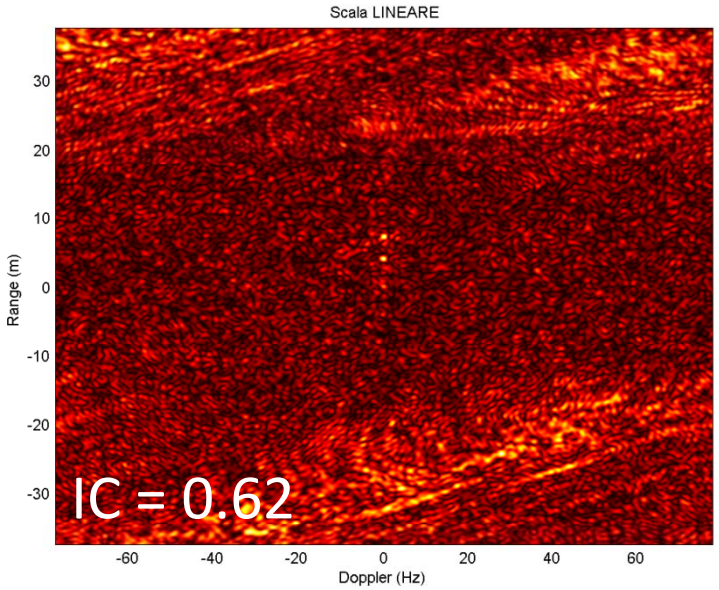

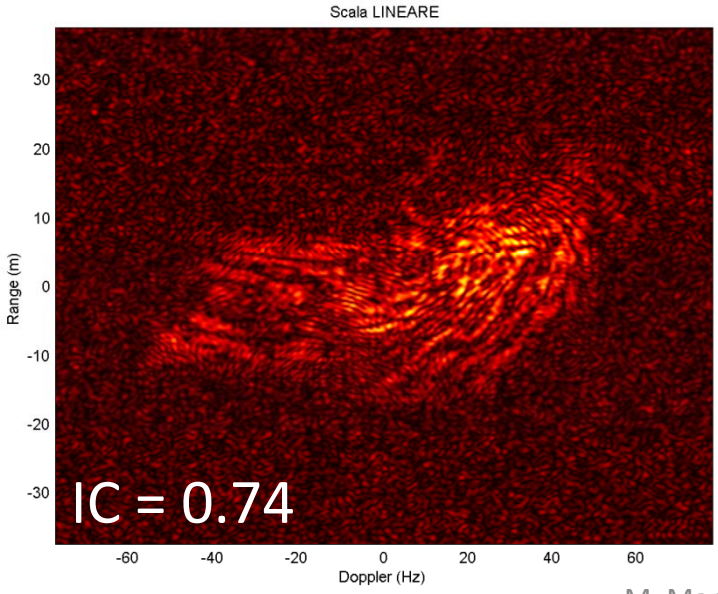

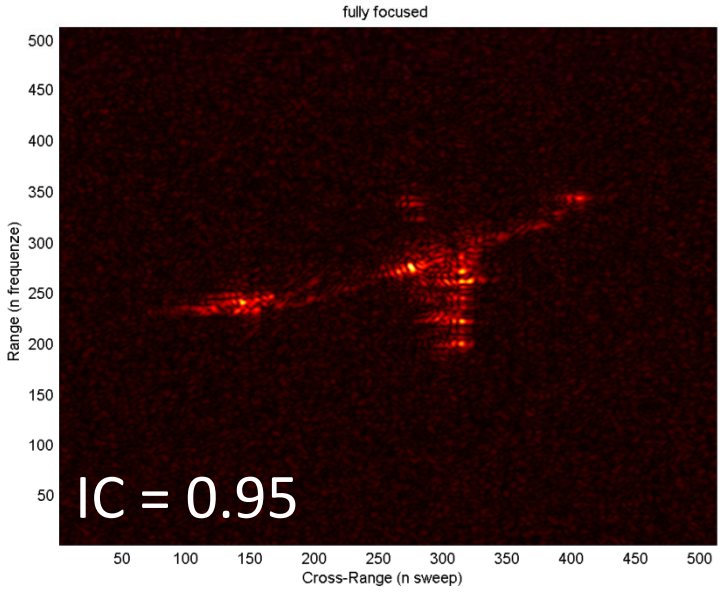

Image Autofocusing by means of Image Contrast Maximisation

By exploiting the definition of IC and its property in relation to the image focus, we can derive an autofocusing technique.

Criterion:

Find the focusing parameter vector $\hat{\alpha}$ that maximises the IC:

$$\hat{\alpha} = \arg\left(\max_{\alpha}\left[IC(\alpha)\right]\right)$$

• The estimation problem is transformed into an **optimisation problem**.

• The solution is not unique and a closed solution of the global maximum cannot be found, hence a numerical technique must be implemented.

• It is important to analyse the cost function IC in order to implement effective optimisation techniqes.

Cost Function

Analysis with two focusing parameters

The optimisation problem becomes:

$$(\ddot{\beta}, \ddot{\gamma}) = \arg\left(\max_{\beta,\gamma} \left[C(\beta,\gamma) \right] \right)$$

With two focusing parameters, the cost function graph can be displayed in a three dimensional domain

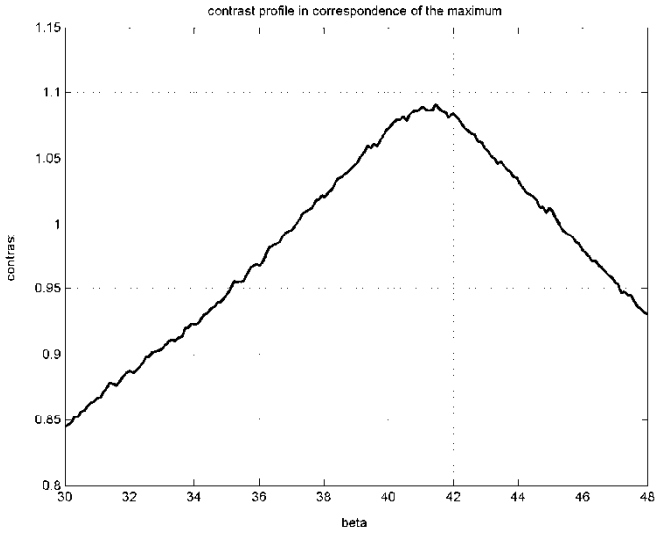

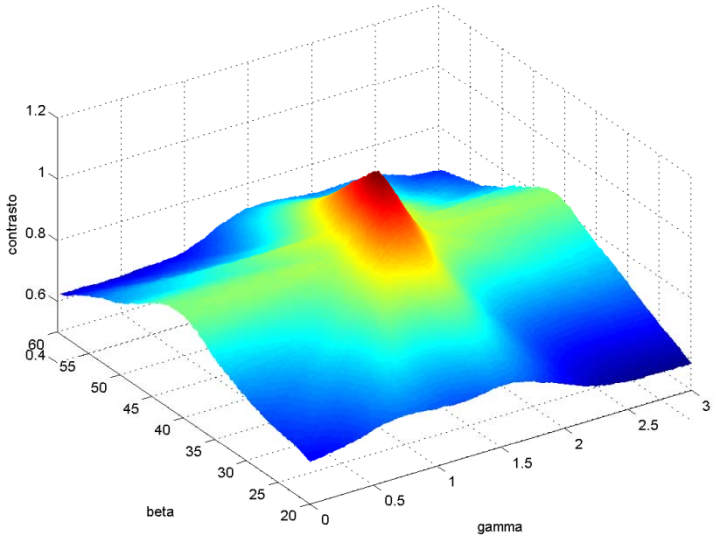

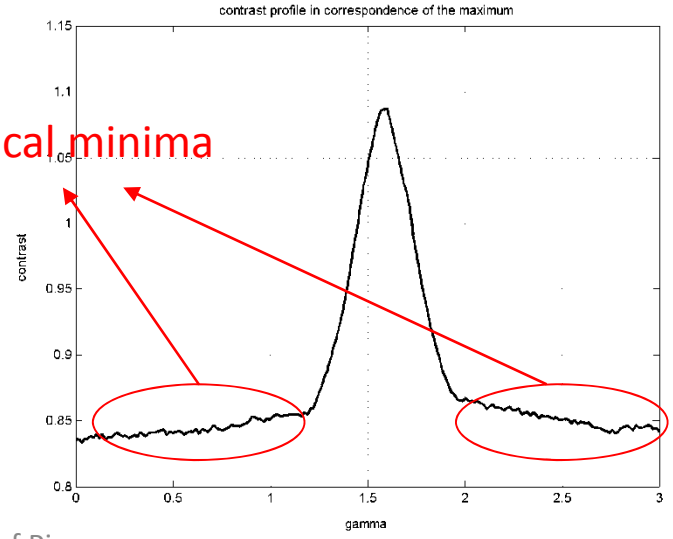

Image Contrast Based Autofocusing

Two focusing parameters

• Classic optimisation techniques, such as Steepest Descend, Newton or Nelder-Mead can be used to find the optimal solution if a good initial guess is provided;

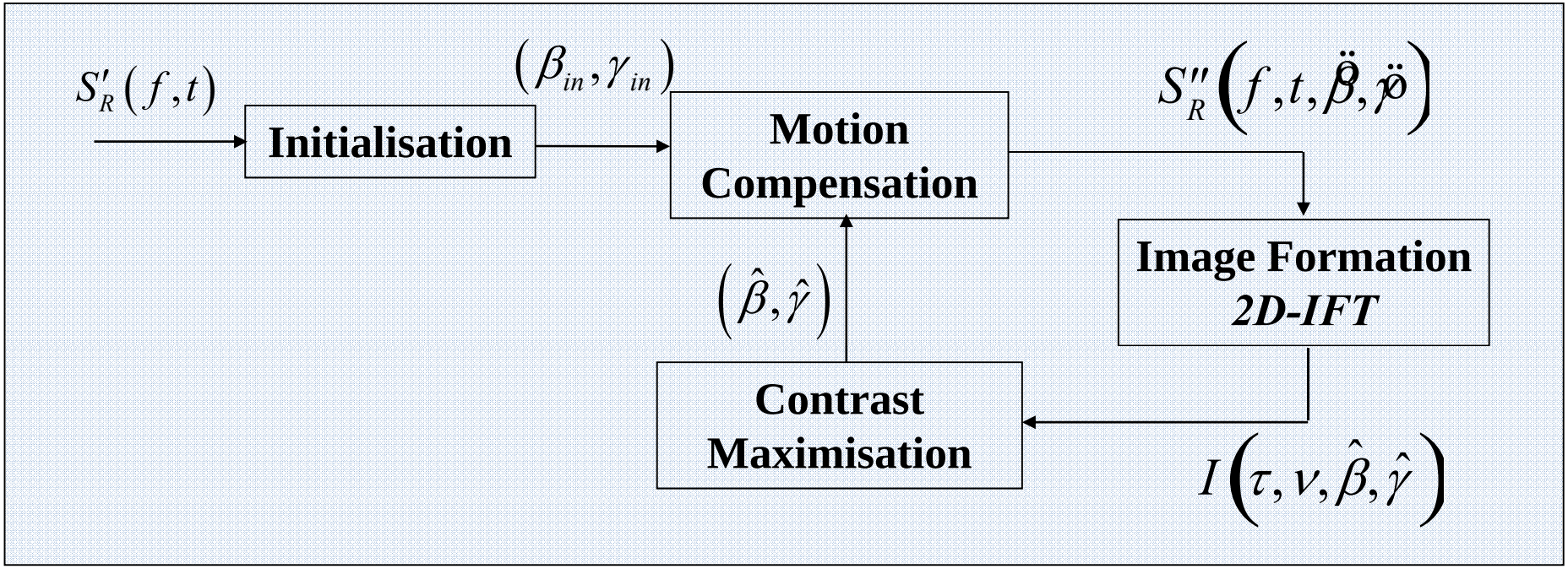

Stop criterion:
The iterations stop when the Euclidean distance between two consecutive estimates is smaller than a given quantity.

Initialisation – estimation of β

$S'_R(f,t)$ → FFT $(f \rightarrow \tau)$ → $\tilde{S}'_R(\tau,t)$

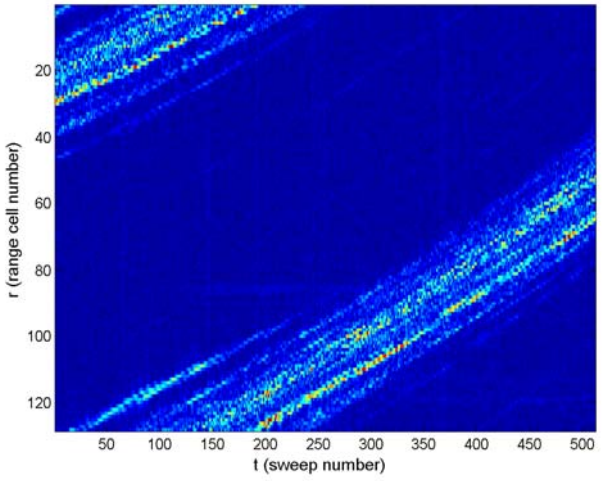

Radon Transform

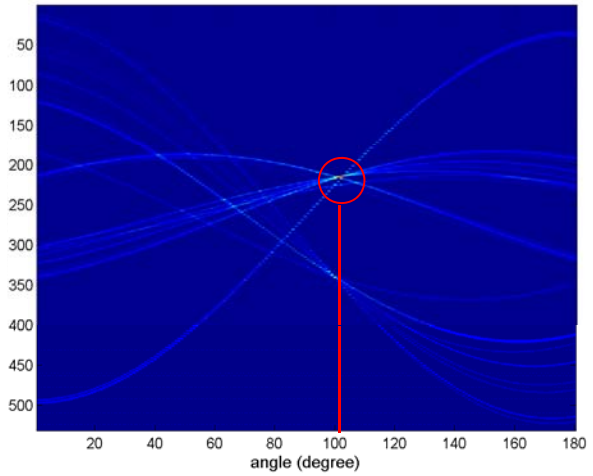

$$\hat{\phi} = \arg\left\{\max_{\phi}\left[RT_{S_R}(r,\phi)\right]\right\} - \frac{\pi}{2}$$

Estimation of the radial velocity (β)

$$\hat{\beta}^{(in)} = tg\left(\hat{\phi}\right)$$

Initialisation – estimation of γ

• The estimate γ^{in} is obtained by means of an exhaustive line search, over the variable γ, of the maximum of the image contrast in a pre-defined interval

$$\hat{\gamma}^{(in)} = \arg\left(\max_{\gamma}\left[IC\left(\hat{\beta}^{(in)},\gamma\right)\right]\right) \qquad \gamma_{\min} \le \gamma \le \gamma_{\max}$$

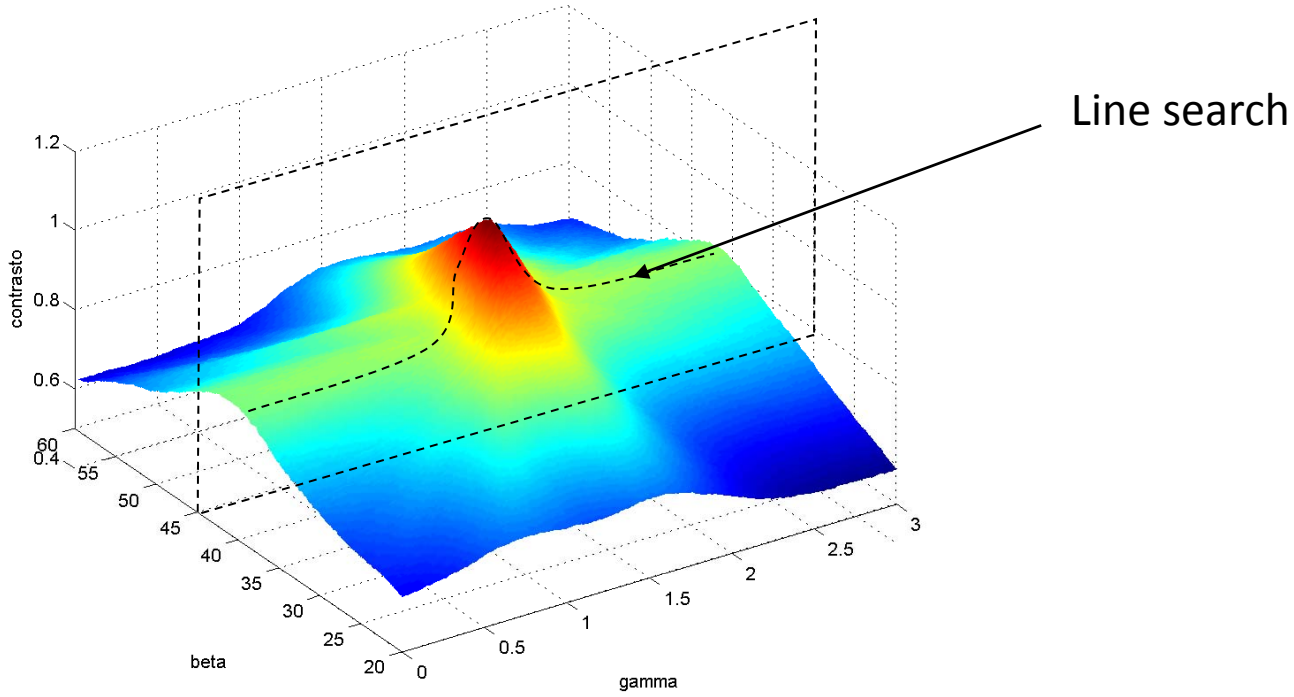

Phase Model Order

The polynomial order of the received signal phase associated with the target phase centre must be chosen wisely:

- high orders give a better approximation of the target radial motion

- low orders provide a faster autofocusing process

Trade off

The polynomial order depends on the length of the integration time and on the target motions.

When the integration time is long, the target radial motion cannot be modeled by, means of low order polynomials

Phase Model Order

Second order model for $R_0(\tau)$

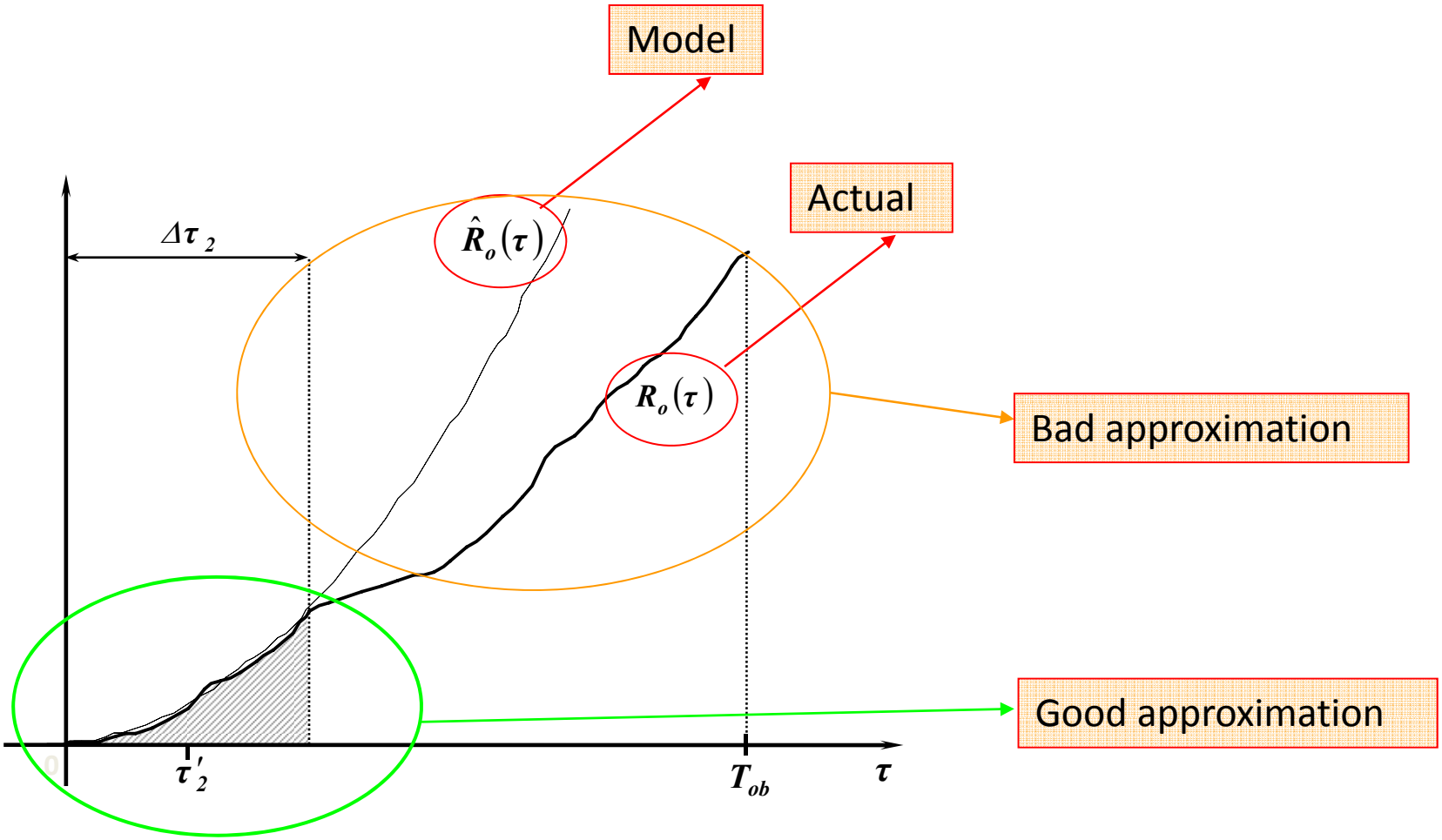

Image Entropy

• The same principle can be applied by using a different cost function. This is the case of the Minimum Entropy Autofocusing (MEA).

• Image Entropy:

$$IE(\alpha) = -\int\int \ln\left(\bar{I}(\tau,\nu;\alpha)\right)\bar{I}(\tau,\nu;\alpha)\,d\tau d\nu$$

where

$$\bar{I}(\tau,\nu;\alpha) = I^2(\tau,\nu;\alpha) \Big/ A\left(I^2(\tau,\nu;\alpha)\right)$$

A = spatial mean operator

The focusing parameter estimates are obtained by solving an equivalent optimisation problem:

$$\hat{\alpha} = \arg\left(\min_{\alpha}\left[IE(\alpha)\right]\right)$$

Non-parametric techniques: Prominent Point Processing (PPP)

The principle ideas for this technique were obtained by delving into two other areas of research, namely time delay estimation and adaptive beamforming.

Step 1: Rough Range bin alignment

A rough range bin alignment can be obtained by means of a cross-correlation. In fact, by assuming that the range profiles do not change too much within two adjacent sweeps, the delay, and hence the range offset, between two adjacent sweeps can be measured and compensated by means of a cross-correlation. Such an operation is iterated through all the range profiles.

$$\Delta\tau_{i,i+1} = \arg\left\{\max_{\eta}\left[\int \left|\tilde{S}'_R(\tau,i)\right|\left|\tilde{S}'_R(\tau+\eta,i+1)\right|d\tau\right]\right\}$$

where

$\tilde{S}'_R(\tau,i)$ is the i-th range profile

$\tilde{S}'^{*}_R(\tau+\eta,i+1)$ is the complex conjugated of the $(i+1)$-th range profile

Range shift (circular):

$$\%\%\left(\tau,i+1\right) = \%\%\left(\tau-\Delta\tau_{i,i+1},i+1\right)$$

Non-parametric techniques: Prominent Point Processing (PPP)

Step 2: Phase Conjugation

The phase Conjugation represents a refinement of the range bin alignment. In fact, in order to obtain a satisfactory motion compensation, it is necessary to align the range bin with an accuracy comparable with one tenth of the radar wavelength.
Because the rough range alignment cannot reach an accuracy finer than the range bin resolution, a refinement must be performed.

- Firstly, the most stationary range cell must be found. Such a selection is performed by measuring the amplitude variance and by choosing the range cell with minimum variance.
- The phase history relative to the selected range cell is stored and used to compensate the phase histories of all the range cells (Phase Conjugation).

$$S_R''(\tau,t) = \tilde{\tilde{S}}_R'(\tau,t)\exp\left[-j\varphi_0(t)\right] \qquad -T_{obs}/2 < t < +T_{obs}/2$$

Where $\varphi_0(t)$ is the phase history of the minimum variance range cell.

Such an algorithm is also called PPP because often the MV range cell is given by a prominent scatterer.

Non-parametric techniques: Prominent Point Processing (PPP)

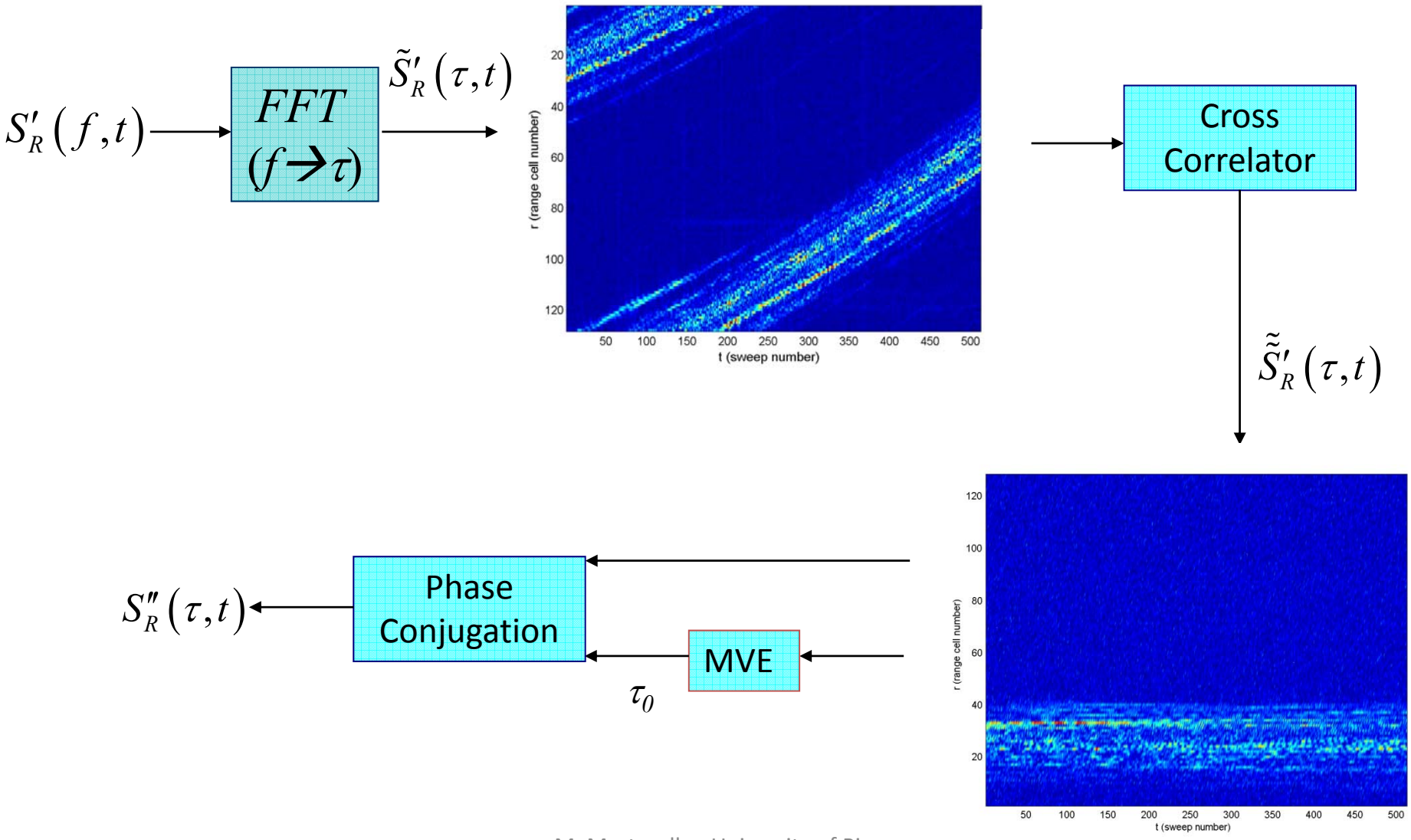

Non-parametric techniques: Phase Gradient Algorithm (PGA)

• The PGA is another technique that is able to perform a phase adjustment. The limitation provided by the PPP regarding the fact that a prominent stable scatterer is needed within the scene, is here overcome.

• In fact, the PGA performs a phase estimation refinement by considering the whole scene.

• The PGA is directly obtained by exploiting the Maximum Likelihood Estimation (MLE).

Let the aligned range bins be represented by the discrete time signal:

$$\tilde{\tilde{S}}'_R(k,n) = S_C(k,n)\exp\left[j\varphi_\varepsilon(n)\right]$$

where $\varphi_\varepsilon(t)$ is the residual phase to be compensated and is the perfectly compensated signal. It is worth noting that the residual phase is assumed to be the same for each range cell *k.*

The phase adjustement can be obtained by estimating the residual phase $\varphi_\varepsilon(t)$

Non-parametric techniques: Phase Gradient Algorithm (PGA)

The residual phase estimation is obtained by means of the sum of the phase difference estimates

Residual phase estimator:

$$\ddot{\varphi}_{\varepsilon}(n) = \sum_{l=2}^{n} \Delta\varphi(l)$$
$$\ddot{\varphi}_{\varepsilon}(1) = 0$$

where

$$\Delta\varphi(n) = \angle \sum_{k=1}^{K} \tilde{\tilde{S}}'_R(k,n)\, \tilde{\tilde{S}}'^{*}_R(k,n-1)$$

The calculation of the angle of the sum of all the range cell contribution is more robust with respect to the noise. Such a result is directly derived from the theory of the MLE.

Non-parametric techniques: Phase Gradient Algorithm (PGA)

The first estimate often shows poor accuracy. An iterative calculation of the residual phase increases the accuracy of the estimator.

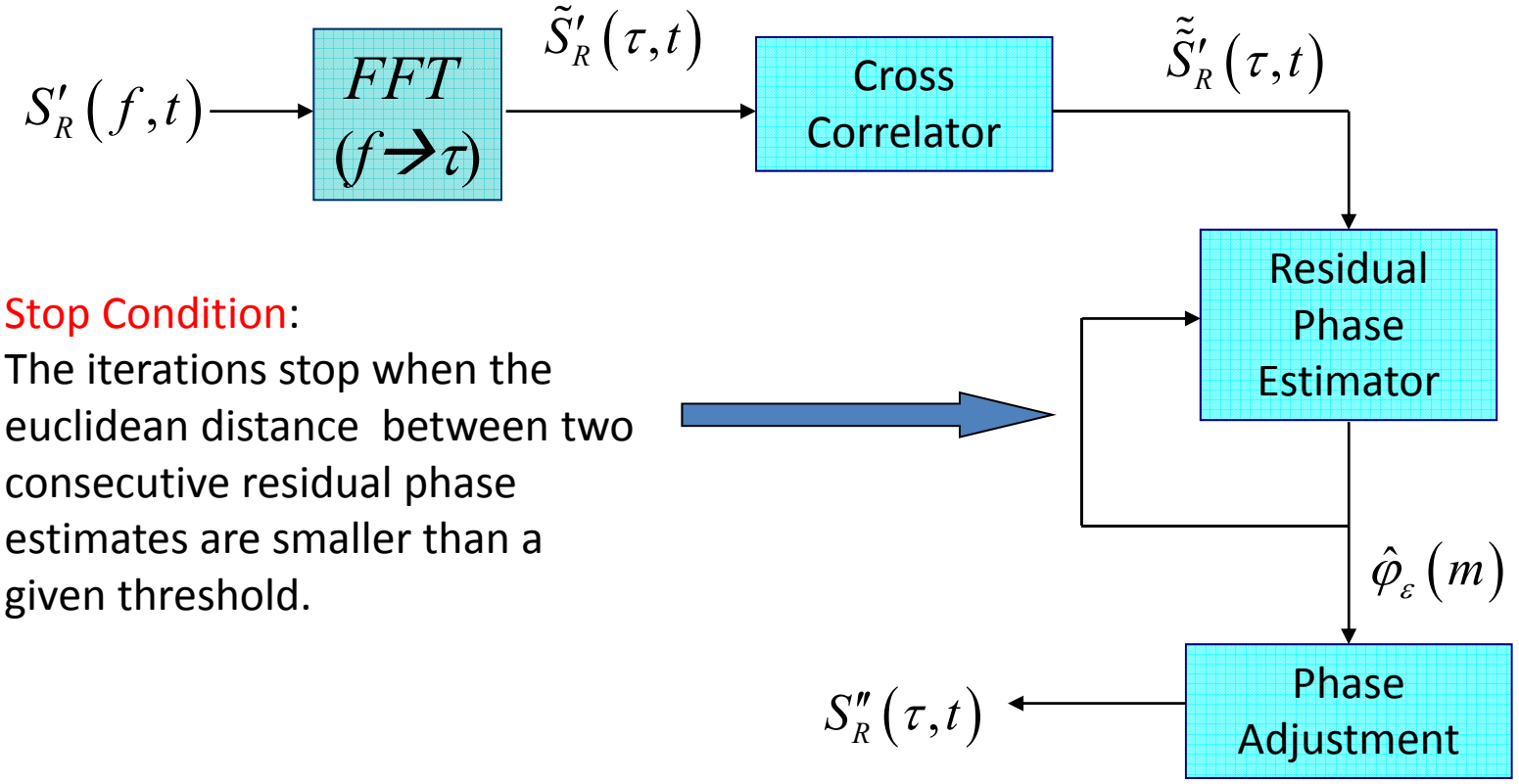

Stop Condition:
The iterations stop when the euclidean distance between two consecutive residual phase estimates are smaller than a given threshold.

Comparisons

- Each of the ISAR autofocusing techniques mentioned here have pro and cons.

- Because the final use of ISAR is the target classification or identification, the choice of the best technique is correlated to the performance of the Automatic Target Recognition (ATR) system.

- Nevertheless, it is possible to evaluate the performances of the autofocusing techniques by defining parameters that act as performance indicators.

- The comparison analysis we proposed is based on the following criteria:

    - Visual analysis

    - Image Contrast (IC)

    - Image Peak (IP)

    - Computational load (CL)

- Two data sets are analysed: one relative to an airplane and one relative to a ship

Real Data Application: Data Set

Boeing 737

N° of sweeps	512
N° of transmitted frequencies	128
Lowest frequency	9.26 GHz
Frequency step	1.5 MHz
Range resolution	0.78 m
Radar height (h_s)	Ground level
Target type	Boeing 737
PRF/Sweep Rate	20 kHz / 156.25 Hz
Data time length	3.27 s

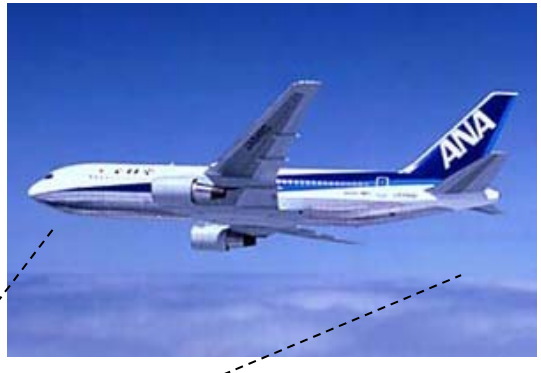

Radar based on the ground

Bulk Carrier

N° of sweeps	256
N° of transmitted frequencies	256
Lowest frequency	9.16 GHz
Frequency step	0.6 MHz
Range resolution	0.97 m
Radar height (h_s)	305 m
Target type	Bulk Loader
PRF/Sweep Rate	20 kHz / 78.13 Hz
Data time length	65 s

Radar carried by a C-130

Visual analysis: airplane

PPP

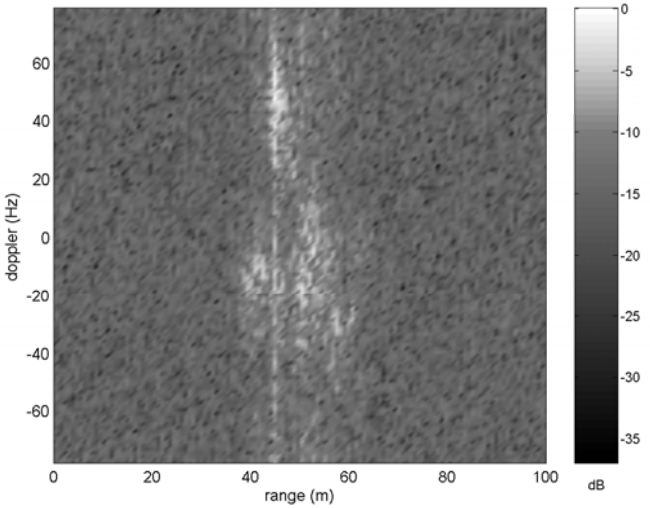

PGA

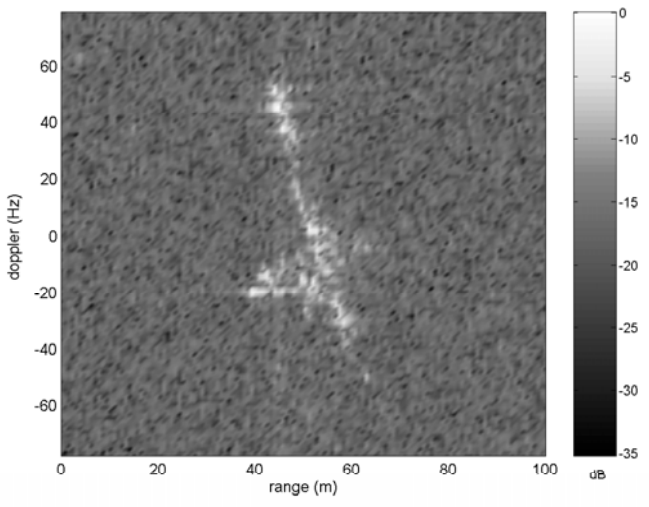

MEA

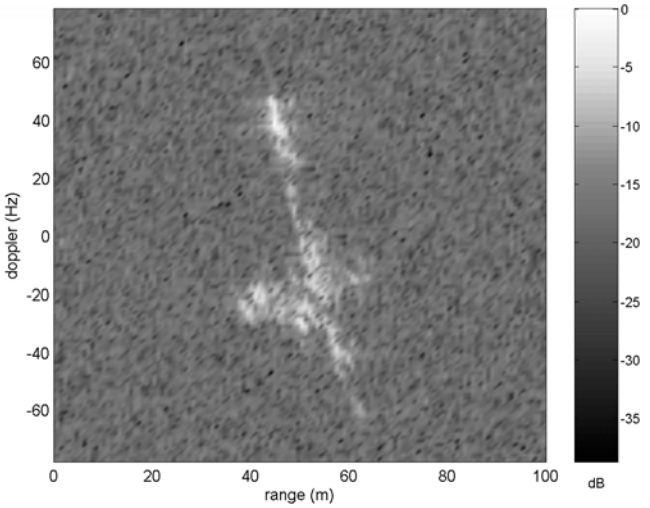

ICBT

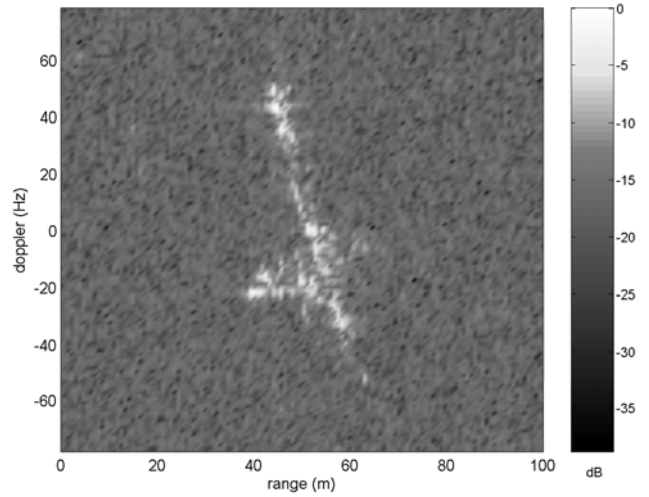

Visual analysis: ship

PPP

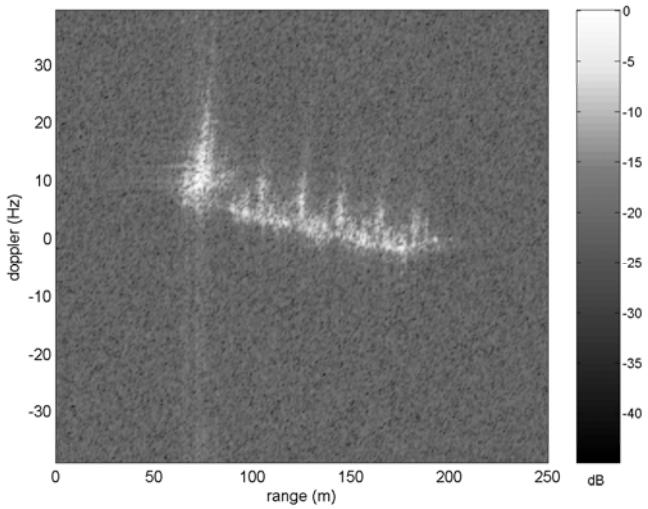

PGA

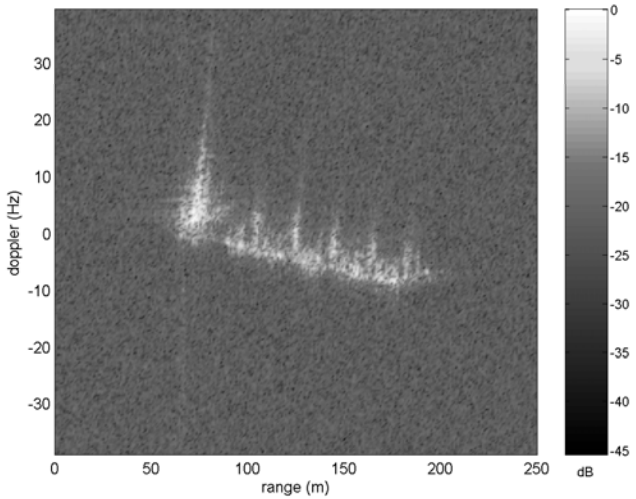

MEA

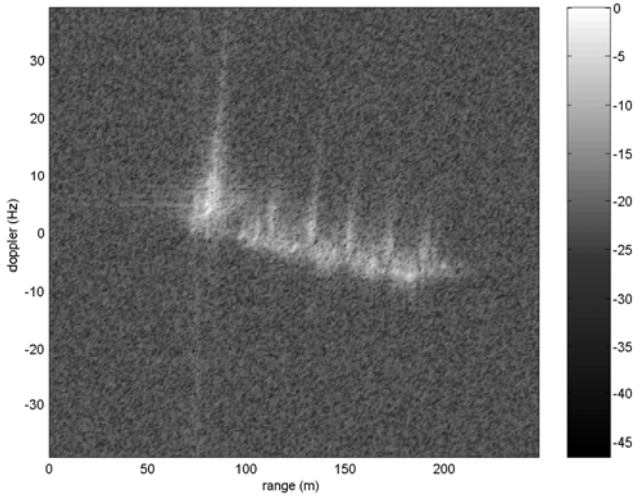

ICBT

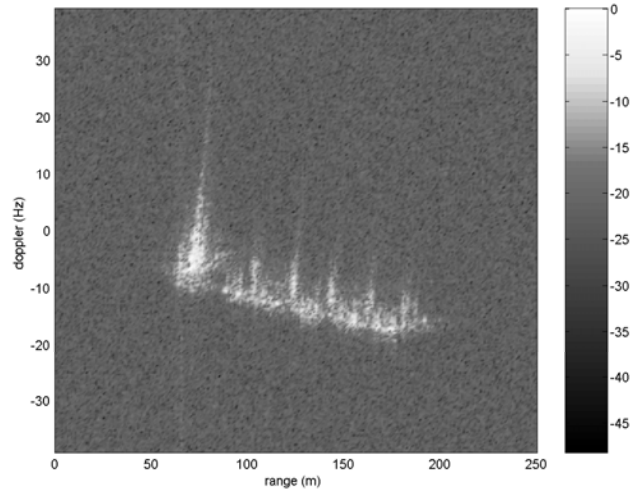

Comparisons

	Image Contrast		
	Bulk loader	***737 1:128***	***737 129:256***
PPP	1.84	1.01	1.14
PGA	1.90	1.24	1.14
MEA	1.88	1.29	1.20
ICBT	1.96	1.29	1.23

	Image Peak (dB)		
	Bulk loader	***737 1:128***	***737 129:256***
PPP	41.96	37.03	38.85
PGA	42.22	39.51	38.62
MEA	44.31	42.30	39.83
ICBT	44.57	42.36	40.20

Computational Load

- Both the PPP and PGA are roughly ten times faster than the MEA nad the ICBT.

- An image of 128x128 pixels can be focused in 0.1 s by means of the PPP and PGA and in 1-2 seconds by means of the MEA and ICBT.

- Even so, the higher CL of the MEA and ICBT is still acceptable for real-time applications.

TIME WINDOW SELECTION

ISAR image Formation

In ISAR scenarios the integration time is strongly affected by the target non-cooperation. In fact, the irregular mapping of the received signal samples onto the Fourier domain provokes image distorsions.

Typical target oscillations, which are usually unknown, produce an irregular and ambiguous mapping on the Fourier domain. The irregularity and ambiguity can be removed only by knowing the time-variation of the target aspect angle.

- In order to have a regularly sampled grid in the Fourier domain, the rotation vector must be constant.

- When the rotation vector is time varying, the polar grid is unevenly sampled

- When the rotation vector is described by a non-monotonic function of the time, the sample locations in the Fourier domain are ambiguous

When the integration time is short, we can assume that a constant or at least almost constant rotation vector is present.

Problem of time-windowing!!!

THE TIME-WINDOW SELECTION PROBLEM

256 sweeps – 3.27 s

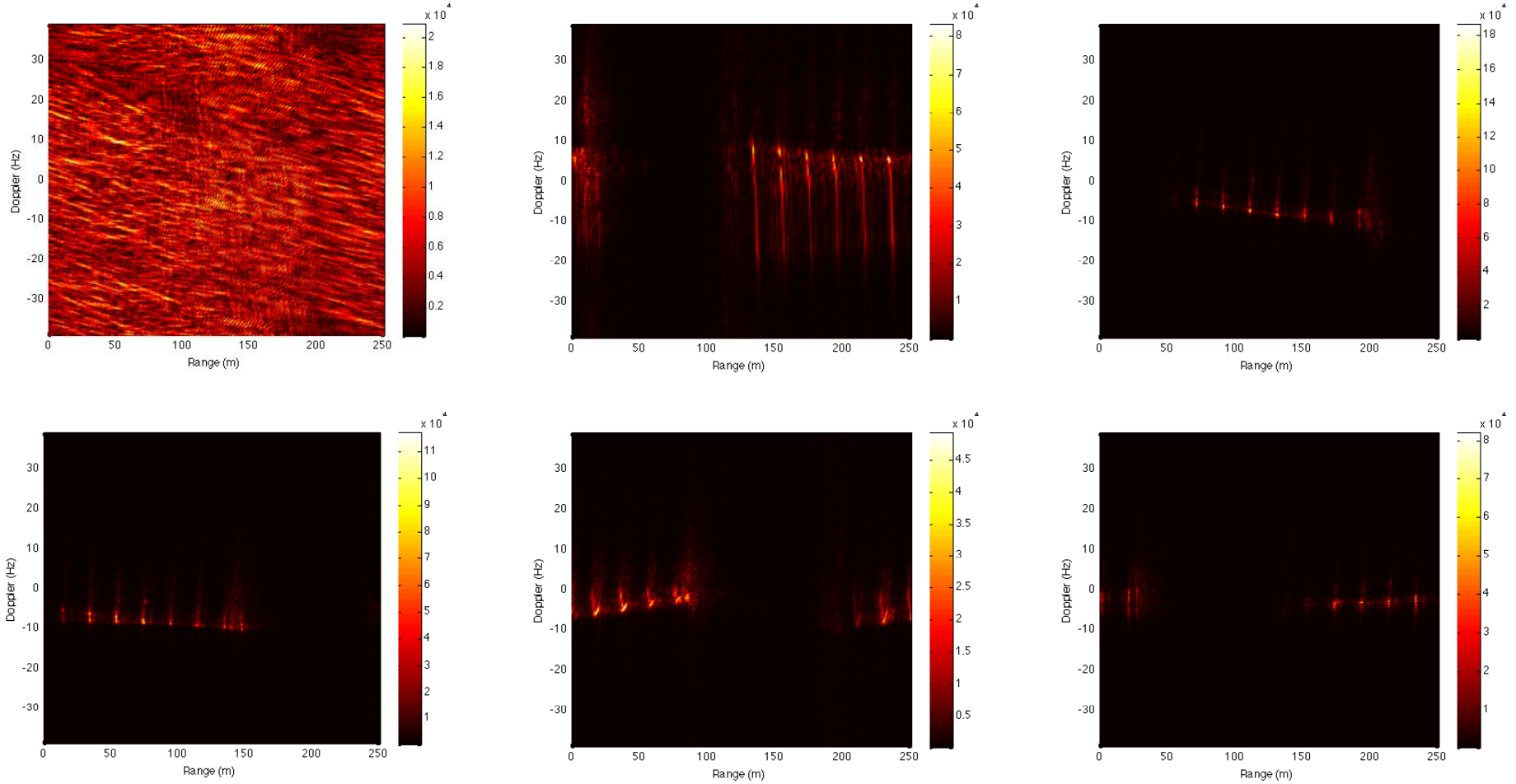

THE TIME-WINDOW SELECTION PROBLEM

64 sweeps – 0.82 s

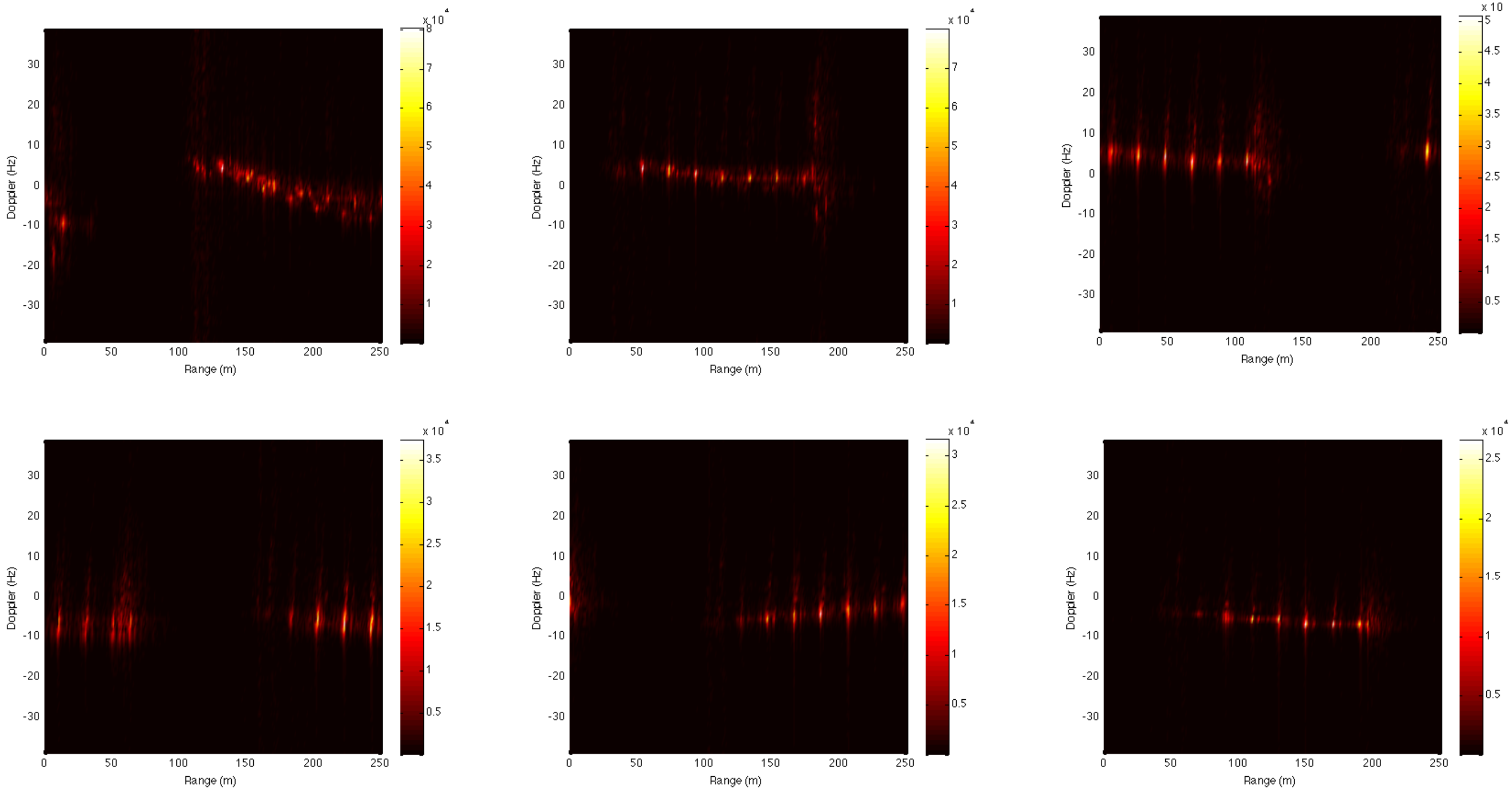

THE TIME-WINDOW SELECTION PROBLEM

96 sweeps – 1.23 s

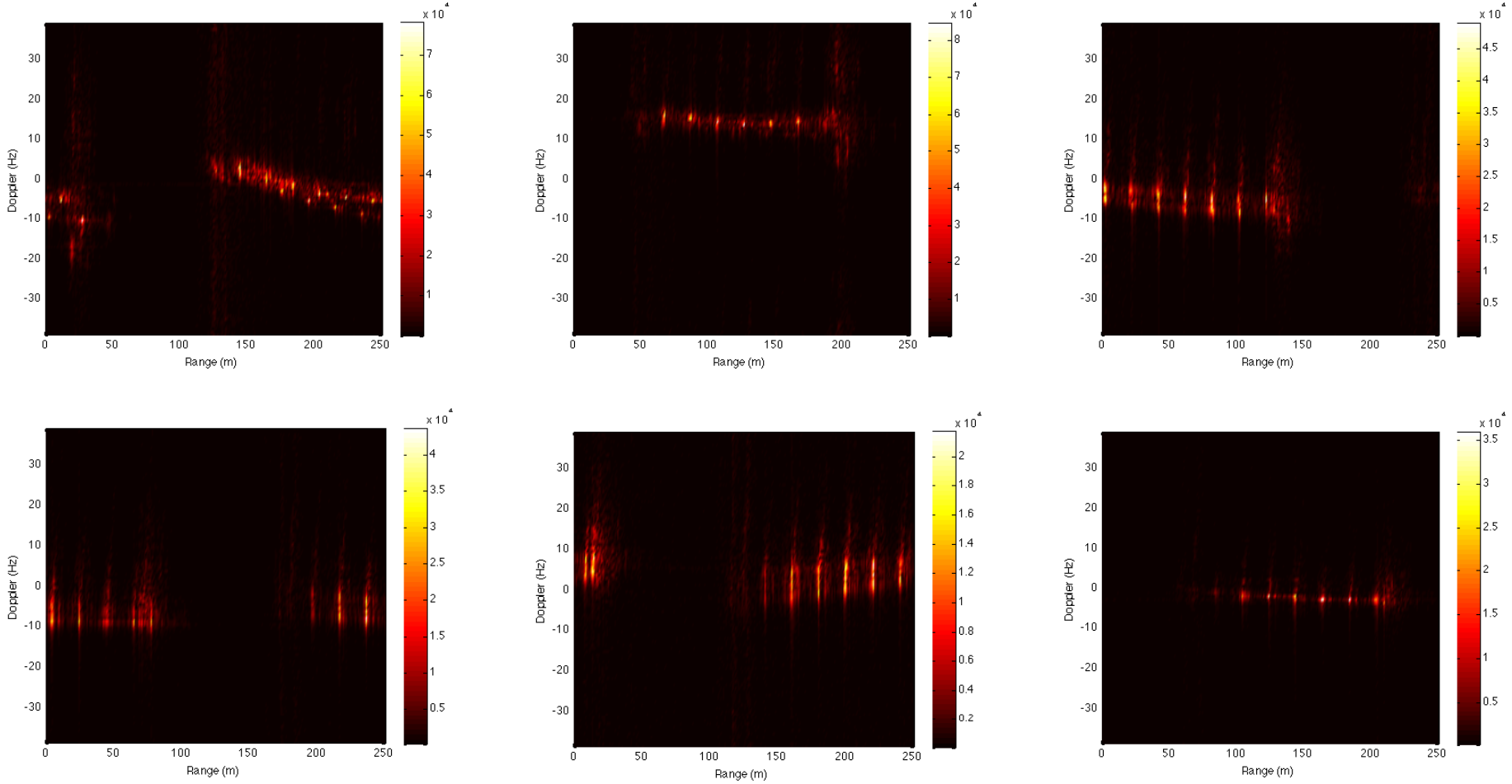

ISAR image Formation

• When a short integration time is used, the total aspect angle variation achieved is generally limited to a few degrees.

• In this condition, the best ISAR image formation to use is the Range-Doppler.

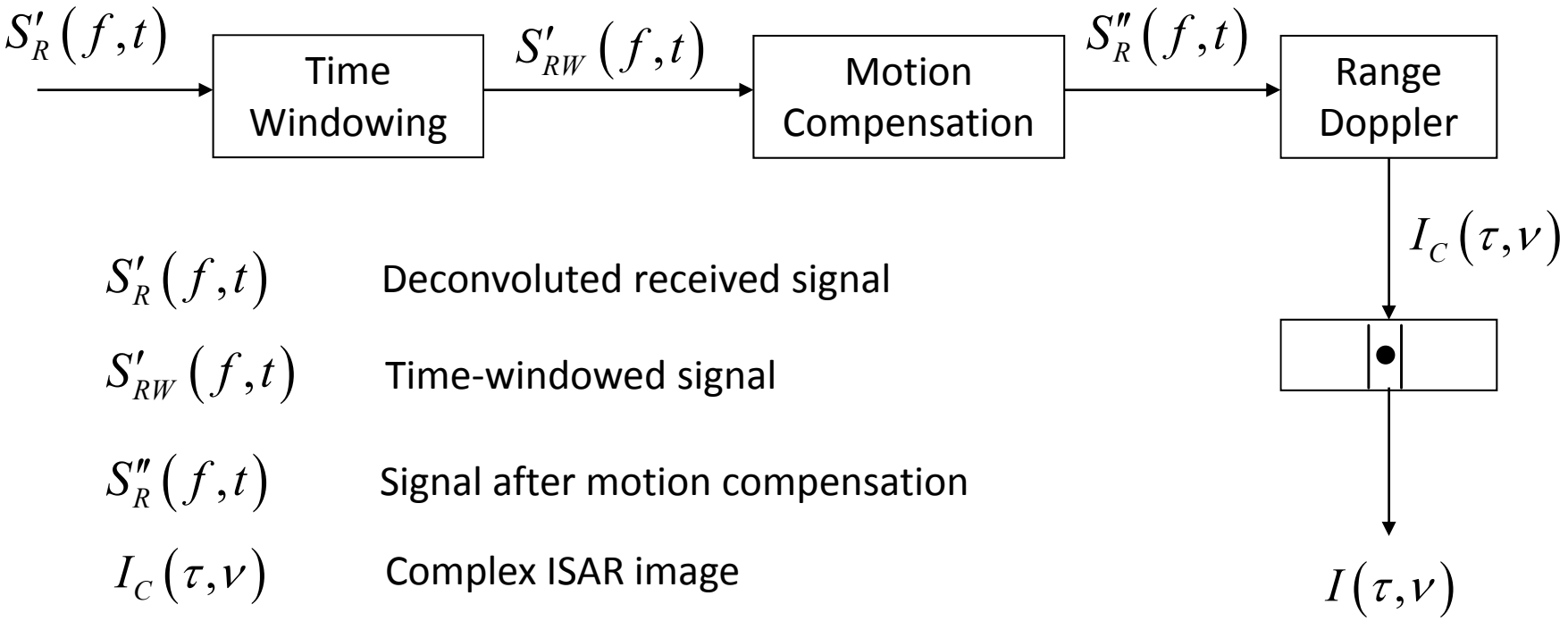

$S'_R(f,t)$ Deconvoluted received signal

$S'_{RW}(f,t)$ Time-windowed signal

$S''_R(f,t)$ Signal after motion compensation

$I_C(\tau,\nu)$ Complex ISAR image

$I(\tau,\nu)$ Intensity ISAR image

Time Windowing

- Given a long recorded data set, we define a window by means of two time parameters, namely τ and Δt_i, which select the data subset to be used to reconstruct the ISAR image.
- By changing the values of τ and $\Delta\tau$, all possible data subsets can be selected.

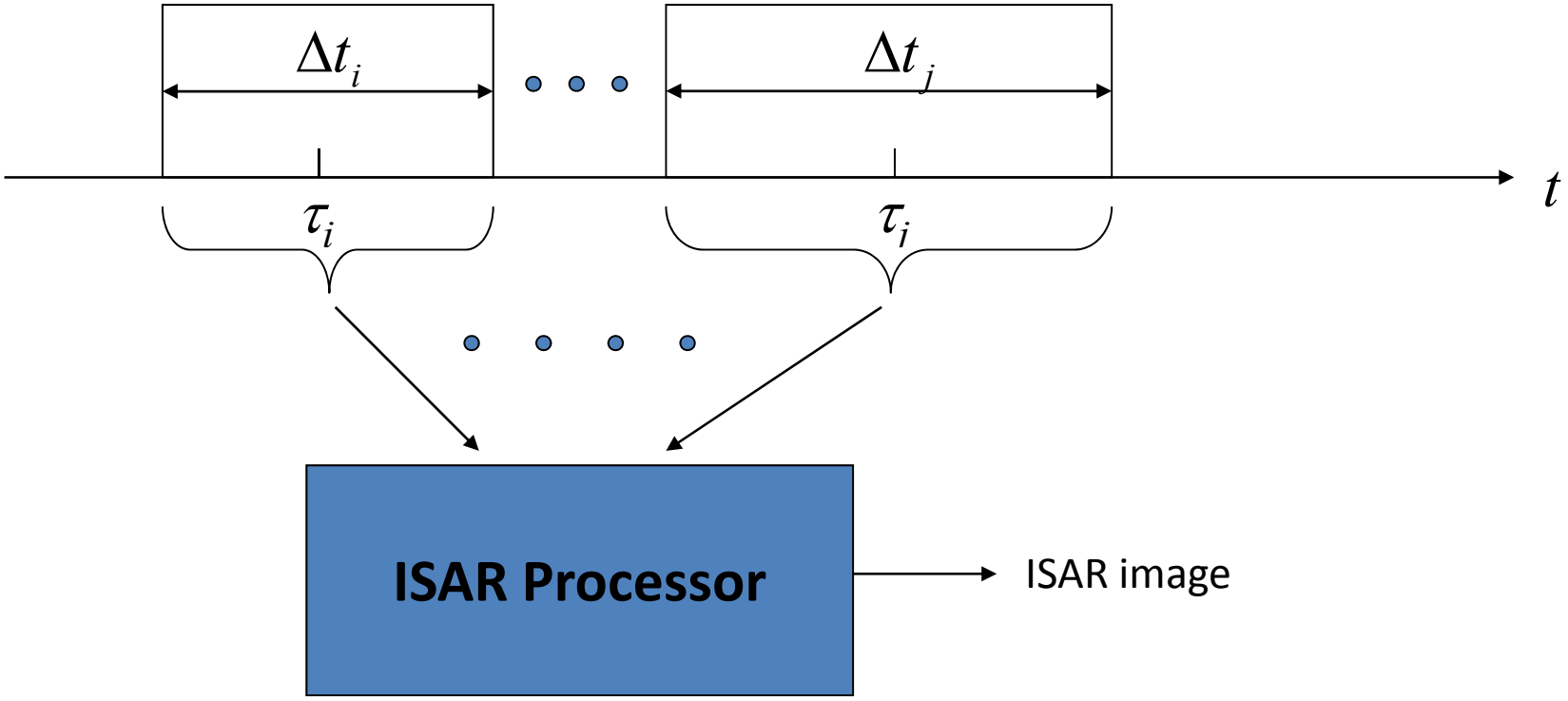

Time Windowing and Contrast Function

As for the motion compensation, we will define an automatic non-aided algorithm for the selection of the optimal time-window for the ISAR image reconstruction.

Given a long recorded data set, we can define two parameters that identify the selection window:

τ = centre of the time window

Δt_i = length of the time window

The optimum criterion is to choose the time window that maximises the IC

$$(\tau, \Delta\tau) = \arg\left\{\max_{\tau,\Delta\tau}\left[IC(\tau,\Delta\tau)\right]\right\}$$

Because τ and $\Delta\tau$ are discrete variables the maximum search problem is not a typical optimisation problem.

A simple solution, based on a trial and error method can be provided by analysing the IC separately for the two variables.

Experimental Results

The analysis of several real data has shown a particular characteristic of the Image Contrast

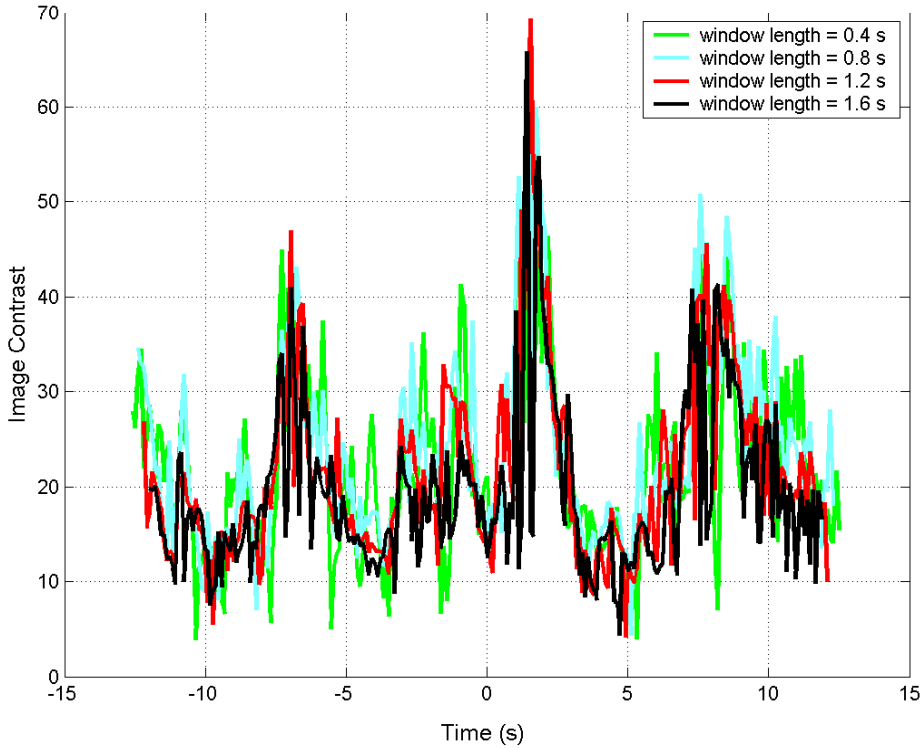

- Apart from slight differences due to noise, the Image Contrast time history looks similar for the four different window sizes;
- Such a characteristic can be exploited to define an optimisation algorithm based on two separated linear searches.

Automatic Search Strategy

Maximum Peak Locator (MPL)

- A sliding window of time length $\Delta t^{(in)}$ is applied to the data in order to produce an Image Contrast time serie $IC(\tau)$;
- The maximum of $IC(\tau)$ is searched and the MPL gives at the output the maximum position τ_{opt}.

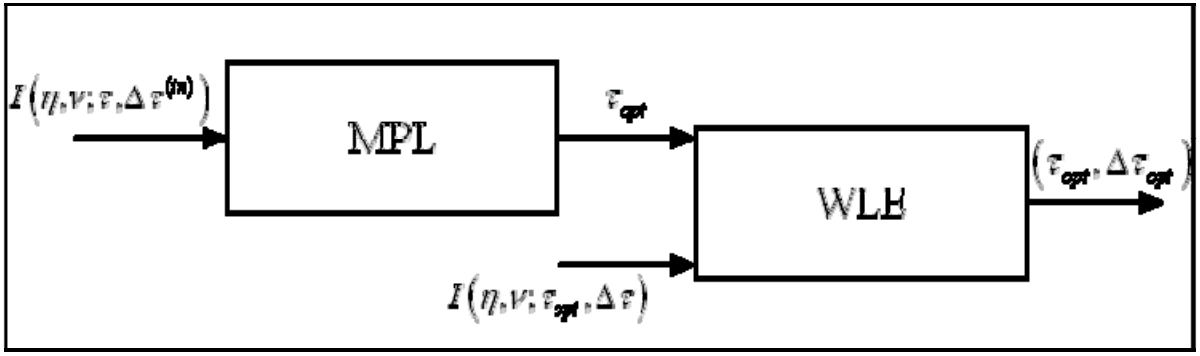

Window Length Estimator (WLE)

- The window time length Δt_{opt} is estimated by defining a new window centred at $\tau = \tau_{opt}$ with a generic time length Δt, which represents the new search domain;
- The maximum of $IC(\tau_{opt}, \Delta t)$ is estimated with respect to Δt and the optimal value of the window length is produced.

Real Data Application: Data Set

Boeing 737

N° of sweeps	512
N° of transmitted frequencies	128
Lowest frequency	9.26 GHz
Frequency step	1.5 MHz
Range resolution	0.78 m
Radar height (h_s)	Ground level
Target type	Boeing 737
PRF/Sweep Rate	20 kHz / 156.25 Hz
Data time length	3.27 s

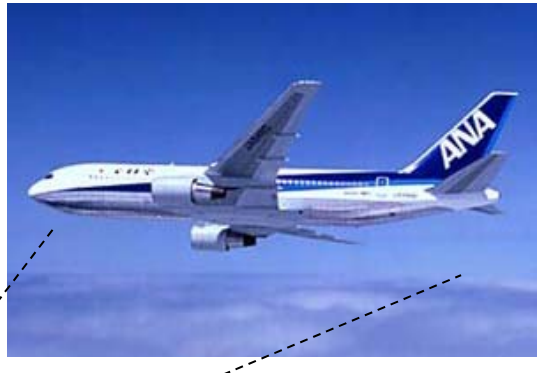

Radar based on the ground

Bulk Carrier

N° of sweeps	256
N° of transmitted frequencies	256
Lowest frequency	9.16 GHz
Frequency step	0.6 MHz
Range resolution	0.97 m
Radar height (h_s)	305 m
Target type	Bulk Loader
PRF/Sweep Rate	20 kHz / 78.13 Hz
Data time length	65 s

Radar carried by a C-130

Real Data Application: Boeing 737

1

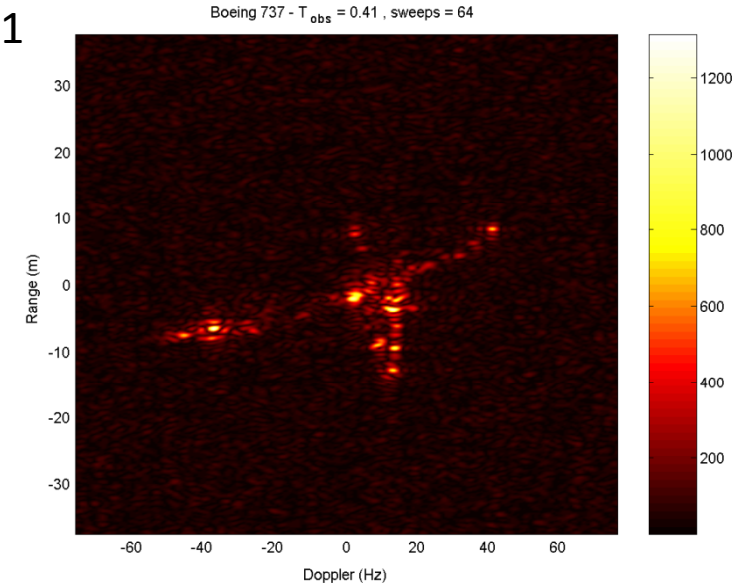

2

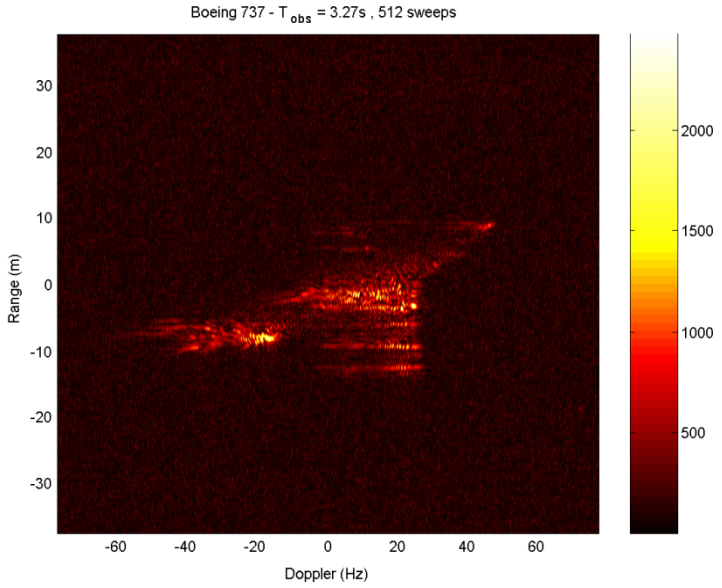

3

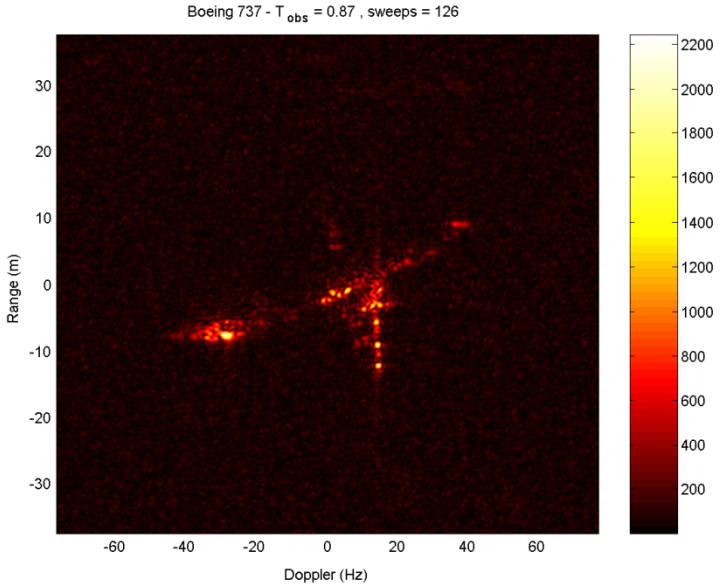

Three ISAR images have been reconstructed by processing different data subsets.

1) Short integration time: Random choice of 64 sweeps (T_{obs} = 0.41 *s*);
2) Long integration time: all the 512 sweeps (T_{obs} = 3.27 *s*);
3) Optimal integration time: 126 sweeps (*Tobs* = 0.87 *s*)

Real Data Application: Bulk Carrier

1

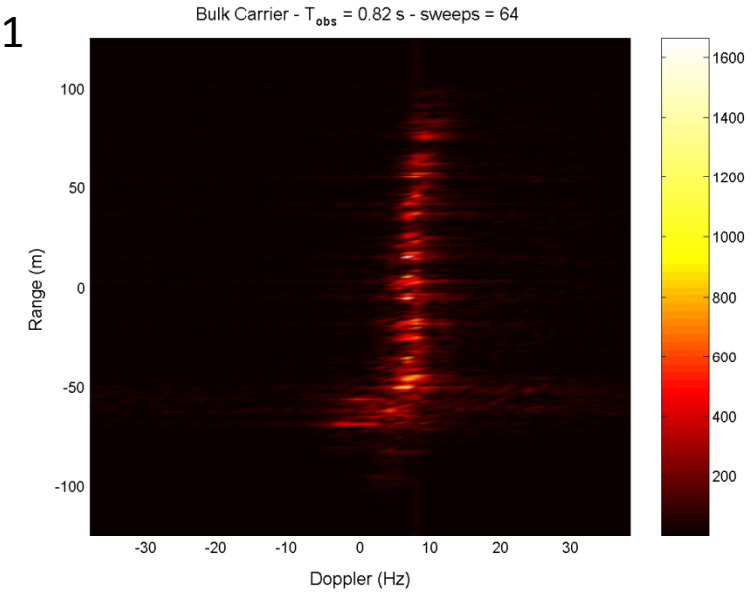

2

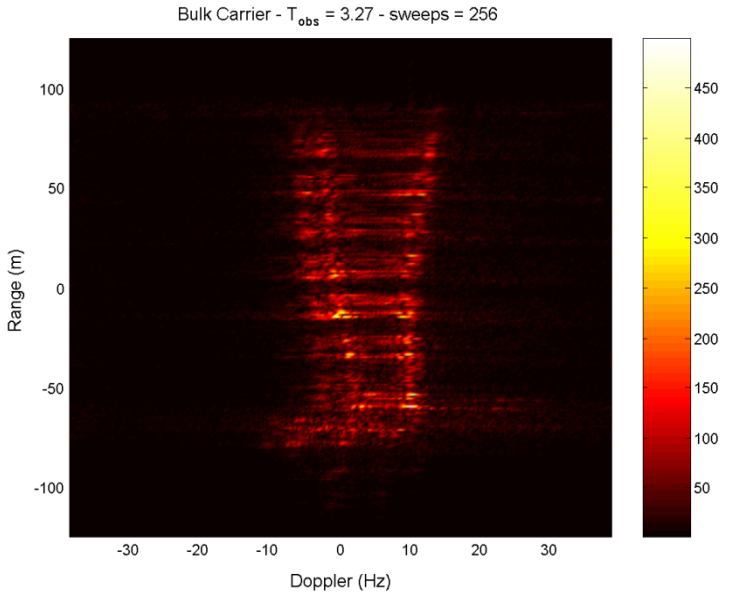

3

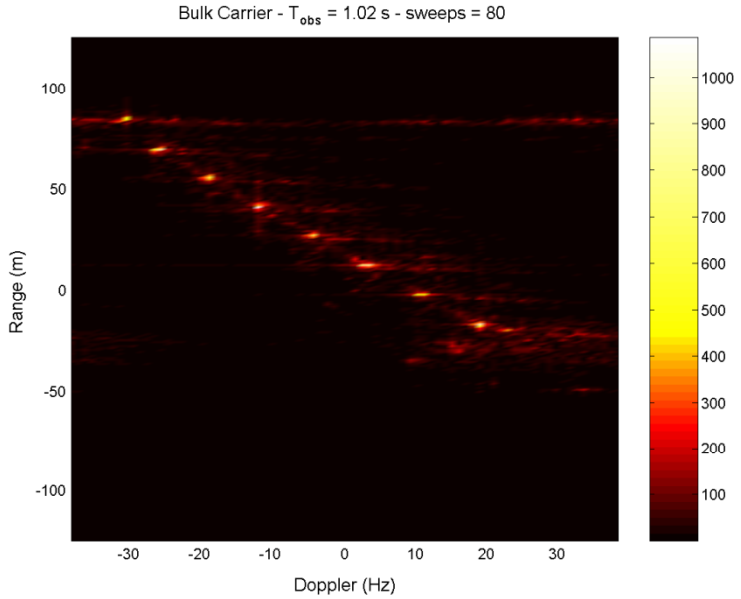

Three ISAR images have been reconstructed by processing different data subsets.

1) Short integration time: Random choice of 64 sweeps (T_{obs} = 0.82 *s*);
2) Long integration time: all the 256 sweeps (T_{obs} = 3.28 *s*);
3) Optimal integration time: 80 sweeps (*Tobs* = 1.02 *s*)

Ad hoc Technique for Ships

Characteristics

- The ship's angular motion is dominant with respect the translational motion
- The Image Plane strongly depends on the target own motions (pitch, roll and yaw)

Idea

- Separate top-view from side-view
- Select the image frame based on the desired view

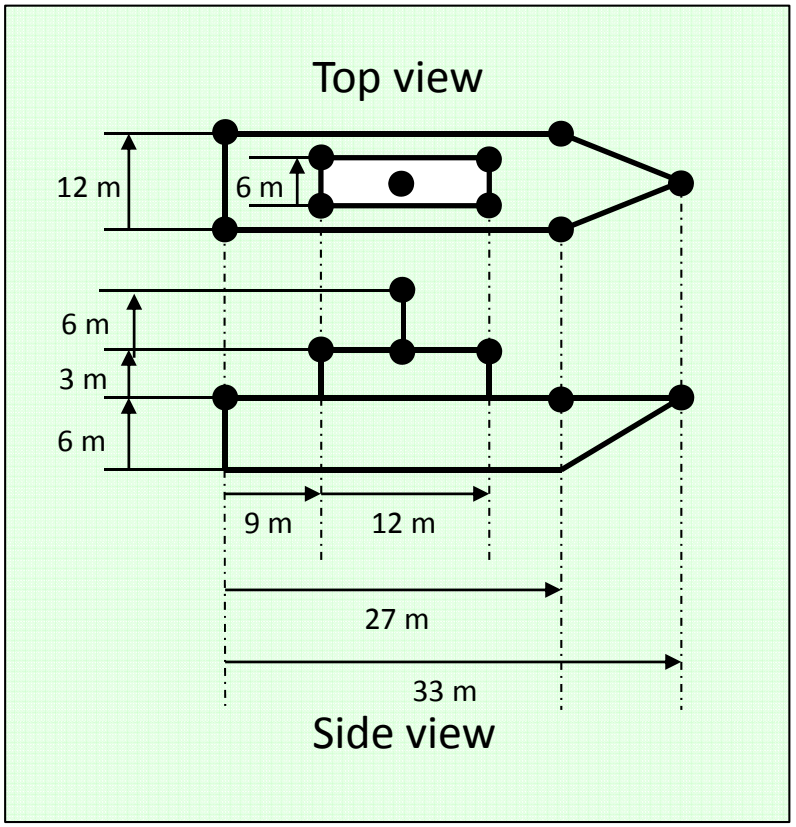

Ad hoc Technique for Ships

Segmentation and time-frame selection

The top-view and side-view portion of the ship ISAR image are quantified as follows:

- A_{tv} = Nr of pixels that are covered by the ship deck
- A_{sv} = Nr of pixels that are covered by the ship superstructure

The top-view images are selected by choosing maximum values of A_{tv} in correspondence of minimum values of A_{sv}

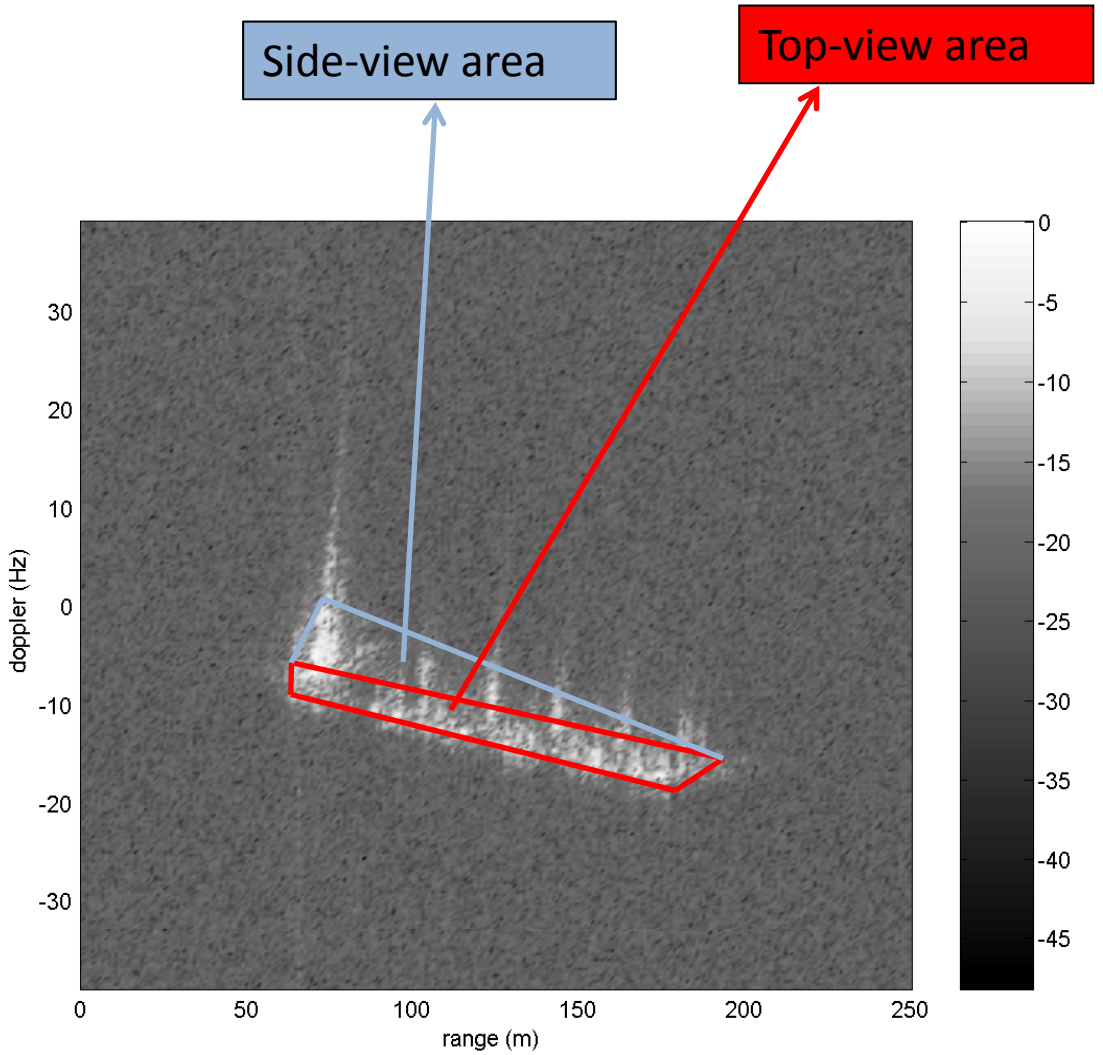

CROSS-RANGE SCALING

Cross-range scaling

• After the application of the Range-Doppler technique, the ISAR image is scaled in fast time ( ) and Doppler ( ).
τ ν

• The ISAR image needs to be scaled in order to be represented in a spatial domain (both range and cross-range)

• The **scaling operations** along the two coordinates are:

$$r = \frac{c}{2}\tau$$ Range coordinate

$$cr = \frac{c}{2 f_0 \Omega_{eff}}\nu$$ Cross-Range coordinate

• In order to scale the **cross-range** coordinate, the knowledge of the modulus of the **effective rotation vector** is required.

• The effective rotation vector depends on the relative motion of the target with respect to the radar, therefore it is usually unknown. Estimation techniques for the effective rotation vector are needed in order to scale the ISAR image.

• When the Image cannot be scaled, it is generally represented in Doppler/meters (**Range-Doppler** representation).

Cross-range scaling

Chirp rate method

Signal modeling

Received signal phase (k-th scattering centre)

$$\varphi_k(f,t) = (-\frac{4\pi f}{c}[(\sin(\Omega_{eff}t))y_{1k} + (\cos(\Omega_{eff}t))y_{2k}])\ rect(\frac{t}{T_{obs}})$$

Received signal phase approximation (k-th scattering centre)

$$\varphi_k(f,t)\ ;\ (-\frac{4\pi f}{c}[(y_{2k} + y_{1k}\Omega_{eff}t - \frac{1}{2}y_{2k}\Omega_{eff}^2 t^2])\ rect(\frac{t}{T_{obs}})$$

Received signal (k-th scattering centre)

$$S_R^{(k)}(\tau,t) = A_k \text{sinc}\left[\text{B}\left(\tau - \frac{2}{c}y_{2k}\right)\right]\exp\left[-j\frac{4\pi f_0}{c}\left(y_{2k} + y_{1k}\Omega_{eff}t - \frac{y_{2k}}{2}\Omega_{eff}^2 t^2\right)\right]\text{rect}\left[\frac{t}{T_{obs}}\right]$$

Cross-range scaling

Chirp rate method

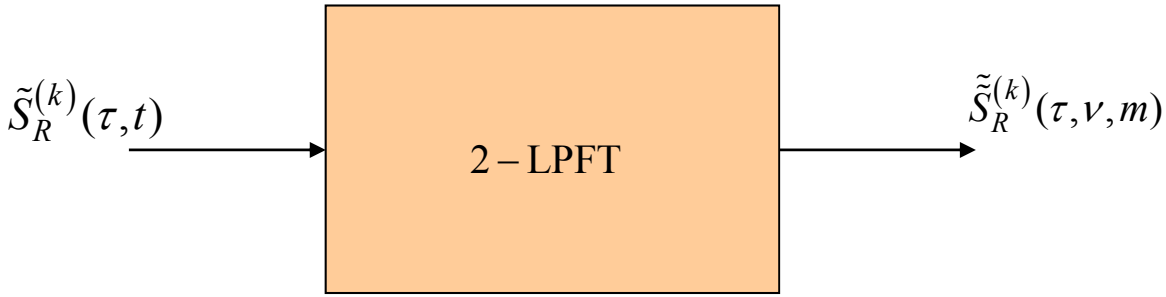

$$\tilde{\tilde{S}}_R^{(k)}(\tau,\nu,m)=\int_{-\infty}^{\infty}\tilde{S}_R^{(k)}(\tau,t)\exp\left[-j2\pi\left(\nu t+\frac{m}{2}t^2\right)\right]dt$$

Relationships

$$m_k = a\, y_{2k}$$

$$a=\frac{2f_0}{c}\Omega_{eff}^2$$

$$\Omega_{eff}=\sqrt{\frac{c}{2f_0}\left|\hat{a}\right|}$$

Estimations

$$\begin{bmatrix}\hat{\nu}_k\\ \hat{m}_k\end{bmatrix}=\arg\max_{\nu,m}\left|\tilde{\tilde{S}}_R^{(k)}(\tau,\nu,m)\right|=\begin{bmatrix}-\frac{2f_0}{c}y_{1k}\Omega_{eff}\\ \frac{2f_0}{c}y_{2k}\Omega_{eff}^2\end{bmatrix}$$

$$\hat{a}=\arg\min_a\left[\sum_{k=1}^{N}\left(m_k-\hat{m}_k\right)^2\right]=\frac{\sum_{k=1}^{N}\hat{m}_k y_{2k}-\frac{1}{N}\sum_{k=1}^{N}\hat{m}_k\sum_{k=1}^{N}y_{2k}}{\sum_{k=1}^{N}y_{2k}^2-\frac{1}{N}\left(\sum_{k=1}^{N}y_{2k}\right)^2}$$

Cross-range scaling

Chirp rate method

The scattering centre separation is accomplished in the image domain

$$I_C(\tau,\nu)=\sum_{k=1}^{K}\tilde{\tilde{S}}_R^{(k)}(\tau,\nu,m=0)$$

via a segmentation approach

$$I_T(\tau,\nu)=\begin{cases} I_C(\tau,\nu) & when \quad |I_C(\tau,\nu)|>\mu \\ 0 & otherwise \end{cases}$$

The image is then segmented by means of a clusterisation

$$I_S(\tau,\nu)=\sum_{n=1}^{N} I_T^{(n)}(\tau,\nu)$$

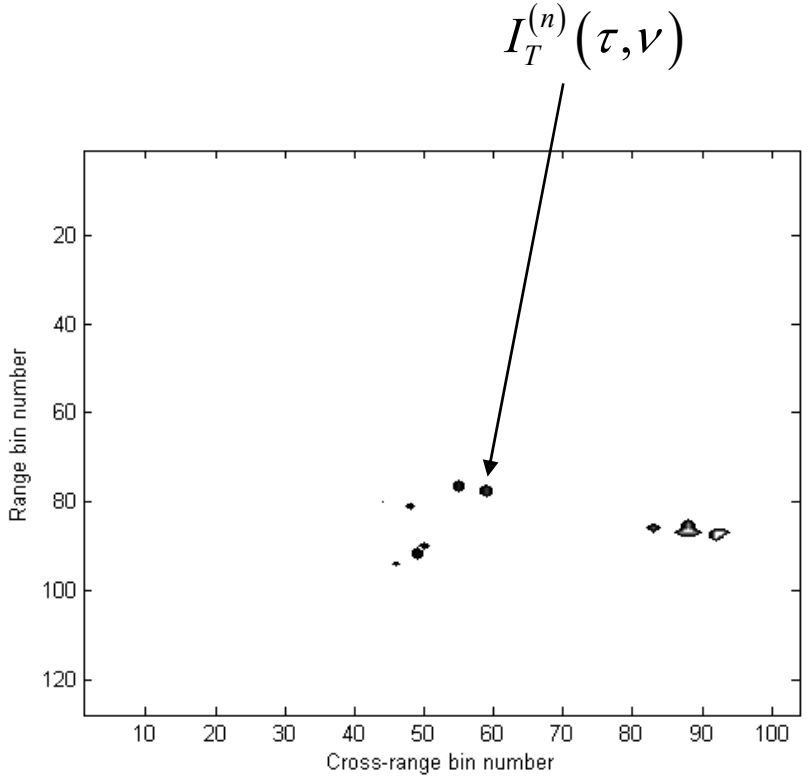

Cross-range scaling

Chirp rate method

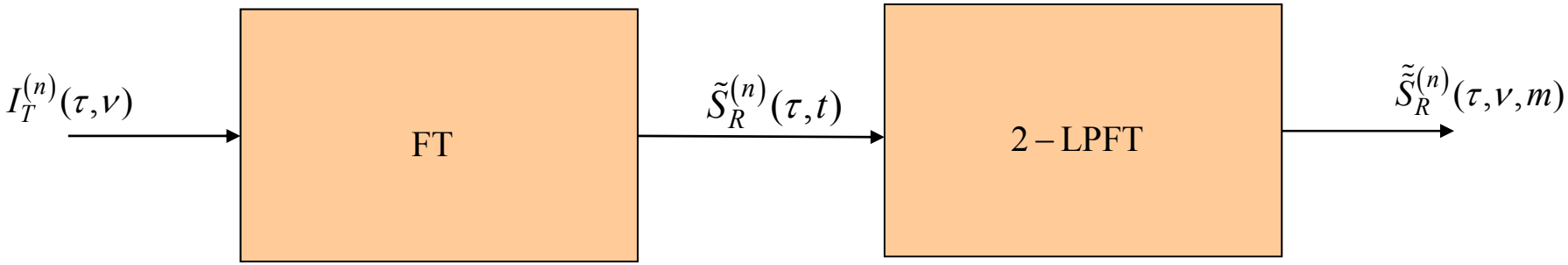

The chirp rate associated with a scattering centre is estimated by maximising the sub-image contrast

$$\hat{m}_n = \arg\max_m \left[IC_n(m) \right]$$

$$IC_n(m) = \frac{\sqrt{A\left\{\left[\left|\tilde{\tilde{S}}_R^{(n)}(\tau,\nu,m)\right| - A\left[\left|\tilde{\tilde{S}}_R^{(n)}(\tau,\nu,m)\right|\right]\right]^2\right\}}}{A\left[\left|\tilde{\tilde{S}}_R^{(n)}(\tau,\nu,m)\right|\right]}$$

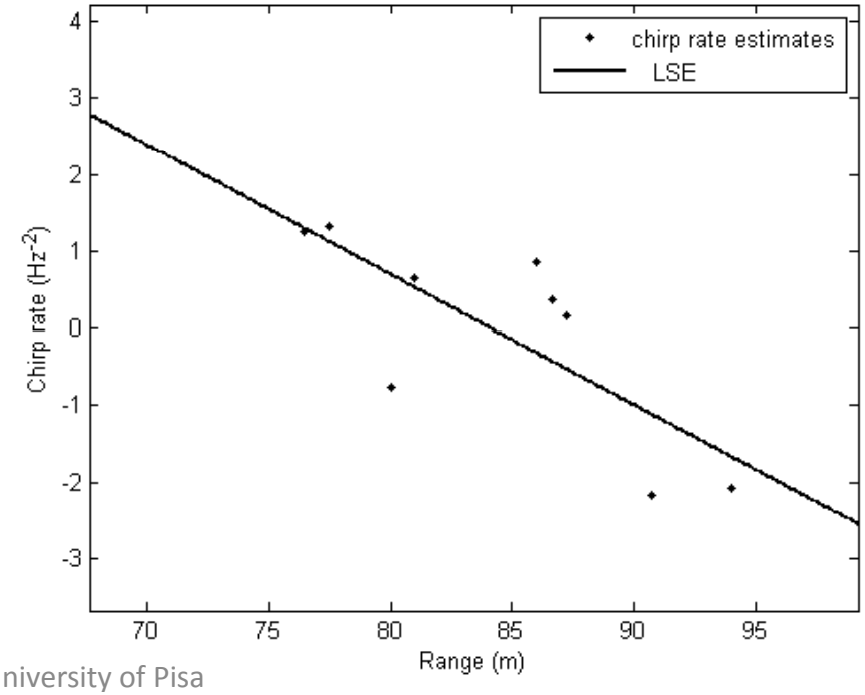

Cross-range scaling

Chirp rate method

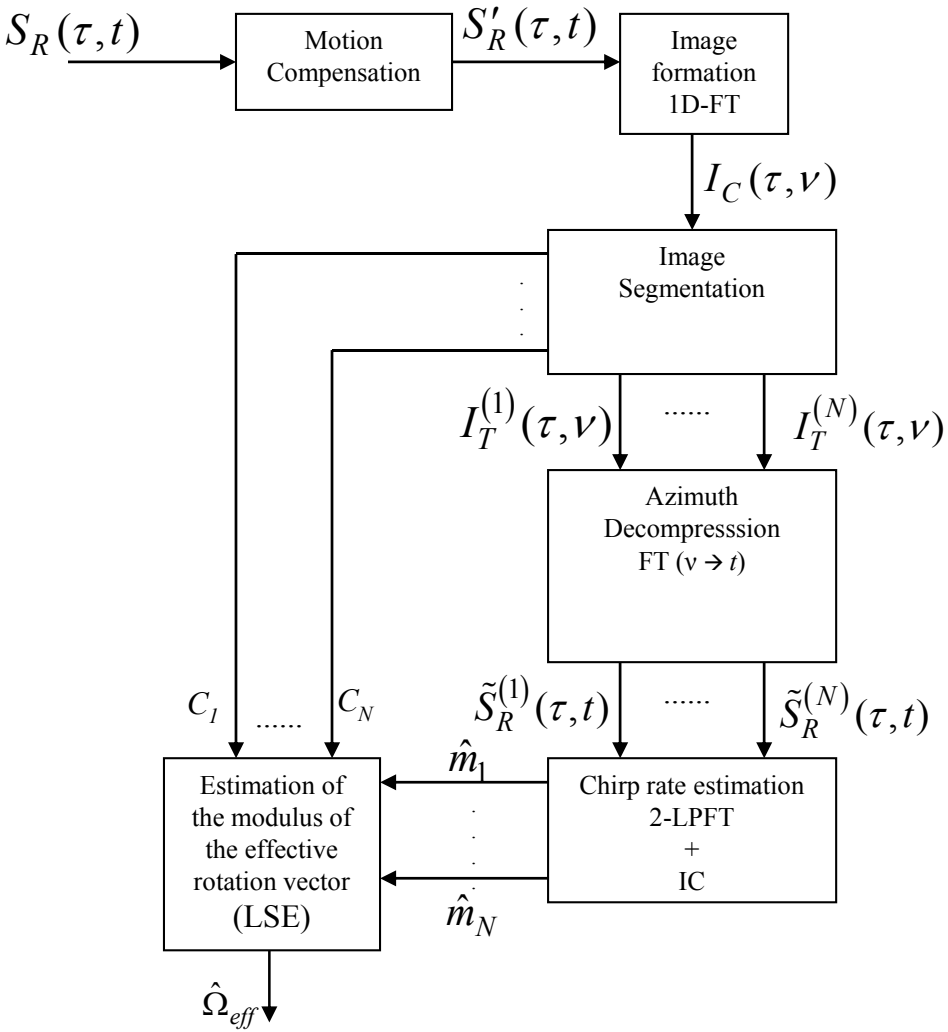

Results

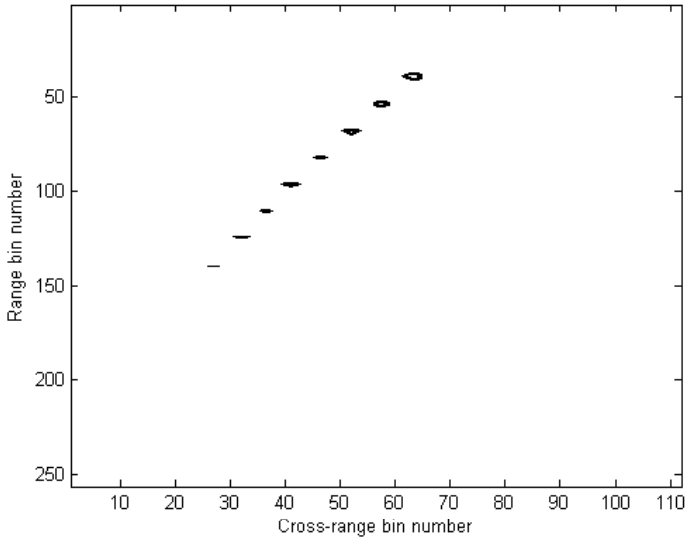
Range bin number
Cross-range bin number
50
100
150
200
250
10
20
30
40
50
60
70
80
90
100
110

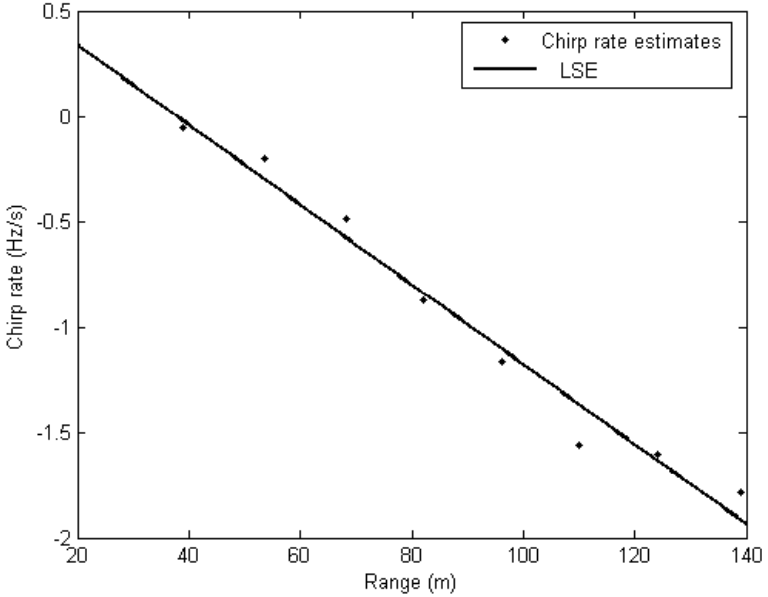
Chirp rate estimates
LSE
Chirp rate (Hz/s)
Range (m)
0.5
0
-0.5
-1
-1.5
-2
20
40
60
80
100
120
140

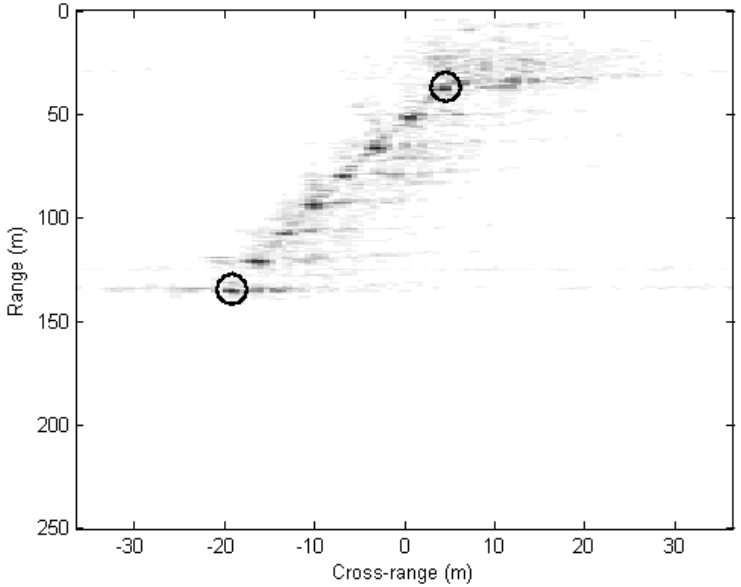
Range (m)
Cross-range (m)
0
50
100
150
200
250
-30
-20
-10
0
10
20
30

Results

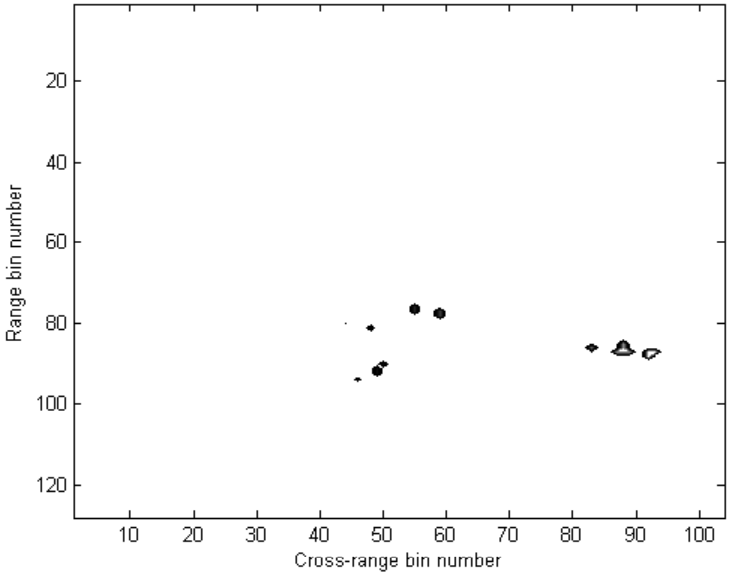

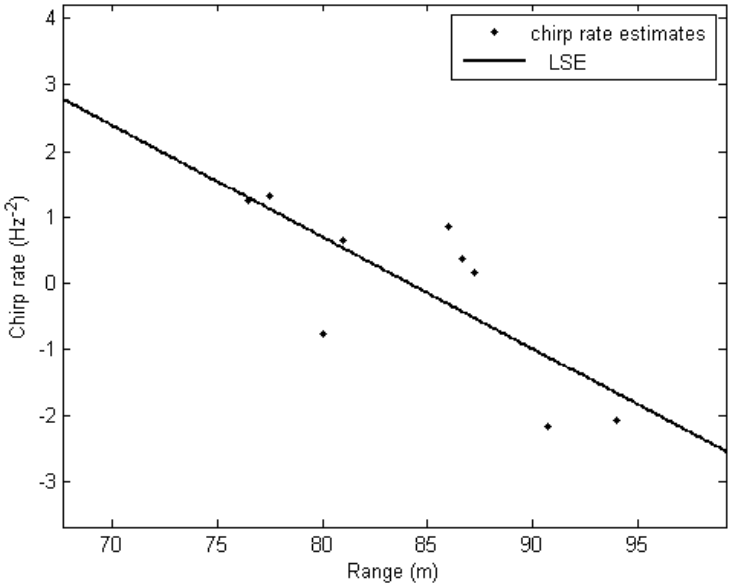

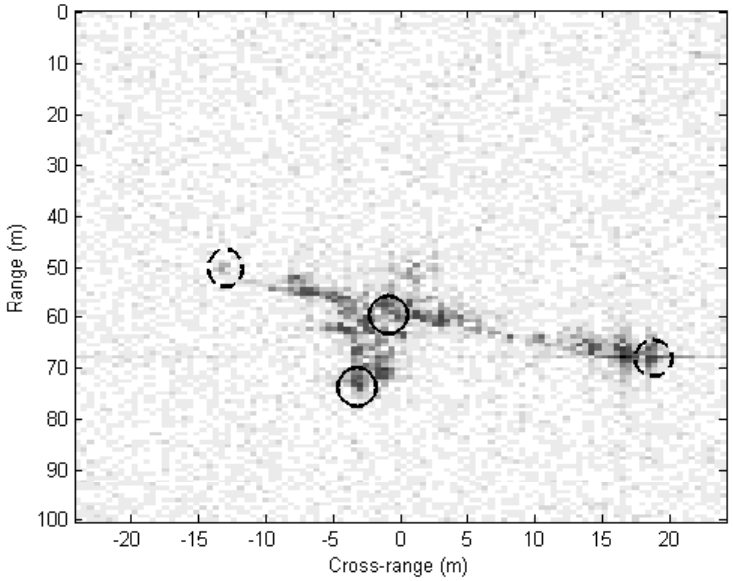

	Boeing 737	*Bulk Carrier*
Actual length (m)	[31.01-36.45]	[150-170]
Estimated length (m)	36.8	144
Actual wing span (m)	28.88	-
Estimated wing span (m)	28.37	-

Backprojection based Cross-Range Scaling

Frequency approach

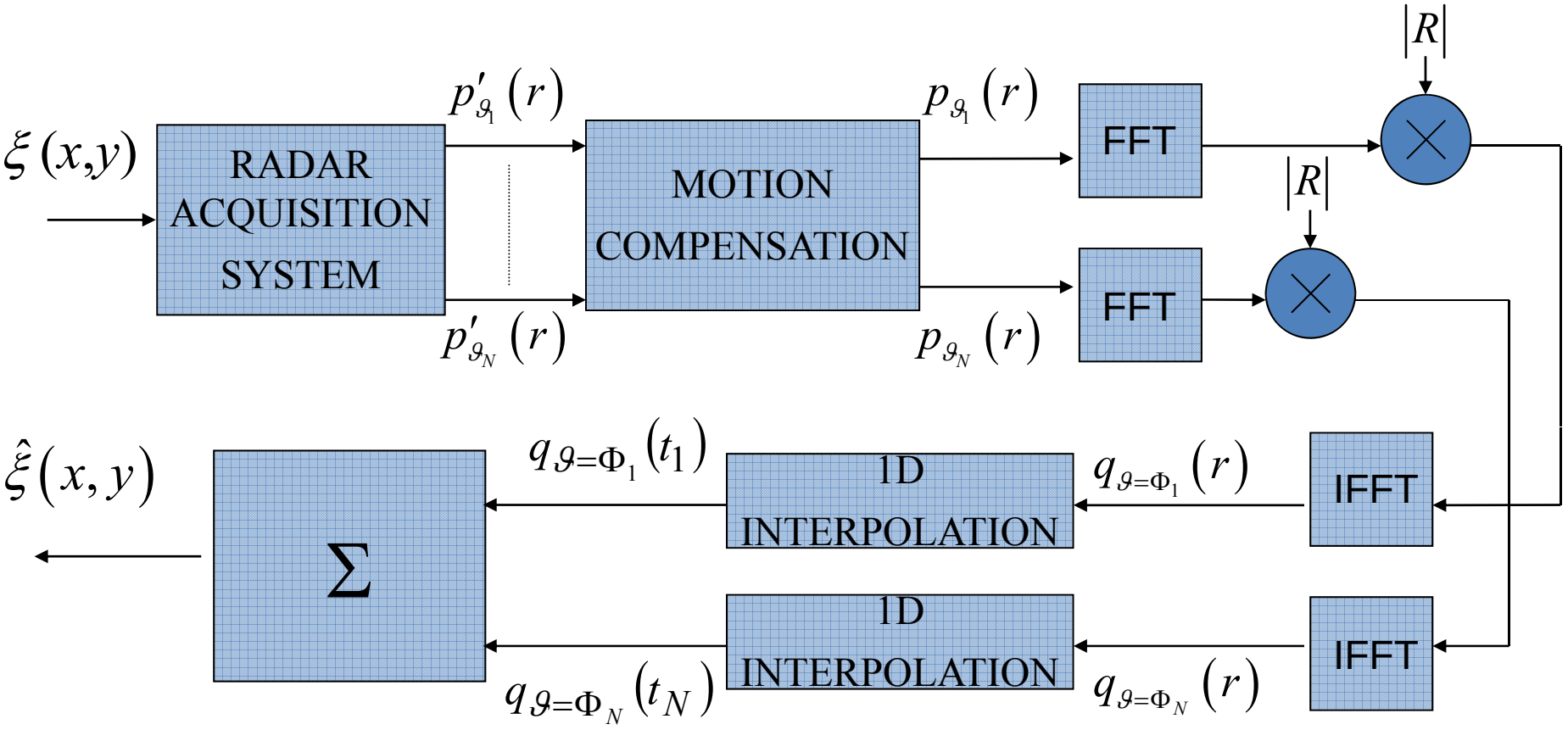

Backprojection based Cross-Range Scaling

$$\delta_{cr} = \frac{c}{2 f_0 \Delta\theta} = \frac{c}{2 f_0 T_{obs} \Omega} = \frac{c}{2 f_0 (N-1) \delta\theta}$$

Assumption of rectangular Fourier domain

Assumption of constant angular rotation

Discrete Time

Angle variation at each radar sweep

- The concept is that of forming sub-images from sub-apertures

- Each sub-aperture will produce an ISAR image with a given cross-range resolution, which will depend on the sub-aperture length

$$\delta_{cr}^{sub} = \frac{c}{2 f_0 (N_{sub} - 1) \delta\theta}$$

Backprojection based Cross-Range Scaling

Insight

- Divide the whole aperture into equal sub-apertures of length

$$N_{sub} = \frac{N}{K} \quad with \ \frac{N}{K} \ an \ integer \ number$$

- Rotate the i-th sub-image by an angle $\theta_0 = N_{sub}\delta\theta$

- Add up all the sub-images coherently

In the case of perfect knowledge of the angle $\delta\theta$, the reconstructed ISAR image is the same as that formed by using the whole aperture
(This can be easily shown by re-interpreting the backprojection algorithm)

Backprojection based Cross-Range Scaling

Insight

- The angle $\delta\theta$ is not known a priori, therefore the method proposed is not directly applicable
- The angle $\delta\theta$ must be estimated
- An error in the estimation of $\delta\theta$ produces an image defocusing
- The level of image focus can be measured by means of IC, IE, IP, etc

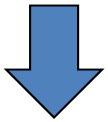

The angle $\delta\theta$ can be estimated by maximising (minimising) some cost function which is able to measure the level of focus

Backprojection based Cross-Range Scaling

Zhishun She et al.

$$\delta\hat{\theta} = \arg\max_{\delta\theta} \left\{ IP(\delta\theta) \right\}$$

Where $IP(\delta\theta)$ is the image peak found in the ISAR image formed by adding sub-images after rotating them of an angle equal to $\theta_0 = N_{sub}\delta\theta$

Other suggestions may be

$$\delta\hat{\theta} = \arg\max_{\delta\theta} \left\{ IC(\delta\theta) \right\}$$

$$\delta\hat{\theta} = \arg\min_{\delta\theta} \left\{ IE(\delta\theta) \right\}$$

Where $IC(\delta\theta)$ and $IE(\delta\theta)$ are the ISAR image contrast and entropy